学位論文

Chemistry of Natural Surface Water in Volcanic Area

火山地域における天然陸水の水質形成機構

平成 17 年 12 月博士（環境学）申請

東京大学

ANAZAWA, Katsuro

穴澤　活郎

Contents

1. Introduction

1.1. Background of the research

Earth has been called "the planet of water" with 14 hundred million km^3 water on the surface, but the fresh water is no more than 2.53%. Furthermore, it is assumed that the available water for human beings is only 0.01%, i.e., 0.1 million km^3 (Berner and Berner, 1996). We human beings are annually wasting 54% of available surface water resources. Management of the flowing water by the mankind has already been playing an important role on the terrestrial water circulation. Furthermore, improvement of the standard of living, increase of population and rapid economic development has brought synergy for a rise of world water demand; water demand has increased to 6 times in 100 years in the 20th century whereas world population increase was 3 times.

Concerning the fresh water resources, "the quality" problem is indwelling in addition to such quantitative problem. Freshwater resources are reduced by pollution besides consumption. Some 2 million tons of waste per day are disposed within receiving waters, including industrial wastes and chemicals, human waste and agricultural waste (fertilizers, pesticides and pesticide residues). There are a few reliable data about the range or seriousness of water pollution, but it is in no doubt that the most victims are poverty layer; about 50% of the people in the developing countries are using polluted water resources (World Water Assessment Program, 2003). Consequently, aquatic environmental issue worsens worldwide, and aquatic environment is regarded the most important issue as "the 20^{th} century was the century of oil, the 21^{st} century will be the century of water" (Alaton, 1999).

Concerning Japanese aquatic environment, Japan is a world's premier rainy region with 1700 mm of annual precipitation. This value is nearly about twice the world average. However, for the precipitation per capita, it is only about 1/4 of world average. Moreover, usable water resource in Japan is really limited; most of rainfall is

concentrated in the rainy season and the typhoon period; the precipitated rainwater flows at a stretch on the ground for the steep topography. In addition, sudden development of Japanese industry and the increasing standard of living are extending the amount of water usage as well as polluting the usable water resources. The severity of the aquatic environmental impact is rapidly increasing in this "Land of the Golden Ears of Rice". Since the available water resources have already been limited, it is essential for us to maintain the quality of water resources or even to improve them. In this manner, the social concern and importance for aquatic environment is shifting from the quantity issue to the quality issue. For the fundamental solution of aquatic environmental problems, it is necessary to quantitatively assess the anthropogenic load on the aquatic environment and to clarify the consequence of water pollution. For this sake, we have to clarify the chemical process on the "natural surface water" in addition to the survey of anthropogenic polluted water.

However, most hydrochemical research works have been emphasizing on geothermal waters or anthropogenically polluted river water (eg. Simeonov, 2001; Ministry of the Environment of Japan, 2004), if not, deep underground water from the aspect of the disposal of high level radioactive waste (eg. Iwatsuki and Yoshida, 1999; Kamei et al., 1999; Sasamoto et al., 2004). In the viewpoint of chemical component, the hydrochemical researches have been emphasizing only health items such as COD, BOD (eg. Ministry of the Environment of Japan, 2002), heavy metals or other trace elements (eg. Anazawa et al., 2004). Hydrochemical research works in volcanic areas are relatively rare for non-geothermal surface water; especially little attention has been paid for the major chemical components, which controls the fundamental water chemistry (eg. Kawakami, 1996; Anazawa and Ohmori, 2001). Little concern has been paid to the major chemical behavior, such as sodium or calcium, which enables us to comprehend the surface water chemistry. Therefore, this research investigated major chemical behaviors on the surface water in typical Japanese volcanic regions, where the source of Japanese river water exists intensively. The major part of this research has involved to

clarify the relation between the volcanic geology and the surface water chemistry and to extract the underlying factor of the hydrochemical processes in the volcanic area.

1.2. Hydrological and hydrochemical characteristics of Japan

1.2.1. Topology and geology of Japan archipelago

Japan archipelago is located in the tectonically active Circum-Pacific Mobile Belt and comprises a narrow island arc extending along the eastern margin of the Asian continent. The nature of this belt is evident in the topography and the geology of the Japanese islands; the topography is mountainous and rugged, and many volcanoes are widely distributed. This is the prominent geographical characteristic of Japanese islands in comparison with Europe or America on the geologically stable continents.

Such natural phenomena emerge on the topography and the geological feature of Japanese islands. The mountains higher than 3,000m form mountain range in the central part of the main island (Honshu Island); about 3/4 of the national land are covered by rugged hills and mountains. Approximately 46 % of the land surface is covered by Paleogene rocks or older rocks, and the residual 54 % is occupied by sedimentary rock and volcanic rock of the Neogene period and the Quaternary period (Geological Survey of Japan, 1982). The rugged topography, many volcanoes and wide distribution of volcanic ejecta, and various kinds of rocks are the important factors to consider the aqueous environmental chemistry in Japan.

A relatively temperate climate, abundant of rainfall is also important features. Japan archipelago extends north and south for 3000 km in the monsoon area, which includes the northern limit of the laurel forest zone. The general trend of the aquatic environment in Japan is characterized as the high precipitation, small scale of river in catchment area and length, rapid flows and the high speed of water circulation. The evapotranspiration for the precipitation is small, and the concentration by evaporation of rivers water ingredient is small; the chemical concentration in the river water is

generally small in comparison with the continental rivers (Table 1-1). The groundwater level is high in Japan and rock formations are saturated with water nearly to the surface. Therefore, the chemistry of river water in Japan is supposed to be largely influenced by groundwater or geological feature.

1.2.2. Comparison between continental and Japanese rivers

In 1960s, chemical researches on the river water were intensively conducted worldwide for the interest in global material circulation between the continent and ocean. Chemical researches of river water were mainly conducted on the continental rivers with wide catchment area in order to determine the representative chemical composition of world river water (eg. Meybeck,1979; Gibbs, 1972; Martin and Meybeck,1979). For example, Livingstone (1963) determined the average chemical composition of world river waters based on over 800 chemical data of the continental river water. The hydrochemical data, which were accumulated in this period, produced many hydrochemical researches; one of the representative works is assumed to be Gibbs (1970). In this classic paper, he described that the continental aquatic chemistry is mainly controlled by three factors; an atmospheric precipitation, carbonate rock weathering, evapotranspiration and dissolution of evaporite. This model was presented by a plot of total dissolved salts (TDS) against $Na^+ / (Na^+ + Ca^{2+})$ or $Cl^- / (Cl^- + HCO_3^-)$. The plot predicted that water with low TDS and high Na^+ and Cl^- had chemistry dominated by atmospheric precipitation; water with moderate TDS and high Ca^{2+} and HCO_3^- by rock weathering, and water with high TDS and high Na^+ and Cl^- by evaporation (Fig. 1-1.). This paper mentioned only little about the weathering of silicate rocks, such as volcanic rock and metamorphic rocks. Piper (trilinear) diagram and Stiff diagram, which are widely applied for the classification of surface waters in Japan, are also based on the continental water chemistry (Piper, 1944; Stiff, 1951). These diagrams are lack of silicon from the chemical item, which is a good indicator of silicate weathering. The silicate minerals such as feldspar or quarts are far more resistant to

weathering than carbonate minerals, such as calcite or dolomite (eg. White, et al., 1999); it is reasonable to focus attention on carbonate weathering for the continental rivers, which flows through sedimentary strata or limestone. On the contrary, as stated above, Japan archipelago differs from continents in geological and hydrological environment, where igneous rocks dominate the geology. It is a questionable research strategy to apply the same methods for the rivers in continents to the rivers in active tectonic zones, where the water resources exist intensively in the volcanic area.

The average chemical composition of river water in the world and Japan is shown in Table 1-1, and the conceptual comparison between Continental river and Japanese river in Table 1-2. The chemistry of Japanese river water is characterized by the small amount of total dissolved solids (TDS), low calcium and magnesium concentrations and high silicon in comparison with the world river water. The comparison between chemical and geographical properties gives general characteristics of chemical mechanism in Japanese river. First, the small amount of TDS would be introduced by the shortness of rivers and the rapid flow rate. The low calcium and magnesium and high silicon concentration is reasoned by the geology of catchment area, which is mainly composed of silicate rocks (igneous rocks). The prominent characteristics of Japanese hydrological or hydrochemical environment is supposed to mainly depend on the Japanese topography and geology.

1.3. Purpose and significance of this research

1.3.1. Purpose

The major part of this research is to quantitatively elucidate the relation between chemistry of surface water and geological environment in volcanic area, where the major water sources in Japan intensively exist (Fig. 1-2). The reasons of lack of researches on the water chemistry in volcanic areas are supposed that the access to the observation areas are usually difficult, obtained water samples are weak solutions,

which is difficult to analyze. In addition, even if the analytical values be precise and accurate, the research significance has not been found; the chemical compositions would be nearly the same as meteoric waters for the water rock interaction is not processed in the mountain area with short residence time. However, the preliminary hydrochemical investigation in the summit area showed significantly different characteristics between lake or spring waters and meteoric waters. Therefore, even waters in high mountains were anticipated to show the early stage in the chemical process of natural surface waters. In this research, the chemistry of surface waters in volcanic areas was intensively studied using statistical techniques and thermodynamic calculations. This study aims to state a comprehensive chemical image of natural surface water in Japan, by elucidating the hydrochemical mechanism of typical volcanic areas.

1.3.2. Methodology

The research process is composed of field work, chemical analysis, statistical analysis, thermodynamic calculation, geochemical interpretation and compilation of the results (Fig. 1-3). The methodological characteristic is applying multivariate statistical analysis for the computation of the massive analytical data set, and conducting thermodynamic and stoichiometric calculation for the quantitative interpretation of the statistical results.

Field work and chemical analysis

In addition to surface waters (eg. river water, spring water and lake water), meteoric waters (eg. rainwater, snow) or geothermal waters, which are supposed to play important roles for chemical process of the surface waters, were collected and analyzed. Over 300 samples were analyzed on the major chemical components altogether. The chemical analysis was performed by ion - chromatography for anions, atomic absorption spectrometry for cations, and colorimetric spectrophotometry for silicon.

Statistical analysis

Multivariate statistical analysis was performed on the chemical compositions to understand the geographical distribution and to extract geochemical potential factors affecting the chemical concentration of waters. Among the bunch of multivariate analysis, principal component analysis (PCA), factor analysis (FA), cluster analysis (CA) and multiple linear regression analysis were mainly applied on the surface water as well as geothermal water and rainwater. The statistical results were interpreted on the basis of geochemical or thermodynamic knowledge.

Geochemical interpretation

Thermodynamic and stoichiometric computations were performed to evaluate the hypothetical models induced by statistical results and the geochemical interpretation. The calculation was based on the computer simulations and the experiments of water-rock interaction.

1.3.3. Anticipated results and significance

Probable factors to control the water chemistry in volcanic areas are supposed to be atmospheric sources (eg. rainwater, snow, and atmospheric fallout), geothermal sources (eg. hot springs, geothermal waters, volcanic gases, sublimate), geological sources (eg. rock weathering, ion exchange, adsorption or deposition of solutes), and subsurface waters. Present research is expected to clarify the influence of those factors to the water chemistry qualitatively and quantitatively (Fig.1-2). The anticipated results will firstly give the chemical classification of water samples to specify the range of chemical variation in natural surface waters. Secondly, the results will clarify the chemical mechanism or causation by calculating prediction equations, which estimate chemical composition of real waters or by elucidating various stoichiometric relations. An application example would be that for the calculation of anthropogenic or other

impact on aquatic environment, this research will provide a fundamental concept to estimate natural hydrochemistry as a background environment.

1.3.4. Site selection

Followings are the requirements of desirable observation site for investigation to clarify the natural surface water chemistry.

(1) Away from major metropolitan areas
(2) No industrial area, no farmland, no residential district exists upstream of the site.
(3) Constant amount of water flows
(4) Typical Japanese geological features in the catchments of rivers.

It is preferable to set a simple function to examine natural mechanism of water chemistry in the early stage. For this sake, it is necessary to take the following conditions into consideration.

(5) Away from the ocean
(6) No volcanic activity

In this research, Norikura volcano was chosen as a major observation area, which satisfied all the above-mentioned conditions. Norikura volcano gives the following characteristics as an ideal research field.

(1) Separated from Tokyo Metropolis or Nagoya area

Mt. Norikura is 200 km away by direct distance from central Tokyo (12 million people) and 120 km from Nagoya (2 million people). Even the nearest city, Matsumoto city (200 thousand people) is 40 km away from the study area.

(2) Restriction of the local development

Norikura volcano is in the Chubu Sangaku National Park. It is strictly restricted or regulated for people to walk in as well as to develop or construct buildings there. Norikura volcano is the third highest volcano in Japan with 3,026 m high, and there are no farmlands or industrial areas upstream of the major observation area.

(3) High rainfall

The summer precipitation at the summit area of Norikura volcano is nearly 1600 mm during summer season, i.e., June to September. Therefore, the observation area is supposed to take more precipitation than Japanese annual average precipitation, which is about 1700 mm (Japan Meteorological Agency, 2005).

(4) Andesitic volcano

Major water resources in Japan is found in volcanic area, most of which are covered with andesitic ejecta or lava. Norikura volcano consists of an elongated group of small andesitic stratovolcanoes and is a typical volcano in Japan.

(5) Separated from ocean

The nearest seacoast of Japan Sea from Norikura volcano is 80 km to the north and the nearest seacoast of Pacific Ocean is 120km to the south; the influence of airborne sea salt to the rain and river water is supposed to be small.

(6) Dormant for over a thousand years.

Norikura Volcano has been inactive during the last 10,000 years, in spite of the activity of the surrounding volcanic mountains. Since then, there has only been small phreatic explosions (Moriya ,1983). The current shape was fixed about 9400 – 9000 years ago (Okuno, et al., 1994). Volcanic activity such as a spout of

steam is no longer seen in the vicinity of the summit area.

As mentioned above, Norikura volcano is an ideal field to observe the chemical mechanism on the natural surface water. Consequently, the present research is expected to give not only the case study of this area, but also to give general and typical concept of the chemical mechanism for Japanese surface waters. In this research, the other type of volcanic area was also studied to generalize the understanding of surface water chemistry.

1.3.5. Definition of water chemistry

The definition of "water quality" or "water chemistry" is multifarious, and is depending on the purpose of investigations. For example, BOD or COD is widely utilized as an official item related to living environment; heavy metals, such as cadmium or copper, are used as chemical indicators in viewpoint of the ecosystem; environmental endocrine disrupter such as dioxin or PCB are applied to know the impact on the human body. The concentration or value of those indices is so called "water quality" or "chemistry". In this research, the "water chemistry" is defined as the "chemicals, which essentially characterize the chemical property of waters". For this sake, the major chemical components are adopted as the indicators, i.e., sodium, potassium, magnesium, calcium, silicon, chloride ion, nitrate ion, sulfate ion, bicarbonate ion. The reasons for choosing these components are described as follows:

(1) Those components are the fundamental and major dissolved components. These components cover over 99 % of the total solutes in weight for river water or other surface waters.

(2) Since most of the natural river water or the shallow groundwater is weak solution, it is generally difficult to obtain an accurate analytical value on dissolved chemical components. Among those components, it is possible for major

components to keep the relative analytical error in low level. Moreover, application of statistical methods, which examines the covariance relation between variables, such as multivariate analysis, enables us to minimize the systematic error of the chemical data and to give reliable results.

(3) The change of the chemical composition in the stock solution is small during the stock time. Even after several months of sampling, the same analytical results can be obtained. Therefore, reanalysis is also possible to confirm the data reliability.

(4) The breakthrough of instrumental analytical techniques, such as ion chromatography or atomic absorption spectrophotometry, enables us to determine the large number of samples on multicomponent in the short time.

The bicarbonate ion of Norikura samples was excluded from the statistical analysis, since bicarbonate concentration was minute to give the reliable data.

1.3.6. Structure of this paper

Chapter 1. Introduction (This chapter)

Define the purpose and scope of this research

Chapter 2. Multivariate analysis on the hydrochemistry of Norikura volcano

Describe the analytical results of major elements in surface waters, i.e., lake water, river water and spring water, and other type of waters, i.e., rainwater and geothermal water.

Perform the multivariate statistical calculation based on the chemical data to understand the geographical distribution and to extract geochemical potential factors affecting the chemical concentration of waters.

Chapter 3. Thermodynamics and stoichiometry

Interpret the major factor, which controls the water chemistry, by thermodynamic and stoichiometric calculations mainly based on chemical weathering and water-rock interaction.

Chapter 4. Water chemistry in Shirasu ignimbrite area

Describe the other volcanic area, Shirasu ignimbrite area in southern Kyushu, and perform the same statistical and thermodynamic calculation as Norikura case.

Chapter 5. Conclusions

Summarize the chemical mechanism, which controls the major chemicals in the surface waters in Japan; describe what factor controls which chemical behaviors, and how much it is.

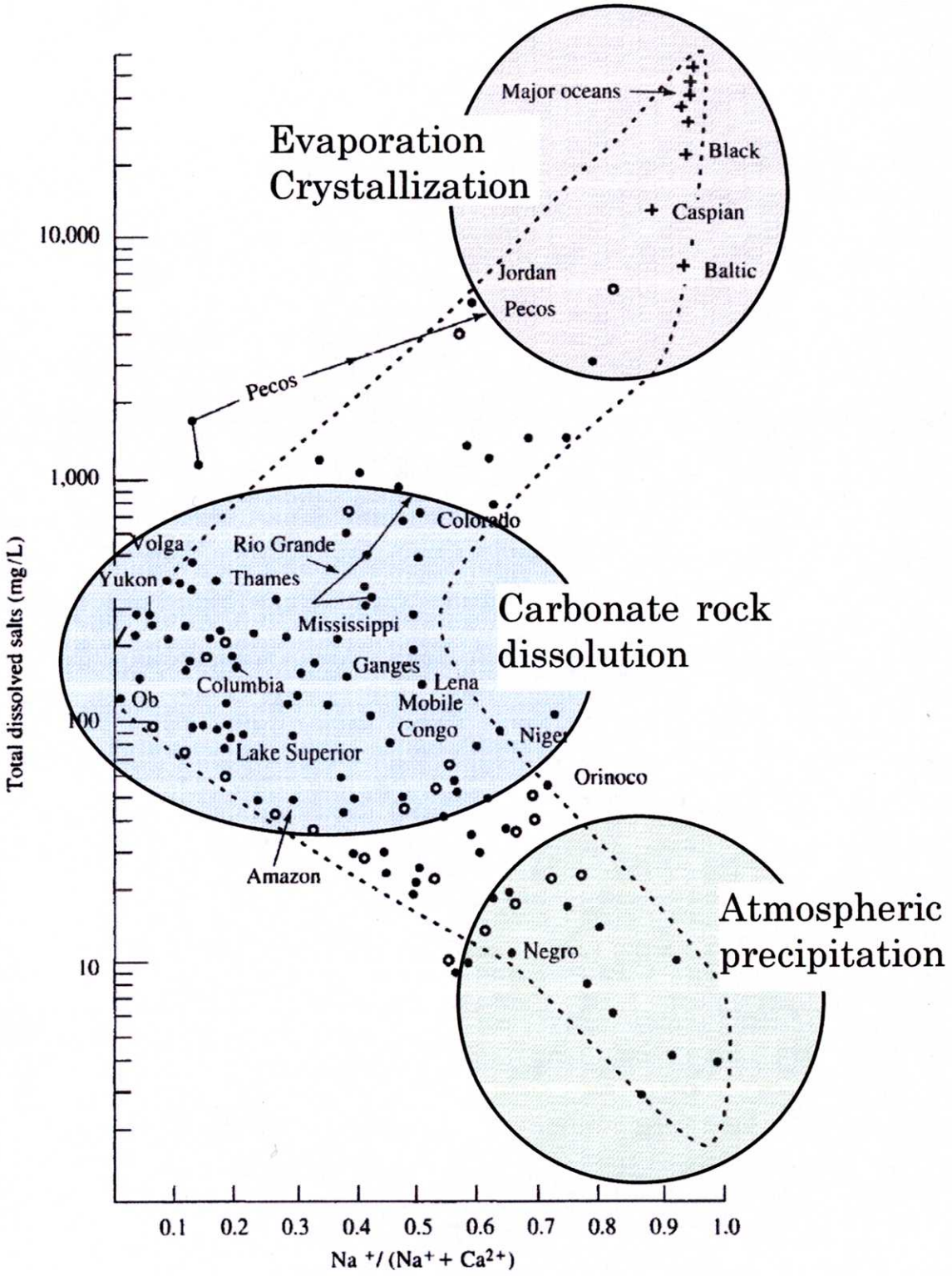

Fig. 1-1. Variation of the weight ratio Na / (Na+Ca) as a function of the total dissolved salts of world surface water. ○, Rivers; ●,lakes; +, oceans (After Gibbs, 1970).

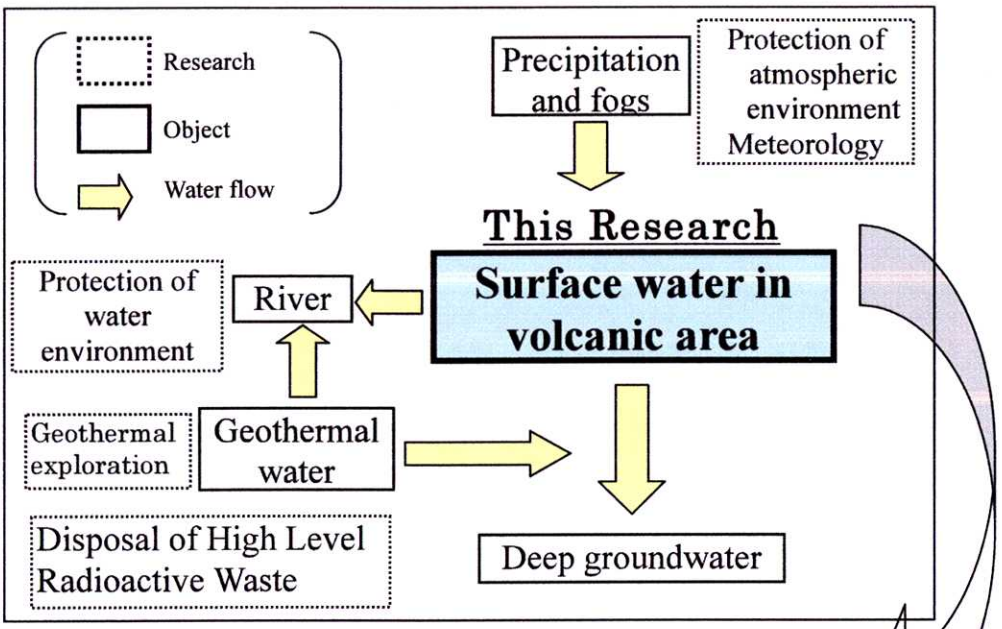

Anticipated Results

Clarify the major factors which control the water chemistry.
Evaluate the influence of those factors.
Classsify catchment areas hydrochemically.
Give the predictive equation for chemical concentrations.

Possibility of the research in the next stage

Elucidation of chemical mechanism of surface waters in Japan
Application to other area.

Fig. 1-2. Scope of this research

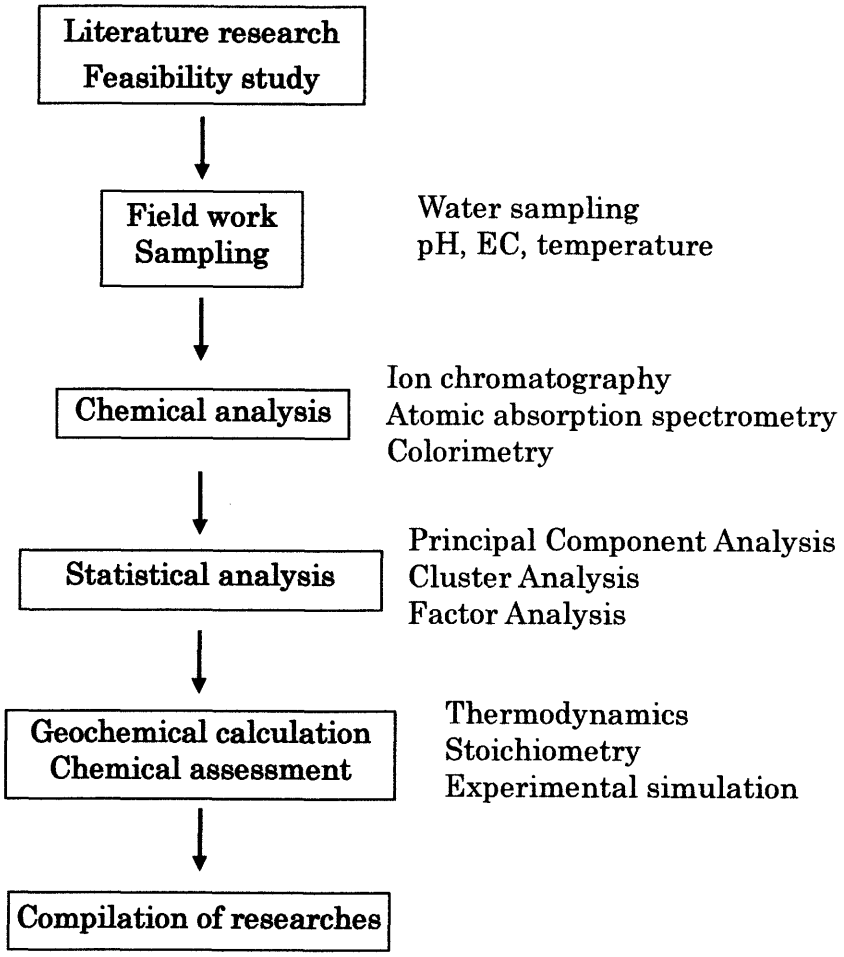

Fig. 1-3. Flowchart of this research procedure.

Table 1-1.
Average chemical composition of river water in Japan (mg dm^{-3})

Na^+	K^+	Mg^{2+}	Ca^{2+}	Cl^-	HCO_3^-	SO_4^{2-}	Si	NO_3^-	TDS	References
6.7	1.19	1.9	8.8	5.8	31	10.6	19	0.26	70.7	Kobayashi (1961)
5.1	1	2.4	6.3	5.2		10.5	17.3			Sugawara(1969)

Average chemical composition of river water in the world (mg dm^{-3})

Na^+	K^+	Mg^{2+}	Ca^{2+}	Cl^-	HCO_3^-	SO_4^{2-}	Si	NO_3^-	TDS	References
6.3	2.3	4.1	15	7.8	58.4	11.2	6.1	0.22	120	Livingstone (1963),
7.2	1.4	3.7	14.7	8.3	53	11.5	4.9		110.1	Meybeck (1979).
6.9	2.1	3.9	15	8.1	55.9	10.6				Gibbs (1972)
5.1	1.35	3.8	14.6				5.4			Martin and Meybeck(1979)

Table 1-2. Comparison of rivers between continents and Japan.

	Continents	Japan
Geographical property		
Geology	Sedimentary rocks (Limestone and evaporate)	Igneous rocks
Length	Long	Short
Flow rate	Slow	Rapid
Scale	Large	Small
Chemical property		
Electrical conductivity	High	Low
Hardness	Hard	Soft
Silicon concentration	Low	High

2. Multivariate analysis on the hydrochemistry of Norikura volcano

2.1. Geographical and geological characteristics of observation area

The observation area, Norikura volcano, is situated in Chubu Sangaku National Park, the access of people and the artificial constructions are strictly restricted there (Fig. 2-1). There are neither big cities nor heavy industrial area located around the mountain. Two local cities, Takayama and Matsumoto, are at the direct distance of 20-30 km from Norikura summit. A bus terminal of a mountain highway is located 1.5 km north from the summit. The area of interest is, therefore, an ideal environment to understand the non-anthropogenic water process.

Mount Norikura is a Quaternary volcano belonging to the Norikura volcanic zone, which overloads on the Hida mountain range. This area is on the west of the Itoigawa-Shizuoka tectonic line, the western part of central Japan. Geological data indicate that Norikura volcano was in active during the Quaternary period, but has been dormant for over last 10,000 years in spite of activity of the surrounding volcanic mountains (Moriya, 1983). Major volcanic ejecta of Mt. Norikura were formed between the Middle Pleistocene and the early Holocene periods (Nakano et al., 1987). Different kinds of geological evidences have been reported to infer that 700-1000 years cycle of volcanic activity had occurred during the Holocene period. Many evidences include the distribution of two-pyroxene dacitic andesite and two-pyroxene dacite around the summit of Norikura were recognized. The existence of thick lava flows and domes with andesitic and dacitic compositions (SiO_2 = 53 - 70%), while pyroclastic materials are restricted. The thickness of volcanic piles is less than 700 m, even under the volcanic center. The eruptive volume is estimated to be approximately 26 km^3 in total, though the present volume shows only about 15 km^3 due to extensive erosion (Nakano et al., 1995). Kengamine peak, which is the highest peak of Norikura volcano, is the highest point of watershed which divides into the Pacific Ocean side and the Sea of Japan side. The normative mineral composition of the major volcanic ejecta is that plagioclase and orthoclase govern 70%, pyroxene is 10%. In the modal mineral composition, plagioclase is 20～30%, pyroxene is 3～6% (after Nakano et al., 1987).

2.2. Sampling and analytical method

The field investigation was performed six times between May 1999 and September 2000, and 260 samples were collected from 100 points altogether. Sampling

points were located in and around Mt. Norikura (Fig. 2-1). They were at altitudes between 250 m and 2800 m above sea level.

The water samples were filtered and placed in polyethylene bottles and transported to the laboratory, then subjected to chemical analysis. The temperature, pH, and electrical conductivity (EC) were determined in the field by a digital pH meter (DKK HPH-130) and digital EC meter (Hach SensIon 5). The estimated uncertainty of pH measurements is 0.01 pH units with the repeatability of 2 %, and that of EC is 0.01 mS/m with 1% repeatability. The standard solutions were prepared from analytical reagent-grade chemicals using deionized water obtained from a Millipore Milli-Q SP water-purification system.

Chemical analyses for major anions were performed by Ion Chromatography (Hitachi L-7470 with Dionex DX-120) at the laboratory. The determination of sodium was performed by flame spectrophotometry (Shimazu AA-646), potassium was determined by atomic absorption spectrophotometry, and magnesium and calcium were determined by atomic absorption spectrophotometry (Shimazu AA-646) coexistence with lanthanum (10 g/dm^3). The silicon determination was performed by the molybdenum ammonium colorimetric method at a wavelength of 410 nm on a spectrophotometer (Hitachi U-1000). The detection limits were 0.05 mg/dm^3 for potassium and magnesium, 0.1 mg/dm^3 for sodium, calcium, silicon and chlorine, 0.5 mg/dm^3 for nitrate and sulfate. The validity of analytical data was maintained by repeated determinations to fall within 5 % of repeatability.

2.3. Statistical strategy

Regarding multivariate analysis, particularly, Factor Analysis (FA) is a widely known statistical technique, which enables us to extract the underlying common factors that control behavioral patterns. In the present work, this technique was applied to extract and understand both the source information and variation of each chemical solute in the natural water samples. The co-variances among chemical components were statistically analyzed, and categorized by Principal Component Analysis (PCA). Under these procedures, the potential factors of chemical variation were extracted by FA.

2.3.1. Principal component analysis (PCA)

PCA is a statistical technique applied to variables when a researcher is interested in discovering which variables in the set from coherent subsets that are relatively independent of one another. The specific goal of PCA is to reduce a large

number of observed variables down to a small number of principal components that reflects underlying processes, i.e., the correlations among variables.

The principal component is expressed by the following linear equation.

$$z_{ij} = a_{i1} \cdot x_{1j} + a_{i2} \cdot x_{2j} + a_{i3} \cdot x_{3j} + \cdots\cdots + a_{im} \cdot x_{mj}$$

where,

a ··· component loading
z ··· component score
x ··· measured value
j ··· sample number
i ··· component number
m ··· total number of variables

2.3.2. Factor analysis (FA)

Factor analysis attempts to extract a lower - dimensional linear structure from the data set. In factor analysis, the basic concept is expressed in the following formula:

$$z_{ji} = a_{j1} \cdot f_{1i} + a_{j2} \cdot f_{2i} + \cdots\cdots + a_{jm} \cdot f_{mi} + e_{ji}$$

z ··· measured value
f ··· factor score i ··· sample number
a ··· factor loading j ··· variable number
e ··· residual term accounting for errors or other sources of variation
m ··· total number of factors

The above two methods are expressed in principle as similar equations. The difference between the two methods is found that in the case of PCA, principal component is expressed as a linear combination of measured variables, while in the other case of FA, measured variable is expressed as a combination of factors and the equation contains residual term. The former method is applicable for any type of multivariate data set, while the latter has some regulations, such as an application on the data set with abnormal distribution.

The following multivariate application was performed as described in the literature (e.g. Davis, 1986).

2.3.3. Multiple regression analysis (MR)

Multiple regression analysis is a method of analyzing the variability of a criterion variable by using information available on a set of explanatory variables. The multiple regression is represented in a model equation of the general form as,

$$Y = b_0 + b_1 \cdot X_1 + b_2 \cdot X_2 + ... + b_m \cdot X_m,$$

where,

Y = criterion variable,
b_0 = constant term,
b_1 .. b_m = (partial) regression coefficient
X = explanatory variable

Multivariate regression analysis was used to identify the valid predictors of surface water chemical process.

2.3.4. Cluster Analysis (CA)

Cluster analysis is a technique used to place objects into groups or clusters based on statistical similarities of their properties. This technique makes no assumptions about the number of groups or the structure of those groups. Instead, groups are formed based on similarities in variable patterns. Therefore, objects in a given cluster tend to be statistically similar to each other in some sense, and objects in different clusters tend to be dissimilar (Johnson and Wichern, 1988). In this research, Ward method, which is a part of hierarchy cluster analysis, was applied for grouping, and the dissimilarity is defined by Euclidean distance (eg. Vega et al., 1998; Santos et al., 2004; Singh et al., 2004).

2.4. Outline of water chemistry

2.4.1. Classification of water samples

The analytical data shows clear correlation between the chemical compositions of the solute and the geographical characteristics of sampling points. The water samples obtained from the summit area of Norikura volcano show low values of electrical conductivity (EC: 0.2-1 mS/m), whereas the samples from the half way down the mountainside show c.10 mS/m, and even over 30 mS/m for the samples contaminated

by geothermal water. Since EC indicates the total concentrations of chemicals in the water, this feature of EC suggests that the dissolved chemicals would be correlated with geographical positions.

In order to classify the water samples, the principal component analysis (PCA) was applied based on the sampling regions and/or the source of waters (i.e. rain water, geothermal water). The chemical variation of each elemental concentration shows distorted distribution from normal distribution; rather similar to Poisson distribution. Since the data set should be normalized before PCA calculation, log-transformation and standardization were applied on each chemical element to revise distribution (Ahrens, 1954). On the other hand, the significant number of samples from summit area shows under determination limit on K^+, Mg^{2+} and Ca^{2+}. In this case, half value of the determination limit (0.05 mg dm^{-3}) was applied to the statistical calculations.

The correlation matrix for the PCA calculation is shown in Table 2-1. The correlation coefficients of logarithmic concentration data are high (0.6-0.9) for significance level of 1% between Si and cations (Na^+, K^+, Mg^{2+} and Ca^{2+}). Since the sole source of silicon is regarded as silicate minerals in volcanic rocks, the above high correlation would show that the volcanic rock dissolution is a major source of those cations.

The result of PCA is shown as eigenvalue and eigenvector of the correlation matrix (Table 2-2). The first principal component is highly loaded by almost all chemicals; this component indicates large proportionate contribution to the most chemicals and is characterized as a "size factor", which implies the integrated variances of the dissolved chemicals. The eigenvalue of this component shows the proportionate contribution of 70%, i.e., this component summarizes 70% of the variability or the information in the data set.

Based on the P1 scores, the water samples were easily classified on the basis of relations between chemical compositions and geographical features (Fig. 2-2). The schematic diagram shows that meteoric and geothermal waters are clearly separated from surface waters. The meteoric water of Norikura summit area (Alt. c.2800 m) lies at the upper left part of the scatter diagram. The P1 scores of surface waters are increasing with decrease in altitude. As a result, the water samples were classified into 8 groups, O to K, under consideration of the geographical features and P1 scores (Table 2-3). The classification of water samples was roughly made by geographically, then meticulous classification was performed under consideration of PCA score.

2.4.2. General characterization of Norikura water

The averages of the chemical concentrations in each group were illustrated in Fig. 2-3 and Fig. 2-4 to compare the geographical characteristics on major chemicals. The meteoric water (group O) shows extremely low concentration for all major elements, which are less than 0.5 mg/dm^3 (EC: < 0.3 mS/m). Even the surface water in the summit area (group A) is also extremely diluted solution; EC is < 0.5 mS/m. The total solute of the surface waters of group B to E increase the values with a decrease in altitude. On the other hand, geothermal waters obtained in the vicinity of Hirayu hot spring village (group K) show high pH (=8.5) and high EC (>30 mS/m). The waters of group H, which were obtained from Hirayu hot spring area, should be pushed up in pH and EC due to geothermal water contaminations.

The extraordinarily low concentration of the solutes shows that the summit area (Alt. c.2800m) takes only little effect from anthropogenic pollution or atmospheric fallout, as well as the neutralization by the eluviation of the basement rocks and soils. With a decrease in altitude, pH and total solutes of the surface water increase, approaching to the average concentration of the river water in Japan (Fig. 2-4). Thus, the chemistry of surface water in the study area would be considered to show one of the typical processes of hydrochemical formation in Japanese rivers.

2.4.3. Chemical ratio of sodium and calcium (Gibbs plot)

As mentioned in chapter 1, a plot of total dissolved salts (TDS) and the chemical ratio of $Na^+ / (Na^+ + Ca^{2+})$ (Gibbs plot; Gibbs, 1970) is widely applied to predict the contributions of atmospheric precipitation, sedimentary rock weathering, and evaporation to global inland water chemistry (eg. Kehew, 2000; Baca and Threlkeld, 2000). The concentration ratio of alkali earth elements and alkali elements of each sample group is presented as a Gibbs plot in Fig. 2-5. The $Na^+ / (Ca^{2+} + Na^+)$ is > 0.6 for the summit samples, and the value decreases with a decrease in altitude. The ratio of $Na^+ / (Ca^{2+} + Na^+)$ in the mountainside samples group E is down to 0.2, which is smaller than the average ratio of the rocks around the observed area, 0.45. This value of 0.2 is almost equal to the experimental value obtained by the powdered andesite elution (Tamari et al., 1988). The general trend of the Na-Ca ratio is firstly Na-type in the summit area, and according to the progress of hydrochemical reactions, the water type is changing into Ca-type in the mountainside region, whereas the geothermal water in the mountainside region shows Na-type again. Although this chemical trend seems similar to the continental water process, the plots of the present samples are out of the continental water range. In addition, since the present research area is covered by volcanic rocks and is separated from the ocean by 80 – 120 km, the contribution of the

atmospheric precipitation, sedimentary rock weathering, or evaporation to the water chemistry is unlikely high. The chemical behavior of the Norikura water should be interpreted in the different way from the continental waters.

2.4.4. Chemical behavior of major ions (Piper plot)

The piper plot or trilinear diagram (Piper, 1944), which is widely used for the classification of the water type (eg. Gieske et al., 2000), shows the other chemical feature (or chemical facies). The ion compositions of surface water, meteoric water of the summit area, geothermal water are presented in Piper plot (Fig. 2-6). This diagram clearly shows the geochemical differences between meteoric water, surface water, and geothermal water in the fluvial sector and the deltaic sector. The meteoric water takes relatively high Na^+, K^+ and Cl^- concentration than surface waters. Those waters are plotted in a typical Na-Cl type, which is found in seawater or seawater mixture. The surface waters in the summit area (A, B) shows relatively high Na^+, K^+, and HCO_3^-, but those values are lower than meteoric water or geothermal water; the water type belongs to the alkaline carbonate type. The relative composition of Ca^{2+} and HCO_3^- is increasing downstream, and the mountainside waters (D, E) are categorized as the alkaline earth carbonate type, which is seen in the typical Japanese shallow groundwater or river water. The geothermal water found in the mountainside (Hirayu area) shows high Na^+, K^+, Cl^- and HCO_3^-. This type of water is classified into the intermediate type, which is found in the circularity groundwater or subsoil water and is categorized in (Na-Ca-HCO_3-Cl) type.

Overall, the chemical evolution of the Norikura surface water is firstly high Na^+ and Cl^- (O: meteoric water) and according to the chemical process, Ca^{2+} and HCO_3^- increase relatively to Na^+ or Cl^-, to form Na-Ca-Cl-HCO_3 type (A, B, C), and Ca-HCO_3 type (D, E). The geothermal water in Hirayu area shows high concentration of Na^+ and Cl^- again (H, K: geothermal water). The details of the water type are found in Table 2-3.

2.5. Water chemistry of summit area

2.5.1. Description of observation area

Beforehand the general observation of the whole Norikura volcano, intensive studies were performed in the two areas; the summit area and the mountainside areas of Norikura volcano. The summit survey was mainly performed within the circle area of Kengamine and Marishiten cone with about 2 km radius (Fig. 2-7). The altitude range is between 2,550-2,845 m. This area is covered with several sheets of lavas, mainly

two-pyroxene andesitic compositions. The water samples were mainly taken from the following ponds; Pond Gongen-Ike, a crater lake of Kengamine Peak with an altitude of 2,845m; Pond Kiezuga-Ike (2,733m), a crater lake of Marishiten Cone; Pond Tsuruga-Ike (2,694m), a trio lake between Ebisu lava cone and Maou-Dake cone; and Ponds Gono-Ike (2,717m), a dammed lake formed by Marishiten-Lava. In addition to the pond and spring water samples, chemical compositions of the remaining snow and rainwater in this area were also determined.

2.5.2. Analytical results

The waters in the Norikura summit area showed extremely low concentrations of chemical solutes. Many samples were found to have below 1 ppm for each chemical solute. This caused the lack of pH buffer action that was proven by the unstable pH measurement during the sampling and it hindered the reliability of the pH data.

The electric conductivity (EC) of water samples were extensively low (< c. 1 mS/m; Table 2-3). The mean values of electron conductivity for each sampling points were 0.34, 0.44, 0.77 and 1.1 (mS/m) for pond Gongen, ponds Gono-Ike, springs at Takamaga-hara side and Kenga-mine peak side, respectively. These values show a negative (inverse) correlation between EC and altitude (Fig. 2-8).

The analytical data of these types of samples are expected to bear appreciable error; hence, an appropriate treatment will be possible only by statistical analysis on the basis of the chemical co-variances rather than by direct interpretation of chemical raw data. Statistical calculations were performed after the standardization of each chemical data to eliminate the variable weights. Most samples have Mg^{2+} concentration less than analytical detection limit (< 0.05 ppm), and so statistical methods were applied without Mg^{2+} data.

2.5.3. Factor analysis

The correlation matrix is shown in Table 2-4. High correlations for significance level of 1% were found among various ions, (eg. between Na^{+} and Cl^{-}). These high correlations are suggesting the possibility that even for these extreme weak solutions, subliminal common factors of geochemical effect can be extracted by statistical calculations.

Three factors were extracted by principal factor method, followed by quartimax rotation method. The number of factors was determined by PCA calculation and analysis of co-variances. The result of FA is shown in Table 2-5. These factor solutions were orthogonal and the interpretation of each factor must be independent from each

other.

2.5.4. Interpretation of factors

Factor 1

The first factor (sF1) showed high loading on all chemical solutes except for Cl^-. The values of factor loading on K^+, Ca^{2+}, SO_4^{2-}, and Si are high as > 0.7, and the loading value on NO_3^- and Na^+, are also significant, 0.3-0.5. The proportionate contribution of sF1 was calculated to be 45%. The cations and silicon of these solutes can be derived from rock dissolution by chemical weathering, however, SO_4^{2-} and NO_3^- are not constituents of rock-forming minerals, and hence the other source should be considered for these anions.

According to a research of fog water at the summit of Norikura volcano, fogs around this area contain significant amount of SO_4^{2-} and NO_3^- (1-1.5μeq/L), making the fog water acidic, to an extent of less than pH 4.0 sometimes (Minami and Ishizuka, 1995). Since Norikura volcano has shown no volcanic activity in the historical era, nor upflow of geothermal water in the summit area, the major source of those anions are assumed to be originated from rainwater.

On the other hand, the source of cations and silicon of the waters is assumed to be resulted from the interaction between rainwater contained the above anions and rocks. The CIPW norm mineral of typical rock composition in this area was calculated on the basis of a previous study (Ishikawa et al., 1992). The result showed that plagioclase occupies >50% of the all minerals, while orthoclase amounted to 13%. This composition suggests that the leaching rate of Ca^{2+}, Na^+ and K^+ should be significant in the initial stage of water and andesitic rock interaction process, according to the Goldich series (Goldich, 1938). Experimental works also demonstrated that plagioclase and orthoclase dissolution affect the initial water formation by water-rock interaction under weak acidic condition (eg. Tamari et al., 1988). The water-rock interaction rate is greatly accelerated by the acidity, approximately pH4 (Kobayashi, 1993), and the neutralization of acidic water by water-rock interaction is completed within several days. A hydrochemical observation of river water at Hida Mountains, which is the vicinity of Norikura volcano, suggested that the major possible source of SO_4^{2-} and NO_3^- ion has been derived from acid rain, and the equivalent cations are dissolved from basement rocks (Sakurai et al., 1998).

The above discussions lead to the consideration that sF1 is a factor related to chemical interaction between acidic rainwater and the basement rocks. Based on the existing influence due to this interaction to the surface waters, chemical composition

may be supported by the fact that statistical treatment of the data showed a negative correlation between sF1 oriented cation (K^+ and Ca^{2+}) and the altitude of each sampling points for the significance level of 1% (Fig. 2-8). This implies that water samples from higher altitude and lower altitude bear noticeable difference of ions concentrations. This implication contradicts the assumption that if surface waters around the summit area mainly come from rainwater, keeping constantly all the other effect, chemical composition is expected to have negligible difference as regardless of altitude. As the water is seeped to the ground, which basically composed of plagioclase and orthoclase, water-rock interaction enhances the leaching of major cations such as Ca^{2+}, K^+ and Na^+. The arriving solution, enriched with leached ions, will in turn increase the ion concentration of surface water at low altitude.

Factor 2

The second factor (sF2) shows high loading on Na^+ and Cl^- with the proportionate contribution of 20%. The sF2 score distribution shows the minimum score on rainwater, and increases from new fallen snow to old remaining snow (Fig.2-9). Remaining snow readily accumulates dustfall and rainwater solutes or any other contaminations, and the sF2 score variation is likely to be connected to this process. The concentrations of Na^+ and Cl^- are predominantly high in seawater (eg. Brewer, 1975), and the presence of these elements in dustfall or rainwater is generally interpreted as seawater origin (eg. Hara, 1999). Similarly, sF2 is interpreted as seawater effect in airborne particles and/or rainwater.

Factor 3

The third factor (sF3) shows high loading on NO_3^- with the proportionate contribution of 10%. The distribution of sF3 scores on pond Gono-Ike shows that the samples of minimum scores are samples on June 1999 (Fig. 2-10). The mean scores of samples at the beginning September take the maximum scores, while those of samples at the end September take intermediate. The differences of means in each sample group are highly significant at 1% (two-tailed T-test). The same pattern is also found in the waters from pond Gongen-Ike.

A hydrochemical study of forest soil reported that positive high correlation is found between inorganic nitrogen in soil water and the temperature of soils (Wu, et al., 1998), and the major NO_3^- source of soil water in forests is from biological nitrogen fixation (eg. Nambu, 1994).

The surroundings of pond Gono-Ike and pond Gongen-Ike are covered with

snow for most of the year and the vegetation is limited. Only during July to September, the nitrogen fixation is active and the NO_3^- concentration is increased in these ponds. The distribution trend of sF3 scores fitted this pattern expected for nitrogen fixation. Thus, sF3 is interpreted as biological activity effect, specifically nitrogen fixation.

2.6. Water chemistry of mountainside area (Hirayu area)

2.6.1. Description of observation area

An intensive survey of the mountainside area was performed around Hirayu geothermal area. The observation area is 6 km north of the summit, with an altitude from 1,260 m to 1,415 m (Fig. 2-11). Hirayu Hot Spring was originally discovered in 16th century when someone saw a monkey washing its wound with water from the hot springs. Since then it has developed and has been known as the healing springs with c. 20 hotels and hostels.

Most of the water samples were taken from the upper area of geothermal basin to avoid the contamination from artificial wastewater as well as the direct inflow of geothermal water. Those samples, which were classified as group E by PCA, are assumed to be non-geothermal waters. On the other hand, some samples were collected around Hirayu area to evaluate the influence of the river water chemistry. Those water samples were classified as group H. At the same time, the hot spring waters from Hirayu area were analyzed to examine the degree of influence of geothermal water for the above samples (group K).

2.6.2. Principal component analysis

For the sake of the water sample classification between non-geothermal water and geothermal contaminated water, PCA was applied on the chemical compositions on both cold waters and geothermal waters. The calculation result of PCA is shown in Table 2-6 as eigenvalues and eigenvectors. The proportionate contribution for the first principal component (mP1) was 74%, and for the second component (mP2) was 12%. The cumulative contribution for these two components was over 80% of the total co-variances. On the scatter plot of mP1 (Fig. 2-12), non-geothermal waters and geothermal contaminated waters were clearly separated.

On the basis of this result, factor analysis was conducted on the non-geothermal water samples. The correlation matrix is far different from that of summit water samples, in which Ca^{2+} and Mg^{2+} showed negatively high correlations with other solutes.

2.6.3. Factor analysis

The correlation matrix of non-geothermal waters and the result of FA are presented in Table 2-7 and 2-8 respectively. The first factor (mF1) showed positive high loading on most of the solutes, i.e. Na^+, K^+, SO_4^{2-}, Cl^-, NO_3^- and Si, except for Mg^{2+} and Ca^{2+}. The proportionate contribution of this factor was 45% of the total co-variances. The previous studies show that the cations of mF1 are the major solutes leached from rocks or discharged from rocks by ion exchange with Ca^{2+} and Mg^{2+} (eg. Iwatsuki, T. and Yoshida, H., 1999). Therefore, mF1 is interpreted as Na^+ and K^+ dissolution from rocks by acid water.

The second factor (mF2) showed positively loading on Ca^{2+} and Mg^{2+} and the proportionate contribution was 20%. The cations of mF2 are easily adsorbed into rocks by ion exchange with Na^+ and K^+ or precipitated by carbonation. Hence, the mF2 may be correlated with cation exchange on the rocks or sediments or precipitation of Ca^{2+} and Mg^{2+}.

2.7. Factor analysis for major cations and silicon on the non-geothermal waters

The intensive observation in the summit area or the mountainside area shows that the major factor to control the surface water chemistry is water and volcanic rock interaction. In the next stage, the major cations and silicon, which are the major elements of the surface waters and volcanic rocks, are intensively studied. The statistical strategy is the same as the above researches.

Firstly, the correlation coefficients were calculated among the major cations (Na^+, K^+, Mg^{2+} and Ca^{2+}) and silicon on the non-geothermal waters (O, A, B, C, D, E). The correlation matrix (Table 2-9) shows that there is high degree of correlation within (Na^+, K^+ and Si: r = 0.66 - 0.82) and (Mg^{2+} and Ca^{2+}: r = 0.89). The correlation coefficients between those two group chemicals take moderate value (r = 0.39 - 0.66).

The factor loading matrix shows that those correlations make clear (Table 2-10). The first two factors (nF1 and nF2) represent over 80% of all the covariance and the loading (eigenvalue) of the second factor is approaching to 1.0; the first two factors (nF1 and nF2) should be examined.

The obtained factor structure is similar to that of the mountainside water. The first factor (nF1) takes high loadings for all cations and silica, of which each factor loading is over 0.5; the proportionate contribution of this factor is 65% among the all cation and silica variances. This major factor shows the same tendency with the rock

dissolution factor obtained in the mountainside area. The second factor (nF2) has positive loadings for Na^+, K^+ and Si, and negative loadings for Ca^{2+} and Mg^{2+}. The proportionate contribution of this minor component is approximately 16%. The cation behaviors expressed by this factor would be interpreted as the ion-exchange between (Na^+, K^+) and (Ca^{2+}, Mg^{2+}) in concerned with the rock dissolution that is represented by [Si]. The chemical behavior presented on the Gibbs plot (Fig. 2-5) is expressed by this factor, i.e., $Na^+ / (Na^+ + Ca^{2+})$ decrease with the increase of total dissolved salts.

In the next chapter, those two types of chemical behaviors will be discussed in detail from the viewpoint of "water – rock interaction" using thermodynamics and stoichiometric calculations.

2.8. Summary

In order to understand the chemistry of the natural water in andesitic volcanic area, the surface waters were analyzed and classified on the basis of geographical feature and confirmed by PCA. The analytical result showed that the chemical process of the surface water in this area is a typical chemical process of Japanese river water.

2.8.1. The hydrochemical overview

(1) The chemical concentrations increase downstream with the decrease of chemical ratio of $Na^+ / (Na^+ + Ca^{2+})$.

(2) The water samples at the summit area take extraordinary low concentrations of the chemicals (EC: 0.2-1 mS/m) and the water type belongs to the alkaline carbonate type.

(3) The waters of the mountainside are categorized as the alkaline earth carbonate type, which is seen in the typical Japanese shallow groundwater or river water.

(4) The geothermal waters found in the mountainside (Hirayu area) are classified into the intermediate type, which is found in the circularity groundwater or subsoil water and water type is (Na-Ca-HCO_3-Cl) type.

2.8.2. Multivariate analysis

The PCA calculation of the whole chemical data set clearly divided the water groups as meteoric waters, non-geothermal waters and geothermal waters. The first principal component (P1) scores of the non-geothermal waters varied linearly with the altitudes of the sampling points. The correlation coefficients among major components in the non-geothermal waters were positively high in the data set of the mountainside

area or in the whole data. These high correlations between silicon and cations suggested that the volcanic rock dissolution plays an important role to the water chemistry in this area.

(1) Summit area (Group A)

The factor analysis showed that in the summit area, leaching of cations in the rocks by acid rainwater was the major contributor of preliminary water formation (proportional contribution was 45% of all co-variances). Airborne sea salt contributed 20%, while the biological activity contributed 10%. These results introduced that the major anions of acid rain rapidly leached out major cations of rock in the summit area of Norikura, and this chemical influence was detectable only under application of multivariate statistical method.

(2) Mountainside area (Group C)

The water formation in the mountainside area of Norikura was exclusively contributed by water-rock interaction; Na^+ and K^+ dissolution from rocks by acid water (proportional contribution was c. 45% of all co-variances), and cation exchange in the rocks or precipitation of Ca^{2+} and Mg^{2+} (c. 20%). The influence of geothermal water was found to be small even though the sampling points were close to geothermal area.

(3) Non-geothermal waters from the whole area

The factors obtained from the whole data shows similar structure to those from the mountainside area. The first major factor shows high correlation for all cations and silica. The second largest factor has positive loadings for Na^+, K^+ and Si, and negative loadings for Mg^{2+} and Ca^{2+}. The first factor shows the simple rock dissolution trend and the second factor shows the ion-exchange between (Na^+, K^+) and (Ca^{2+}, Mg^{2+}).

Fig. 2-1

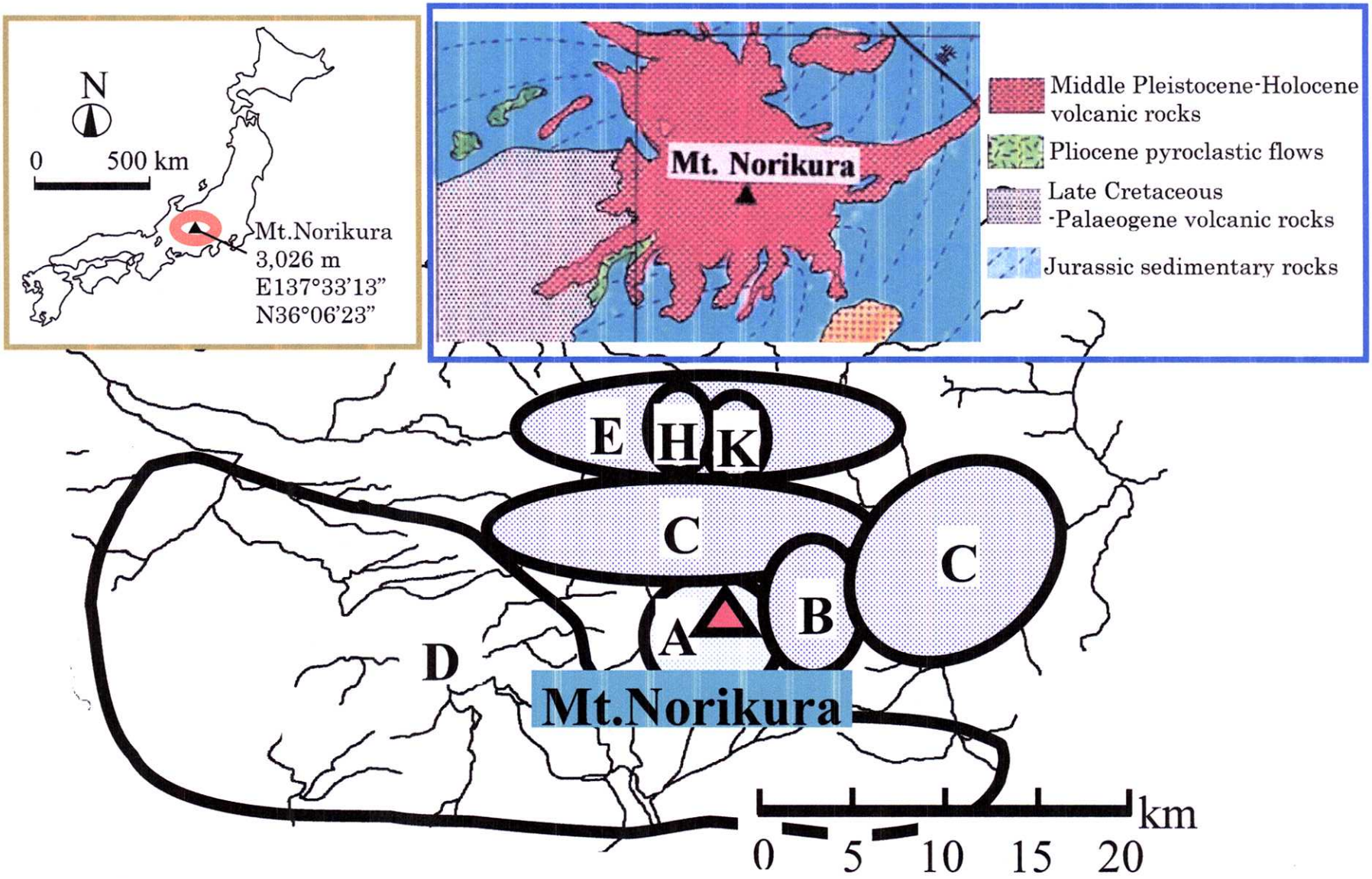

Fig. 2-1. Geological map and location map of observation area, Norikura volcano, in central Japan archipelago.

Fig. 2-2

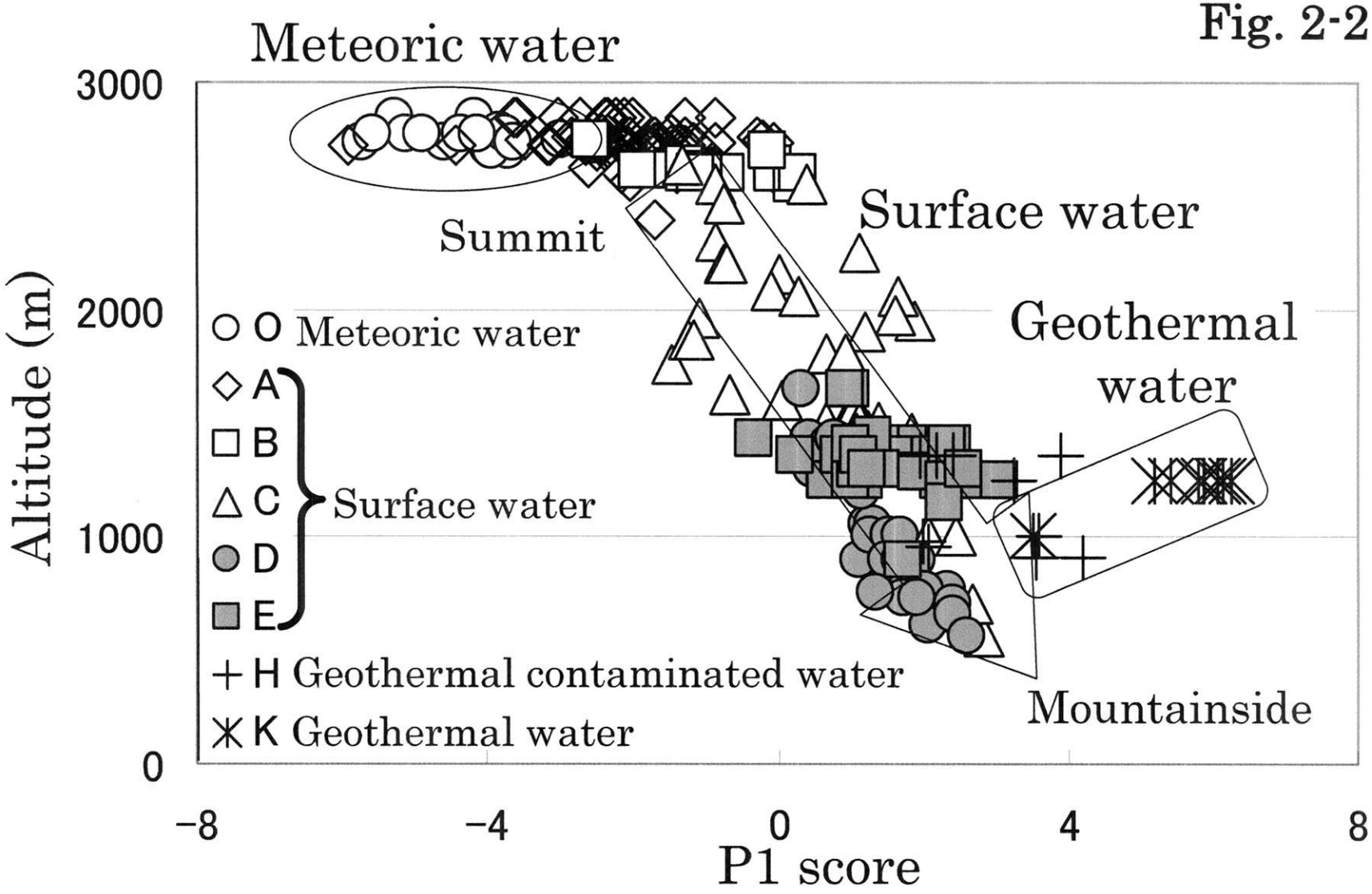

Fig. 2-2. Scatter plot of PCA scores (P1) vs altitude of the sampling points. Arrow indicates the direction of change in water chemistry with a decrease in altitude. Sample classification was performed by geographical feature under consideration of PCA scores. The sample group description is found in Table 2-3.

Fig. 2-3

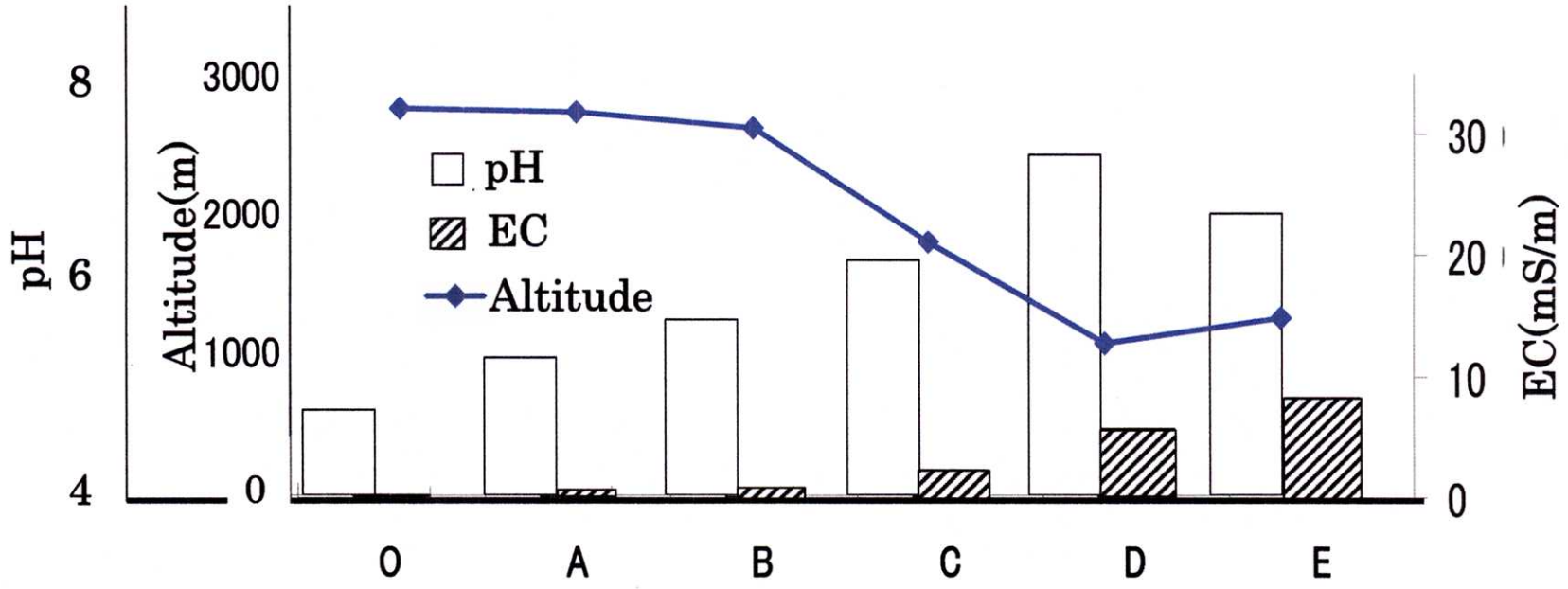

Fig. 2-3. Average data of each water group for altitude, pH and electrical conductivity (EC: mS/m). The group definitions are found in Table 2-3.

Fig. 2-4

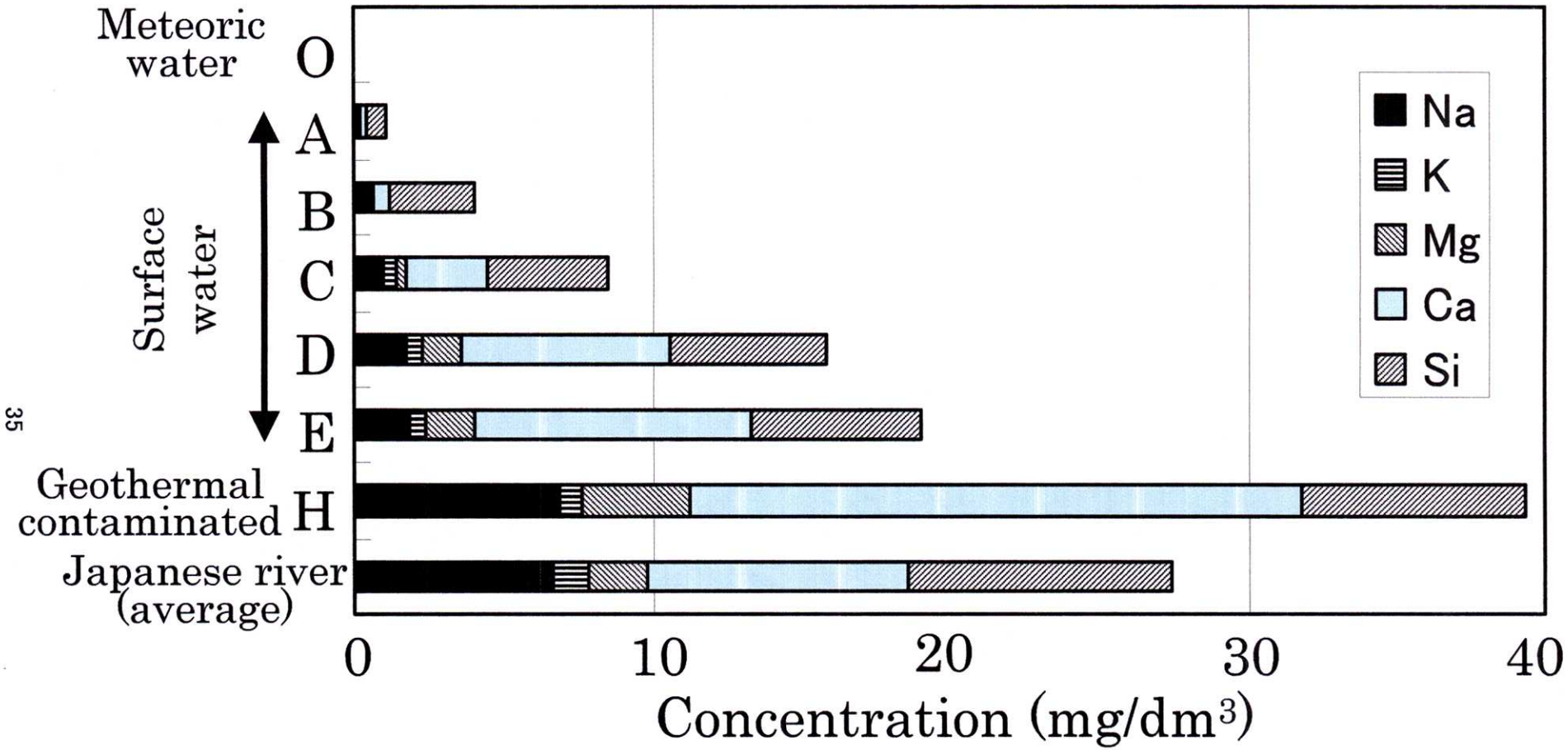

Fig. 2-4. Average concentrations of major cations and silicon in the meteoric and surface water groups. The group definitions are found in Table 2-3. The value of Japanese river water is after Kobayashi (1961).

Fig. 2-5

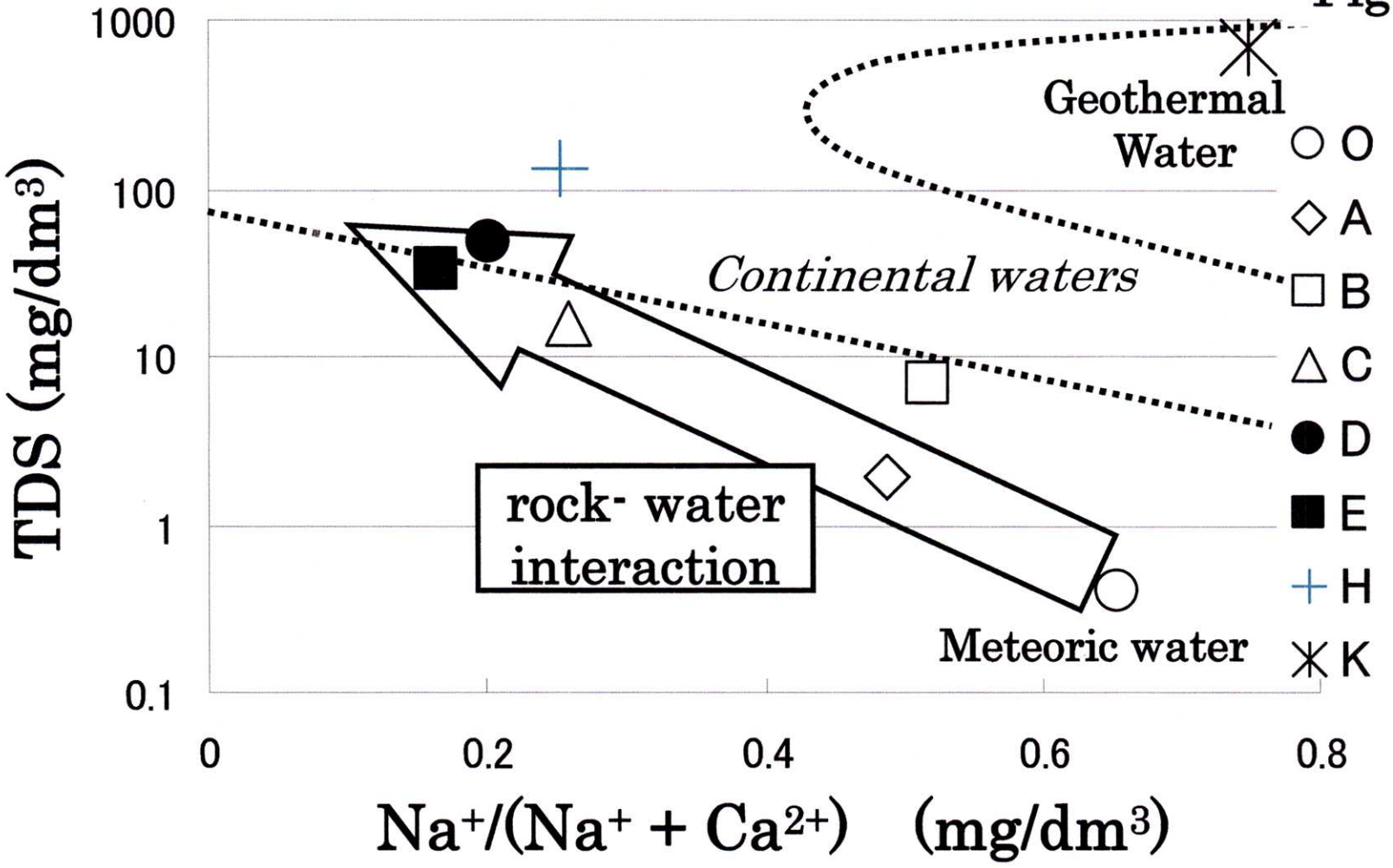

Fig. 2-5. Variation diagram of the concentration ratio of $Ca^{2+}/(Ca^{2+} + Na^{+})$ as a function of the total dissolved solids of surface waters. Inside of the dashed line describes typical continental river waters (Gibbs, 1970). Symbols are the same as in Table 2-3.

Fig. 2-6

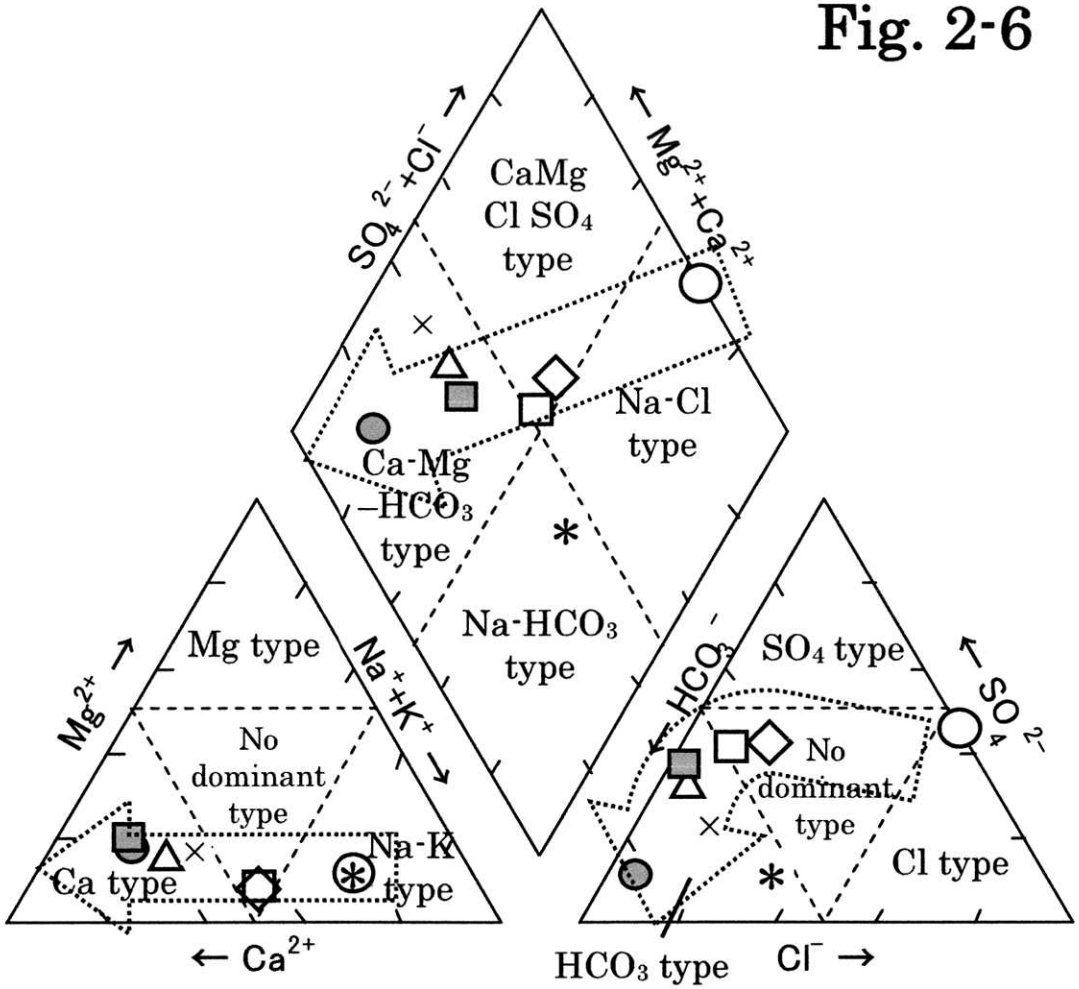

Fig. 2-6. Piper plot (trilinear diagram) of the surface water, meteoric water and geothermal water in Norikura volcano. Cation percentages in milliequivalents per dm^3 (meq dm^{-3}), plotted on three axes on the left triangle, and anions plotted in same way on the right triangle. The arrows show the hydrochemical process downstream.

Fig. 2-7

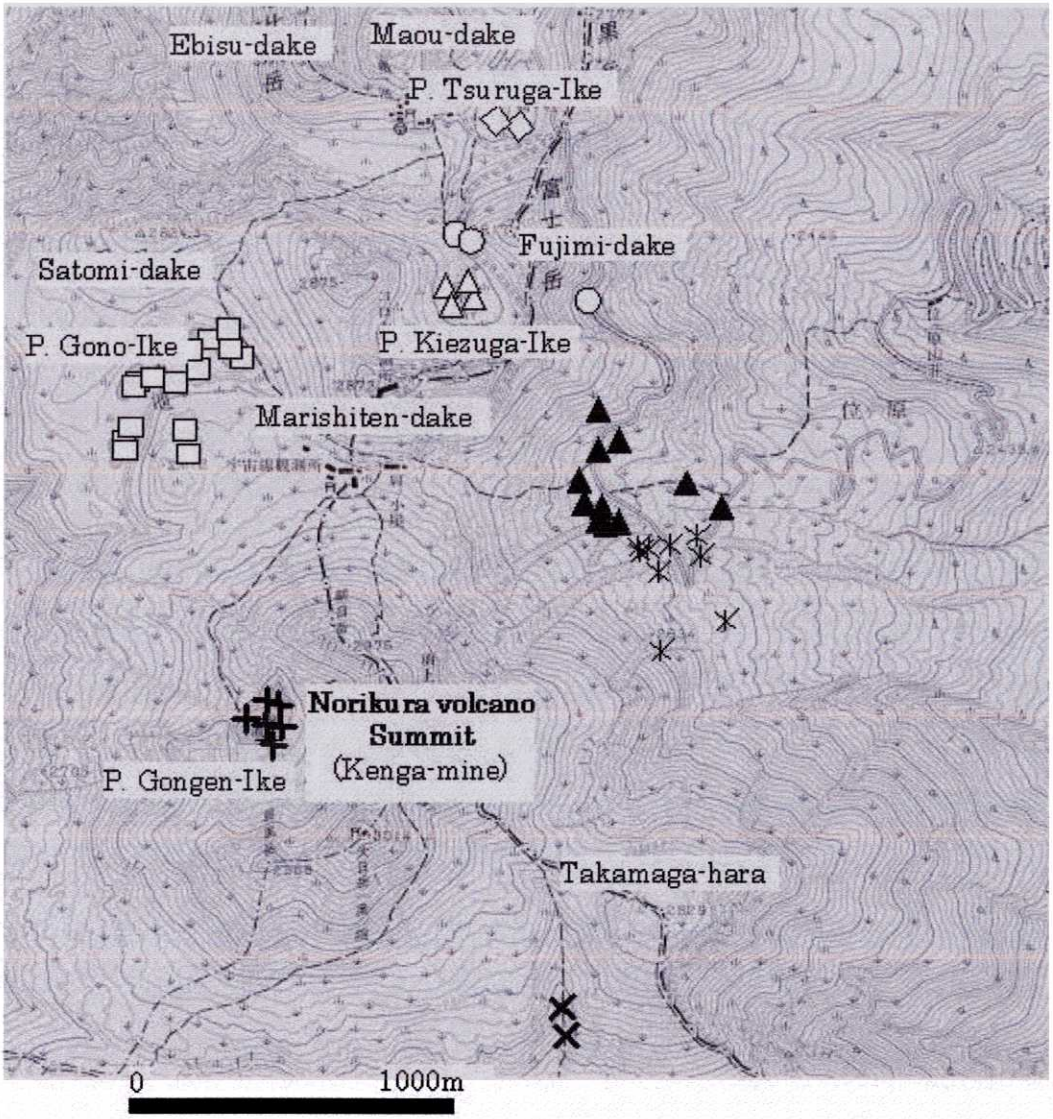

Fig. 2-7. Sampling points of the summit area of Norikura volcano. Symbols are; +, Pond Gongen-Ike; ×, Springs of Takamaga-Hara; ＊, Springs and streams of Kenga-Mine; □, Ponds Gono-Ike; □, Pond Kiezuga-Ike; □, Pond Tsuruga-Ike; ○, Springs of Fujimi-Dake; ▲, Springs and streams of Marishiten-Dake..

Fig. 2-8

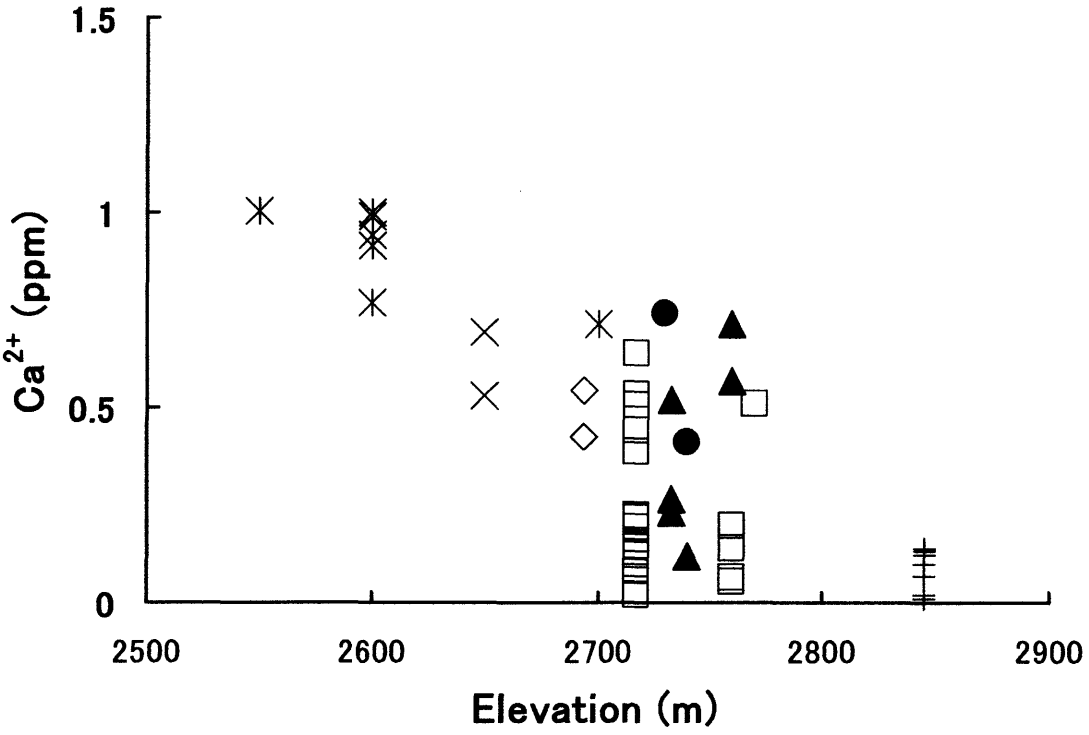

Fig. 2-8. Scatter plots of the sF1 oriented cation (Ca^{2+}) vs the altitude of sampling points in the Kengamine catchment basin. Symbols are the same as in Fig. 2-7.

Fig. 2-9

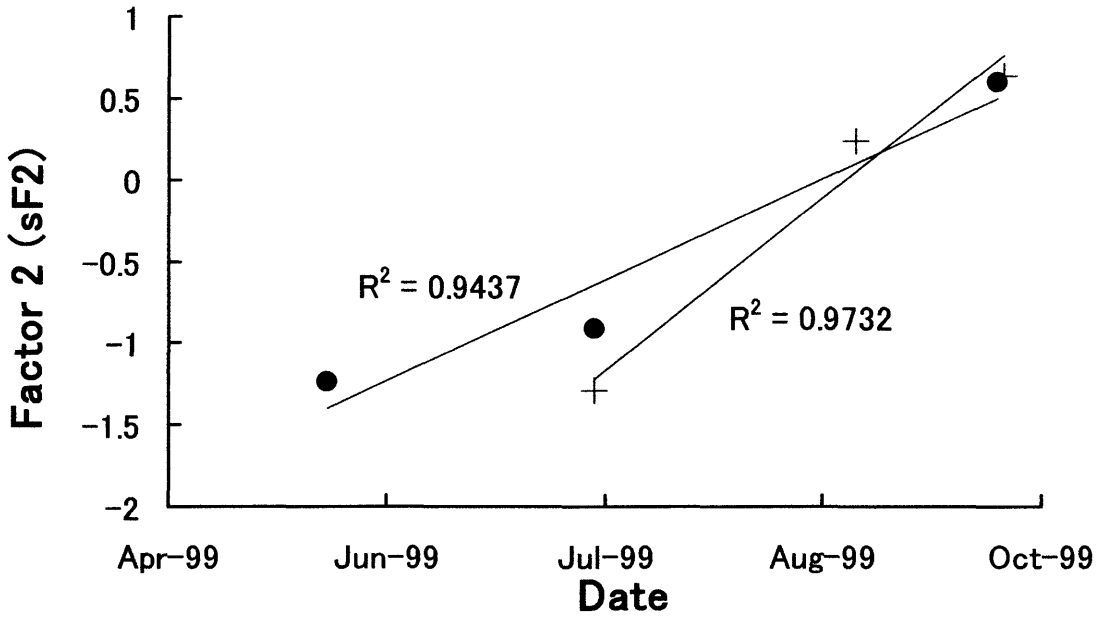

Fig. 2-9. Scatter plots of factor scores (sF2) vs sampling date for lake waters and lingering snow. Each point shows the mean value of the sampling date. Symbols are; +, Pond Gongen-Ike; ●, lingering snow.

Fig. 2-10

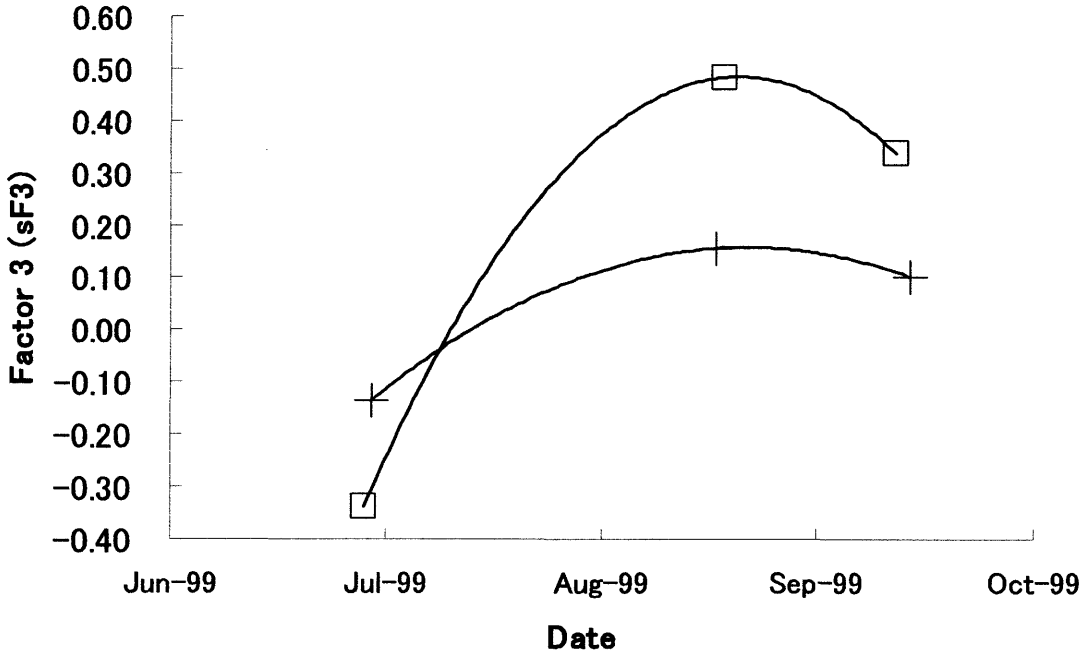

Fig. 2-10. Scatter plots of factor scores (sF3) vs sampling date for lake waters. Each point shows the mean value of the sampling date. Symbols are; + , Pond Gongen-Ike; □, Ponds Gono-Ike.

Fig. 2-11

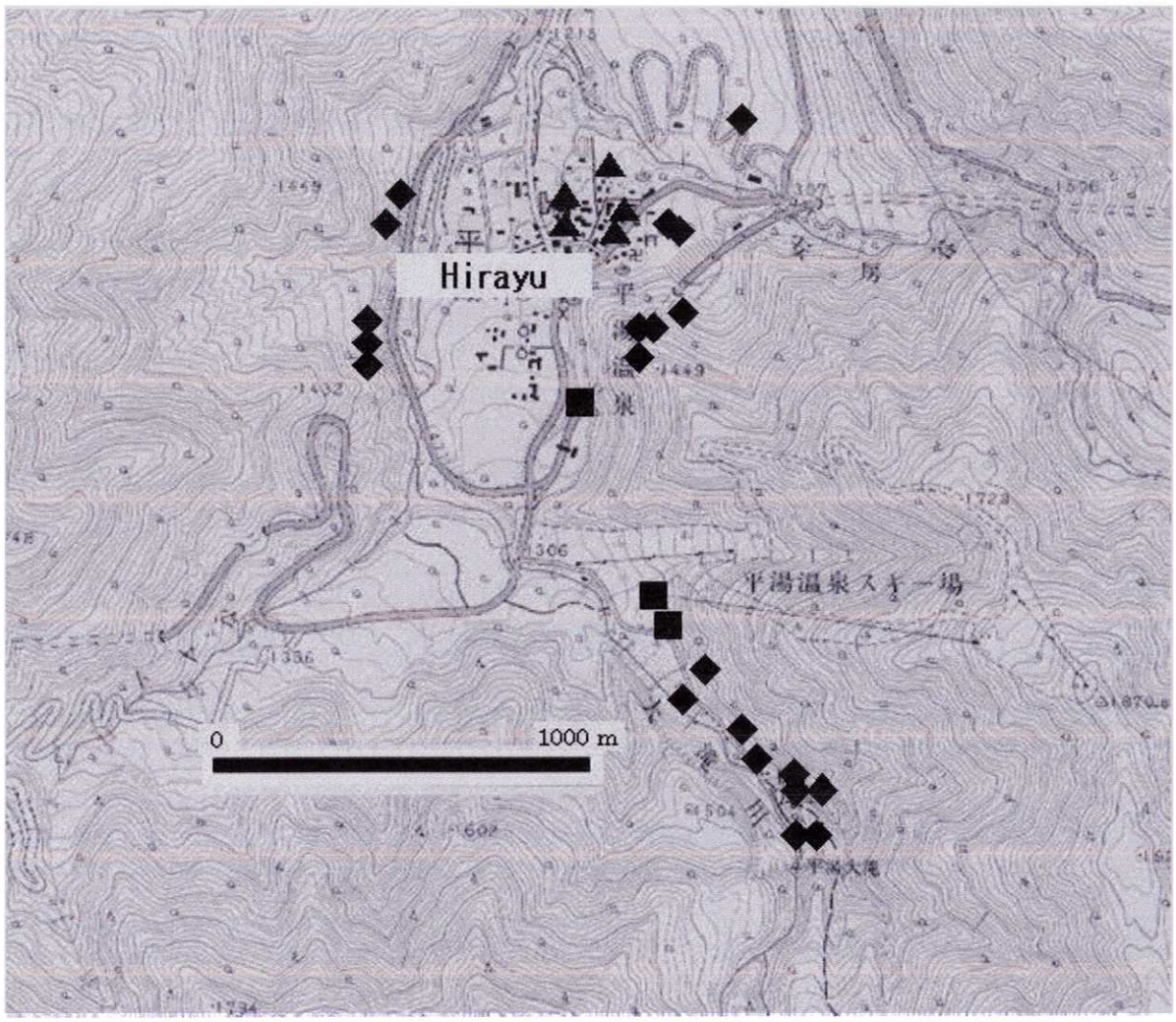

Fig. 2-11. Sampling points of the mountainside area (Hirayu area). Symbols are ◆, non-geothermal waters; ■, geothermal contaminated waters; ▲, hot springs.

Fig. 2-12

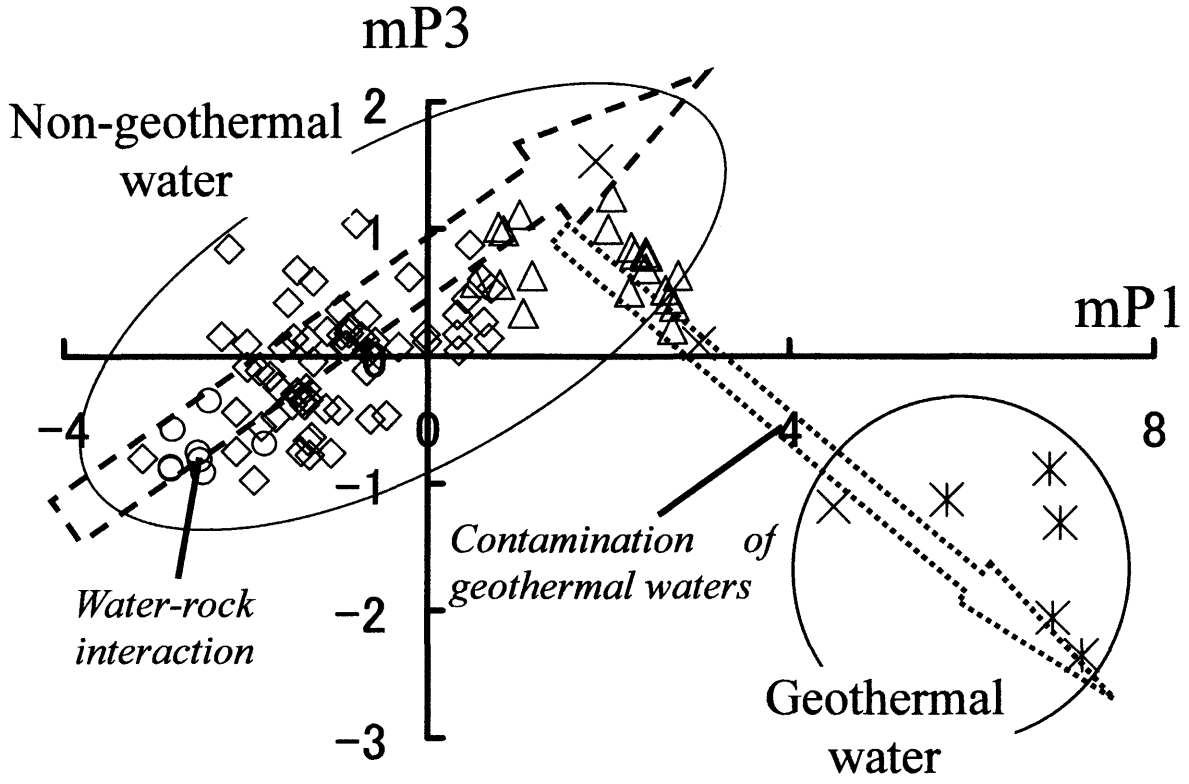

○ Meteoric water (summit area)
◇ Surface water (summit area)
△ Non-geothermal water (Hirayu area)
× Geothermal contaminated water (Hirayu area)
∗ Geothermal water (Hirayu area)

Fig. 2-12. Scatter plots of PCA scores, mP1 vs mP3 for the summit and the mountainside samples, and the geothermal waters.

Table 2-1. Correlation matrix of the chemical concentration in meteoric water, surface water and geothermal water (n=260).

	log(Na)	log(K)	log(Mg)	log(Ca)	log(Si)	log(Cl)	log(NO_3)	log(SO_4)
log(Na)	1.00							
log(K)	0.64	1.00						
log(Mg)	0.85	0.69	1.00					
log(Ca)	0.79	0.73	0.91	1.00				
log(Si)	0.80	0.64	0.80	0.79	1.00			
log(Cl)	0.82	0.62	0.71	0.66	0.61	1.00		
log(NO_3)	0.19	0.15	0.20	0.23	0.15	0.25	1.00	
log(SO_4)	0.74	0.66	0.84	0.83	0.72	0.64	0.20	1.00

Table 2-2. Eigenvectors and eigenvalues on the correlation matrix of the chemical concentration in meteoric water, surface water and geothermal water (n=260).

Element	P1	P2
log(Na)	0.39	-0.05
log(K)	0.34	-0.08
log(Mg)	0.40	-0.06
log(Ca)	0.40	-0.03
log(Si)	0.37	-0.12
log(Cl)	0.35	0.08
log(NO_3)	0.11	0.98
log(SO_4)	0.38	-0.04
Eigenvalue	5.50	0.95
Proportion (%)	0.69	0.12
Cum.Proportion (%)	0.69	0.81

Table 2-3. Classification and chemical composition of water samples; chemical concentrations in μmol dm^{-3}.

Group	Mark	n	Water description	Location	Altitude (m)	pH	EC (mS/m)	Na	K	Mg	Ca	Si	Cl	NO_3	SO_4
O	○	19	meteoric water ; rain water, snow	summit area	2800	4.9	0.28	5.36	1.04	0.62	1.20	6.27	3.79	3.03	1.65
A	◇	73	surface water; lake water, spring water	summit area	2700-2800	5.5	0.58	14.1	1.76	1.40	7.91	54.1	5.25	3.37	6.66
B	□	21	surface water; river water, spring water	summit area	2600-2750	5.9	0.80	25. 4	4.53	2.73	15.0	150	6.00	6.04	12.3
C	△	41	surface water; river water, spring water	north-east side	1000-2600	6.7	3.72	64.0	15.2	27.5	106	202	18.60	5.05	56.7
D	●	43	surface water; river water, spring water	south-west side	600-1600	7.7	6.60	83.7	14.8	62.8	217	196	34.1	13.6	38.7
E	■	44	surface water; river water, spring water	north side; Hirayu area	1000-1300	6.9	9.02	95.4	16.7	84.7	276	240	22.2	6.18	155
H	+	10	surface water; contaminated with geothermal water	north side; Hirayu area	1000-1300	7.7	21.1	559	41.2	180	547	307	287	11.7	250
K	*	9	geothermal water	north side; Hirayu area	1000-1300	8.5	85.2	6905	502	674	1299	1502	3693	20.7	670
Japanese river [1)]		225	river water			7.0		291	30.4	78.2	220	317	164	18.6	110
Fog water [2)]			Fog water at the Norikura summit			3.3-4.25		231-43110	0.00-934	24.69-1703	7.49-1677	0.00-0.00	203-39880	0.00-51790	447-37740
Seawater [3)]			Seawater			8.2		459161	9719	52335	10280	71.21	547200	0.00	28221

1) Kobayashi (1961), 2) Minami and Ishizuka(1996), 3) Brewer(1975)

Table 2-4. Correlation matrix of the Norikura summit waters.

	Na^+	K^+	Ca^{2+}	Cl^-	NO_3^-	SO_4^{2-}	Si
Na^+	1.00						
K^+	0.09	1.00					
Ca^{2+}	**0.55**	**0.57**	1.00				
Cl^-	**0.54**	0.01	**0.42**	1.00			
NO_3^-	0.27	**0.42**	**0.40**	0.02	1.00		
SO_4^{2-}	**0.44**	**0.67**	**0.73**	0.14	**0.43**	1.00	
Si	**0.55**	**0.64**	**0.80**	**0.39**	**0.33**	**0.83**	1.00

Bold values are 1% significant correlations.

Table 2-5. Factor loadings of the Norikura summit waters (Principal factor analysis with Quartimax rotation).

	sF1	sF2	sF3
Na^+	0.34	**0.80**	0.24
K^+	**0.82**	-0.20	0.01
Ca^{2+}	**0.78**	0.39	0.01
Cl^-	0.15	**0.66**	-0.13
NO_3^-	**0.48**	0.00	**0.45**
SO_4^{2-}	**0.87**	0.12	0.08
Si	**0.88**	0.36	-0.20

Table 2-6. Eigenvalue and eigenvector of the mountainside waters (including hot springs).

	mP1	mP2
Na^+	**0.39**	-0.15
K^+	**0.38**	-0.30
Ca^{2+}	**0.38**	0.16
Mg^{2+}	**0.31**	**0.36**
Cl^-	**0.39**	-0.07
NO_3^-	0.19	**0.81**
SO_4^{2-}	**0.35**	-0.07
Si	**0.39**	-0.25
Eigenvalue	5.96	0.93
Proportion	0.74	0.12
Cum.Proportion	0.74	0.86

Table 2-7. Correlation matrix of the non-geothermal mountainside waters.

	Na^+	K^+	Ca^{2+}	Mg^{2+}	Cl^-	NO_3^-	SO_4^{2-}	Si
Na^+	1.00							
K^+	**0.86**	1.00						
Ca^{2+}	0.10	-0.01	1.00					
Mg^{2+}	-0.42	-0.49	**0.77**	1.00				
Cl^-	0.40	0.47	0.15	-0.16	1.00			
NO_3^-	0.08	0.29	0.03	-0.13	0.43	1.00		
SO_4^{2-}	0.53	**0.80**	-0.41	**-0.62**	0.31	0.28	1.00	
Si	**0.73**	**0.91**	-0.20	**-0.63**	0.46	0.31	**0.85**	1.00

Bold values are 1% significant correlations.

Table 2-8. Factor loadings of non-geothermal mountainside waters (Principal factor analysis with quartimax rotation).

	mF1	mF2
Na^+	**0.89**	0.12
K^+	**0.98**	-0.00
Ca^{2+}	-0.02	**0.96**
Mg^{2+}	**-0.52**	**0.77**
Cl^-	**0.46**	0.14
NO_3^-	0.24	0.00
SO_4^{2-}	**0.76**	-0.42
Si	**0.91**	-0.22

Table 2-9. Correlation matrix of the chemical concentration in non-geothermal surface waters for group A-E. (n=222).

	Na^+	K^+	Mg^{2+}	Ca^{2+}	Si
Na^+	1.00				
K^+	0.82	1.00			
Mg^{2+}	0.59	0.50	1.00		
Ca^{2+}	0.60	0.52	0.89	1.00	
Si	0.66	0.74	0.39	0.39	1.00

Table 2-10. Factor loadings of the chemical concentration in non-geothermal surface waters for group A-E. (principal factor method) (n=222).

Element	F1	F2
Na^+	0.85	0.21
K^+	0.86	0.41
Mg^{2+}	0.81	-0.48
Ca^{2+}	0.82	-0.47
Si	0.68	0.36
Eigenvalue	3.27	0.79
Proportion(%)	65	16
Cum.Proportion(%)	65	81

3. Thermodynamics and stoichiometry

3.1. Introduction

The previous geostatistical research showed that in the summit area of Norikura volcano, there are three major contributors of preliminary water formation; the leaching of major cations from the host rocks, whose proportionate contribution is 45% of all co-variances; airborne sea salt, which contributes 20%; the possible vegetation influence with 10% contribution. The above results, however, gave only general idea concerning the covariance of the analytical data. The factor interpretation is conceptual basis and rather vague. In this chapter, the thermodynamic and stoichiometric calculation was performed in order to interpret those factor contributions to the surface water chemistry quantitatively. Since it takes long time range to reach the full equilibrium in water – rock interaction, the thermodynamic methodologies based on the chemical equilibrium are exclusively applied in geothermal exploration or researches on oceanic chemical distribution. In this research work, by use of silicon as an indicator to evaluate the dissolution rate of volcanic rocks or the degree of the water-rock interaction, stoichiometric calculations were performed. The results were certified by the chemical equilibrium information. And also the silicon concentrations of the water samples were evaluated by the induced theoretical equation.

3.2. Methods

On the basis of the statistical results given in Chapter 2, the thermodynamics and stoichiometric calculation were performed. The analytical data set is the same as in Chapter 2.

3.2.1. Stability diagram

The stability diagram, which draws the dynamic equilibrium between the solutions and coexistent solid phases, is frequently applied to interpret the chemical behavior of natural spring waters in terms of water-rock interaction (Garrels and Christ, 1965). Using the stability diagrams of major cations and silica relations, the present study attempted to survey how water-rock interaction is involved each stage of the hydrochemical process. The ion activities were calculated as an ionic-strength term in the Debye Hückel expression, on the basis of the thermodynamic constant (ΔG) for

stable minerals and ions given by the published data set (Berner, 1971; Helgeson, et al., 1978).

3.2.2. Theoretical solution by CIPW norm minerals

During the water-rock interaction processes, the primary mineral dissolution is generally followed by the formation of the secondary minerals, which is termed incongruent dissolution. Therefore, even if the rock dissolution plays the major role in explaining the obtained water chemistry, the chemical composition of the solution may be far different from the primary rock compositions. In addition, for examining water-rock interaction, the resistance of minerals to weathering must be taken into consideration. Consequently, in order to evaluate the water-rock interaction quantitatively, on the basis of the mineral weathering series, composition of the theoretical solution was calculated, and was compared with the real sample compositions.

Firstly, the CIPW normative mineral composition was calculated (after Kelsey, 1965; Best, 1982) based on the mean chemical composition of the basement rocks of Mt. Norikura (Ishikawa et al., 1992). A norm is a means of converting the chemical composition of an igneous rock to an ideal mineral composition (Cross, et al., 1902). Among the various norm calculations, most popular one is the CIPW norm, which is named for the four petrologists, Cross, Iddings, Pirsson and Washington. The CIPW norm calculates mineral composition as if the magma were anhydrous (water is simply treated as a separate phase). The details of the CIPW norm calculation is found in the literatures (eg. Kelsey, 1965).

During the water-rock interaction process, primary minerals with high susceptibility to weathering, such as Ca-plagioclase or pyroxene, form secondary stable minerals, such as gibbsite or kaolinite. In the case of the formation of gibbsite as a secondary mineral, the cations and silica ratio are preserved in the generated solution:

Albite → Gibbsite

$$2NaAlSi_3O_8 + 13H_2O + 2CO_2 \rightarrow 2\underline{Na^+} + 2HCO_3^- + 6H_4\underline{Si}O_4 + Al_2O_3\downarrow$$

In the above example, 2 moles of albite give 2 moles of sodium ion and 6 moles of silica solution. On the other hand, in the dissolution process of volcanic minerals to form kaolinite or its adjacent mineral of halloysite as secondary minerals, part of silicon is consumed to form kaolinite, whereas all cations dissolve into the solution as follows:

Na^+—Si : Albite → Kaolinite

$2NaAlSi_3O_8 + 11H_2O + 2CO_2 \rightarrow 2Na^+ + 2HCO_3^- + 4H_4\underline{Si}O_4 + Al_2\underline{Si_2}O_5(OH)_4\downarrow$

Ca^{2+}—Si : Anorthite → Kaolinite

$CaAl_2Si_2O_8 + 3H_2O + 2CO_2 \rightarrow Ca^{2+} + 2HCO_3^- + Al_2\underline{Si_2}O_5(OH)_4\downarrow$

As the equations describe above, in the (Na^+ - Si) reaction system, 2 moles of sodium ion and 4 moles of silicic ion dissolve from 2 moles of albite, and then, 2 moles of silicic ion gets adsorbed into solid phase as kaolinite. In the (Ca^{2+} - Si) reaction system, 1 mole of calcium ion dissolves from 1 mole of anorthite, and then, all silicic ions from anorthite get absorbed into kaolinite. As a result, the (Σcation/Si) ratio rises in comparison with the original minerals.

In the arithmetic procedure, the elution of pyroxene was considered in addition to the above mentioned dissolution reaction of the feldspar. The chemical concentration ratio of the solution was calculated from average CIPW normative mineral composition of the rocks around the observation area. The calculation was performed by the following procedure.

1. Calculate the CIPW normative minerals from the chemical composition of the host rocks.
2. K-feldspar, plagioclase, diopside and hypersthene are allotted for the primary solution.
3. An amount of aluminum in the primary solution is allotted for precipitation of gibbsite, kaolinite and pyrophyllite.
4. The residual cations are allotted to form the theoretical solution.
5. The composition of the theoretical solution is given by the ratio form of cations / silicon.
6. Comparison of real solution with theoretical solution.

3.3. Cation and silicon behavior

3.3.1. Ratio of major cations and silicon

The first major factor (nF1) on the non-geothermal water is highly correlated with all cations and silicon (Table 2-10). The major source of silicon in natural water is, in general, silicate rocks or soils, and the observation area is covered by andesitic rocks; this factor is assumed to be concerned with host rock dissolution. In order to understand the cation-silica processes in detail, the cation behavior was considered in terms of Σcation/silicon ratio. The samples show a wide range in the ratio of Σcations/silicon (Fig. 3-1). The meteoric waters, which are least influenced by host rock components, show high value of Σcations/silicon, with high fluctuations (Range:1-50, geometric mean: 2.46). The high ratio and wide range of the summit waters are mainly due to their quite low silicon concentrations, which may be caused by little supply of silicon from silicate rocks.

On the contrary, despite the similar EC value with the meteoric water, the water samples of the summit area (Group A and B), which show the similar electrical conductivity (EC) with the meteoric water, take the least values with narrow range of variation (Range:0.3-2, geometric mean: 0.62), which is close to the ratio of host rocks around the observation area (0.4). The low ratio is mainly due to the relatively higher concentration of silicon than other cations. Since the ratio of Σcations/silica of this water group is similar to the host rocks around the area, this phenomenon may represent the rapid progress of the simple rock dissolution.

However, the surface waters gradually increase the ratio with an increase in the Σcations, up to nearly five times higher than that of the host rocks (~2). The 5 times higher ratio of the mountainside waters than the host rocks is not interpreted by a simple congruent dissolution of the silicate rocks; the description of the silicon removal mechanism from the solution is required to understand this high ratio. On the basis of the chemical proportion resulting from the weathering of silicate minerals, the chemical processes are examined in the following sections.

3.3.2. Theoretical solution

Average composition of the major elements and CIPW normative minerals of the rocks from the Norikura area is shown in Table 3-1, and the chemical ratio of the theoretical solution obtained by CIPW normative mineral composition is shown in Table 3-2. The relation on each sample group between cation/silicon ratios and Σ cation is shown in Figs. 3-2 (a)-(d).

The meteoric water shows higher Σ cation/Si value than that of the theoretical

solution, which forms gibbsite or kaolinite. The samples from the summit area, i.e. group A and B, take values almost as low as that of the theoretical solution of gibbsite field. The cation ratio of the waters in the mountainside area (group C-E), increases with a decrease in altitude, and the Na/Si and K/Si value are close to the theoretical solution of kaolinite or its adjacent minerals.

The Mg/Si and Ca/Si show the similar trend with Na/Si and K/Si, though exceptions were found in some cases. The mountainside waters show relatively low value of Mg/Si, lower than that of theoretical solution of the kaolinite coexistent field. Unlike other major cations, magnesium is not preserved in feldspar, but is mainly found in pyroxene, which is comparatively strong against weathering (Nesbitt and Wilson, 1992). Due to the relatively higher weathering resistance of the source mineral of Mg, the increase rate of the Mg/Si ratio may be lower than others.

The Ca/Si ratios of the sample groups D and C exceed that of the kaolinite coexistent solution, and even group H, which are contaminated with geothermal water, exceeds the pyrophyllite value (Fig. 3-2(d)). This high ratio of Ca/Si is mainly interpreted as the dissolution of calcite. The dissolution rate of calcite is approximately 7 orders of magnitude faster than that of plagioclase at near neutral pH (White et al. 1999), and calcium would be added into the solution from calcite, which is a minor mineral in the mountainside area.

Thus the surface water in the summit area is formed under the condition of gibbsite generation as a secondary mineral, whereas the waters of mountainside region are formed under the coexisting condition of kaolinite or its adjacent minerals (eg. halloicite). In this manner, the stoichiometric calculation indicated that the major cations and silicon behavior in this area is mainly controlled by the incongruent dissolution of silicate rocks. Thus the nF1, which has high loadings for major cations and silicon, is interpreted as the "incongruent" dissolution of the host rocks.

3.3.3. M^+ (cation) - Si stability diagram

In order to confirm the thermodynamic stability of such secondary minerals coexistent with specific waters, stability diagrams of cation-Si plot were drawn (Figs. 6 (a)-(d)). The diagrams show that the chemical behavior of water samples in this area is similar to the shallow spring waters (Garrels and Mackenzie, 1967), as which the water dissolves plagioclase to form kaolinite (Garrels, 1967).

Since the meteoric waters contain only little silica and cations, the sample groups are situated far left-down in the diagram, where gibbsite [r-$Al(OH)_3$] is the stable mineral. The lake and spring waters in the summit area (group A and B) are

plotted also in the same area. On the other hand, the sample groups C, D and E, which are the samples of the mountainside region, are plotted within the kaolinite field. Geothermal waters are coexistent with pyrophyllite or smectites. Thus, the summit waters, which are similar in composition to the host rocks, are stably coexistent with gibbsite; the mountainside waters, which takes higher cation/Si ratio than that of the host rocks are coexistent with kaolinite. The diagram shows that the mineral phases, which were suggested by the stoichiometric calculations above, are stably coexistent with waters in the thermodynamic point of view. In this way, the incongruent dissolution system, which controls the cation/Si ratio, was interpreted by thermodynamic stability as well as by stoichiometry.

3.3.4. Chemical composition of the final equilibrium solution

When a rock - water interaction reaches the final chemical equilibrium state under certain temperature and pressure, the secondary mineral composition and the chemical composition of the solution should be uniquely determined. If the rock-water interaction is the major factor to determine the water chemistry, the chemical composition of the final equilibrium solution (final product) gives significant information to survey the direction of the water formation process.

The final mineral product of weathered andesite under the normal temperature and pressure is characterized as albite, K-feldspar, 14-A clinochlore, Laumontite and pyrophyllite. The major chemical solute Na^+ is included into albite, K^+ is into K-feldspar, Ca^{2+} is into laumontite and 14-A clinochlore for Mg^{2+}. For aluminum, K-feldspar play a role as buffer to absorb the residual Al^{3+} (Coombs, 1959, Giggenbach, 1988). Thermodynamically, the most stable silica mineral is quartz, but many ground waters with long retention time show that the silica concentration is often supersaturated by quartz, and the silica concentration of the final solution should be discussed on the amorphous silica as the silica solid phase.

Thus under the assumption that the final minerals should take the following idealized chemical formula, the composition of the equilibrium solution was calculated using the set of thermodynamic data under 25 C and 1 atm (Helgeson, 1978, Berner, 1971, see Appendix A).

albite	$NaAlSi_3O_8$
K-feldspar	$NaAlSi_3O_8$
pyrophyllite	$Al_2Si_4O_{10}(OH)_2$
clinochlore-14A	$Mg_5Al(AlSi_3O_{19})(OH)_8$

laumontite $CaAl_2Si_4O_{12}\ 4H_2O$

amorphous silica SiO_2

The following chemical relations are given by the equilibrium calculations and ion balance.

$\log(a_{Na+}/a_{H+}) = 5.26$

$\log(a_{K+}/a_{H+}) = 2.22$

$\log(a_{Mg2+}/a^2_{H+}) = 12.82$

$\log(a_{Ca2+}/a^2_{H+}) = 13.23$

$\log(a_{H4SiO4}) = -2.54$

Here, the character "a" is the ion activity of the subscript chemical species.

The stability diagrams (Figs. 3-3(a)-(d)) shows that the meteoric water is plotted at the lower left and the surface waters forms zone to the upper right area toward the theoretical final product. Geothermal waters are plotted around the theoretical final productive solution. The water process seems to seek for the final solution. This calculation also suggests that the chemistry of those waters be mainly controlled by the water- rock interaction.

3.3.5. Estimation of Si by Cation concentrations

In this section, the other stoichiometric calculation was performed. As mentioned above, rock components do not dissolve uniformly during chemical weathering, but mineral, which is less resistant to weathering, dissolves more rapid than more resistant minerals (Goldich, 1938). Moreover, part of element such as aluminum forms secondary minerals (clay minerals), and is removed from the aqueous phase. Therefore, the chemical composition of bedrock in the catchment area does not exactly reflect the aqueous chemical composition. The stability diagram shows that the river water in the summit area is thermodynamically coexistent with gibbsite, and the secondary minerals produced by rock weathering are most likely gibbsite or its adjacent minerals.

Among the major minerals found in volcanic rocks in Norikura volcano, the possible source mineral for sodium is albite, for potassium is K-feldspar, for magnesium is enstatite and for calcium is anorthite. Therefore, the weathering equations of these minerals in the summit area are shown as follows.

Na^+—Si : Albite → Gibbsite

$$NaAlSi_3O_8 + 11/2\ H_2O + H^+ \rightarrow \underline{Na^+} + \underline{3}\ H_4\underline{Si}O_4 + 1/2\ Al_2O_3\downarrow \quad (3\text{-}1)$$

K^+—Si : K-feldspar → Gibbsite

$$KAlSi_3O_8 + 11/2\ H_2O + H^+ \rightarrow \underline{K^+} + \underline{3}\ H_4\underline{Si}O_4 + 1/2\ Al_2O_3\downarrow \quad (3\text{-}2)$$

Mg^{2+}—Si : Enstatite → Solution (No aluminum)

$$MgSiO_3 + H_2O + 2H^+ \rightarrow \underline{Mg^{2+}} + H_4\underline{Si}O_4 \quad (3\text{-}3)$$

Ca^{2+}—Si : Anorthite → Gibbsite

$$CaAl_2Si_2O_8 + 3\ H_2O + 2H^+ \rightarrow \underline{Ca^{2+}} + \underline{2}\ H_4\underline{Si}O_4 + Al_2O_3\downarrow \quad (3\text{-}4)$$

If the above chemical weathering controls the river water chemistry, 3 moles of silicon dissolve with 1 mol of sodium dissolution; 3 moles of silicon dissolve with 1 mol of potassium; 1 mol of silicon dissolve with 1 mol of magnesium; 2 moles of silicon dissolve with 1 mol of calcium. Thus, if the above chemical reactions (1) - (4) play a major role to control the river water chemistry, the following simple equation will be applicable.

$$[Si] = 3\ [Na^+] + 3\ [K^+] + [Mg^{2+}] + 2\ [Ca^{2+}] \quad (3\text{-}5)$$

Scatter plot of predicted [Si] (= 3 $[Na^+]$ + 3 $[K^+]$ + $[Mg^{2+}]$ + 2 $[Ca^{2+}]$) and measured [Si] is shown in Fig. 3-4(a). In this figure, surface waters of the summit area (i.e., A and B) are plotted on the predicted line. Meteoric water (O), which is least influenced by rock dissolution, is deficient in silicon and takes higher estimated [Si] value than the real [Si] value (above the predicted line). For the mountainside waters (i.e., C, D and E), or geothermal waters (H and I), the predicted [Si] is significantly higher than the real value. In the case of mountainside waters, silicon is saturated in gibbsite and coexistent with kaolinite (Figs. 3-3 (a)-(d)); the secondary mineral is most likely kaolinite and the weathering reaction would be expressed as the following equation.

Na^+—Si : Albite → Kaolinite

$$NaAlSi_3O_8 + 9/2\ H_2O + H^+ \rightarrow \underline{Na^+} + 2\ H_4\underline{Si}O_4 + 1/2\ Al_2Si_2O_5(OH)_4\downarrow \quad (3\text{-}6)$$

K^+—Si : K-feldspar → Kaolinite

$$KAlSi_3O_8 + 9/2\ H_2O + H^+ \rightarrow \underline{K^+} + 2\ H_4\underline{Si}O_4 + 1/2\ Al_2Si_2O_5(OH)_4\downarrow \quad (3\text{-}7)$$

Mg^{2+}—Si : Enstatite →Solution (same as gibbsite case)

$$MgSiO_3 + H_2O + 2H^+ \rightarrow \underline{Mg^{2+}} + H_4\underline{Si}O_4 \quad (3\text{-}8)$$

Ca^{2+}—Si : Anorthite → Kaolinite

$$CaAl_2Si_2O_8 + H_2O + 2H^+ \rightarrow \underline{Ca^{2+}} + Al_2Si_2O_5(OH)_4\downarrow \quad (3\text{-}9)$$

In this case, 2 moles of silicon dissolve with 1 mol of sodium dissolution; 2 moles of silicon dissolve with 1 mol of potassium; 1 mol of silicon dissolve with 1 mol of magnesium. On the other hand, in the dissolution of potassium and calcium, no silicon dissolves, since all silicon is consumed to form kaolinite. Thus, if the above chemical reactions (6) - (9) play a major role to control the river water chemistry, the following simple equation will be applicable.

$$[Si] = 2\ [Na^+] + 2\ [K^+] + [Mg^{2+}] \quad (3\text{-}10)$$

In this case, the predicted silicon concentrations of the mountainside waters (D and E) are good coincidence with the real value (Fig. 3-4(b)). Only group C is deficient in cations and slightly lower than the predicted line. As shown in the stability diagrams (Figs. 3-3 (a)-(d)), the waters of group C are scattered near the boundary line between gibbsite and kaolinite. In this water group, gibbsite may be contained as a minor secondary mineral as well as kaolinite. The predicted silicon value of the water sample C fits well with the real value under the assumption that 85 % form kaolinite as secondary mineral and 15 % form gibbsite. In the same manner, the other samples were calculated using the following equation.

$$\text{Gibbsite : Kaolinite} = X: (1 - X) \quad (3\text{-}11)$$

$$\text{Real } [Si] = X\ (3\ [Na^+] + 3\ [K^+] + [Mg^{2+}] + 2\ [Ca^{2+}]) + (1 - X)\ (2\ [Na^+] + 2\ [K^+] + [Mg^{2+}]) \quad (3\text{-}12)$$

$$\therefore X = \frac{\text{Real}[Si] - (2[Na^+] + 2[K^+] + [Mg^{2+}])}{(3[Na^+] + 3[K^+] + [Mg^{2+}] + 2[Ca^{2+}]) - (2[Na^+] + 2[K^+] + [Mg^{2+}])} \quad (3\text{-}13)$$

$$\left(X = \frac{[Si] - 2[Na^+] - 2[K^+] - [Mg^{2+}])}{[Na^+] + [K^+] + 2[Ca^{2+}]} \right) \quad (3\text{-}14)$$

The result is shown in Fig. 3-5, which is well fitted to the chemical feature given by the stability diagram (Figs. 3-3 (a)-(d)); for group A, secondary mineral is gibbsite or its adjacent minerals (80-151 %); for C, kaolinite is the major secondary mineral (85%) and gibbsite is minor (15%); for D and E secondary mineral is kaolinite (98 - 100%). Here, kaolinite contribution to Group B gave negative value; consequently, the gibbsite ratio was over 100% (151%). As mentioned in Chapter 2, the chemical concentrations of the group A and B are significantly low, and the accuracy of the analytical value is somewhat ambiguous. At least it is clear that gibbsite is more likely coexistent with those samples (group A and B) than kaolinite.

In this manner, the water chemistry of major component was quantitatively explained by chemical weathering of basement rocks using thermodynamics and stoichiometry.

3.4. Relation between (Na^+, K^+) and (Ca^{2+}, Mg^{2+})

The second factor (nF2) has positive loadings for Na^+, K^+ and Si, and negative loadings for Ca^{2+} and Mg^{2+} (Table 2-10). This factor structure shows that there are subliminal factor to induce the negative correlation between M^+ and M^{2+} type of cations. In order to interpret this factor, the cation ratios of monovalent and bivalent ions (M^+/M^{2+}) have been observed to overview the major solutes behavior.

The concentration ratio of alkali earth elements and alkali elements of each sample group is shown by $Na^+/(Ca^{2+}+Na^+)$ in Fig. 2- 5. The general trend of the Na-Ca ratio is firstly Na-type in the summit area, and according to the progress of hydrochemical reactions, the water type is changing into Ca-type in the mountainside region, whereas the geothermal water in the mountainside region shows Na-type again.

The $Na^+/(Ca^{2+}+Na^+)$ is >0.6 for the summit samples, and the value decreases with a decrease in altitude. The ratio of $Na^+/(Ca^{2+}+Na^+)$ in the mountainside samples group E is down to 0.2, which is smaller than the average ratio of the rocks around the

observed area, 0.45. This value of 0.2 is almost equal to the experimental value obtained by the powdered andesite elution (Tamari et al., 1988).

When water-rock interaction progresses, Ca^{2+} is absorbed into the ion exchangeable clay minerals, such as smectites, and Na^{+} is emitted into solution (eg. Garrels and Christ, 1965), as the following equation:

$$Ca^{2+} + 2\ [\text{Na-smectite}] = [\text{Ca-smectite}] + 2Na^{+} \qquad (3\text{-}15)$$

The above reaction reaches chemical equilibrium rapidly, compared with most of the other silicate hydrolysis reactions (Chou and Wollast, 1989). The decrease in dissolved Ca^{2+} is associated with equivalent increase in Na^{+} concentrations with progress of water-rock interaction (eg. Iwatsuki et al., 1995).

However, in the present result, progressing of water-rock interaction causes rapid increase in $[Ca^{2+}]$ under the control of $[Na^{+}]$ behavior. Consequently, the $Na^{+}/(Ca^{2+}+Na^{+})$ decrease with the progress of water-rock interaction. As shown in the M^{+}-silica section, the non-geothermal waters in this area show little interaction with rocks and do not reach chemical equilibrium with smectite (Figs. 3-3 (a)-(d)). Thus, the variation of cation ratio is not interpreted by the ion exchange on smectite.

The scatter plot of (a_{Ca2+}/a^{2}_{H+}) - (a_{Na+}/a_{H+}) shows that the most samples except meteoric water and geothermal water are on the straight line (Fig. 3-6(a)), which is expressed by the following equation (5).

$$\log (a_{Ca2+}/a^{2}_{H+}) = 2 \times \log (a_{Na+}/a_{H+}) + 4.5 \qquad (3\text{-}16)$$

Here, if the increase of Ca^{2+} and Na^{+} could be explained by the simple dissolution of plagioclase, the inclination should be 1 regardless of the dissolution rate. However, the actual inclination shows approximately 2, which suggests ion-exchange equilibrium. The cation variation of non-geothermal waters (group A-E) fits in well with the above equation, with a high correlation coefficient of $r = 0.98$.

This correlation would be interpreted that Ca^{2+} and Na^{+} in the surface waters are in the transitional equilibrium on an unknown ion-exchangeable phase (mineral).

$$2Na^{+} + \text{Ca-X} \rightarrow Ca^{2+} + 2\text{Na-X} \qquad (3\text{-}17)$$

Here, X is the ion-exchangeable mineral produced during the chemical processes. This

transitional chemical equilibrium equation introduces the following formula to give the a_{Ca2+}/a^2_{Na+}.

$$K = \frac{a_{Ca^{2+}}}{a^2_{Na^+}} = \frac{(a_{Ca^{2+}} / a^2_{H^+})}{(a_{Na^+} / a_{H^+})^2} \qquad (3\text{-}18)$$

The log transformation gives the following equations.

$$\log (a_{Ca2+}/a^2_{H+}) = 2\times\log (a_{Na+}/a_{H+}) + \log K \qquad (3\text{-}19)$$

$$\log (a_{Ca2+}/a^2_{Na+}) = \log K \qquad (3\text{-}20)$$

The common-logarithmic value of K (log K) is set to 4.5 by least-squares method (Fig.8(a)). On the other hand, the logarithmic value of the equilibrium constant on the Na-Ca smectite phases is -1.25 (log K = -1.25), which is far smaller than the above constant value. Therefore, the high correlation between (a_{Ca2+}/a^2_{H+}) and (a_{Na+}/a_{H+}) seems to be controlled by an ion-exchangeable solid phase, but other than smectites. The same relations were found between (Na^+, Mg^{2+}), (K^+, Ca^{2+}) and (K^+, Mg^{2+}) in Figs. 3-6(b)(c)(d).

The F2 is, thus interpreted as the ion-exchange reaction between (Na^+, K^+) and (Mg^{2+}, Ca^{2+}), though what mineral controls this relation is remained for further study.

3.5. Summary

The factor analysis (FA) and thermodynamic calculations revealed that the water chemistry is mainly controlled by water-rock interaction. The chemical process of the non-geothermal surface waters in the observed area may be summarized in the following formula.

(1) Rock + $H^+ \rightarrow M^+$ + H-Clay (gibbsite/kaolinite or adjacent minerals) + H_4SiO_4
(2) 2(Na^+, K^+) + (Ca^{2+}, Mg^{2+})-$Clay_2$ = (Ca^{2+}, Mg^{2+}) + 2(Na^+, K^+)-Clay

The chemical process expressed in the (1) reaction contributes 65% for forming water chemical composition, whereas the reaction of (2) contributes 16%. In this manner, the

behavior of the major cations and silica in the non-geothermal water was interpreted by the comparatively simple water-rock interaction.

Those theoretical models introduced the following equations, and the well fitted chemical compositions of real waters were certified the validity of the model.

Summit area; gibbsite dominant as a secondary mineral

$$[Si] = 3\,[Na^{+}] + 3\,[K^{+}] + [Mg^{2+}] + 2\,[Ca^{2+}]$$

Mountainside area; kaolinite dominant as a secondary mineral

$$[Si] = 2\,[Na^{+}] + 2\,[K^{+}] + [Mg^{2+}]$$

Fig. 3-1

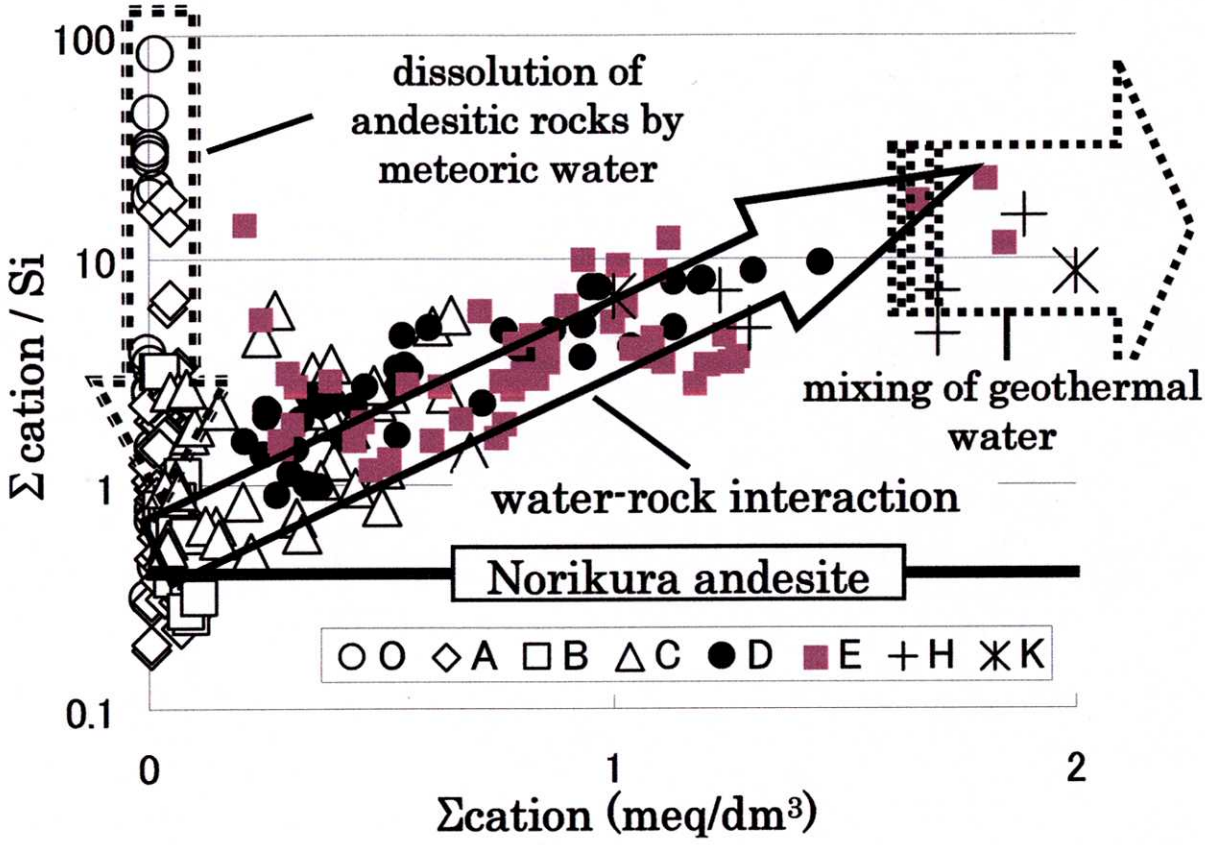

Fig. 3-1 Scatter plot of (total cations / silicon) ratio against total cations (meq/dm^3). The solid line is the average ratio of the volcanic rocks obtained from Norikura volcano. Symbols are the same as in Table 2-3.

Fig. 3-2(a)

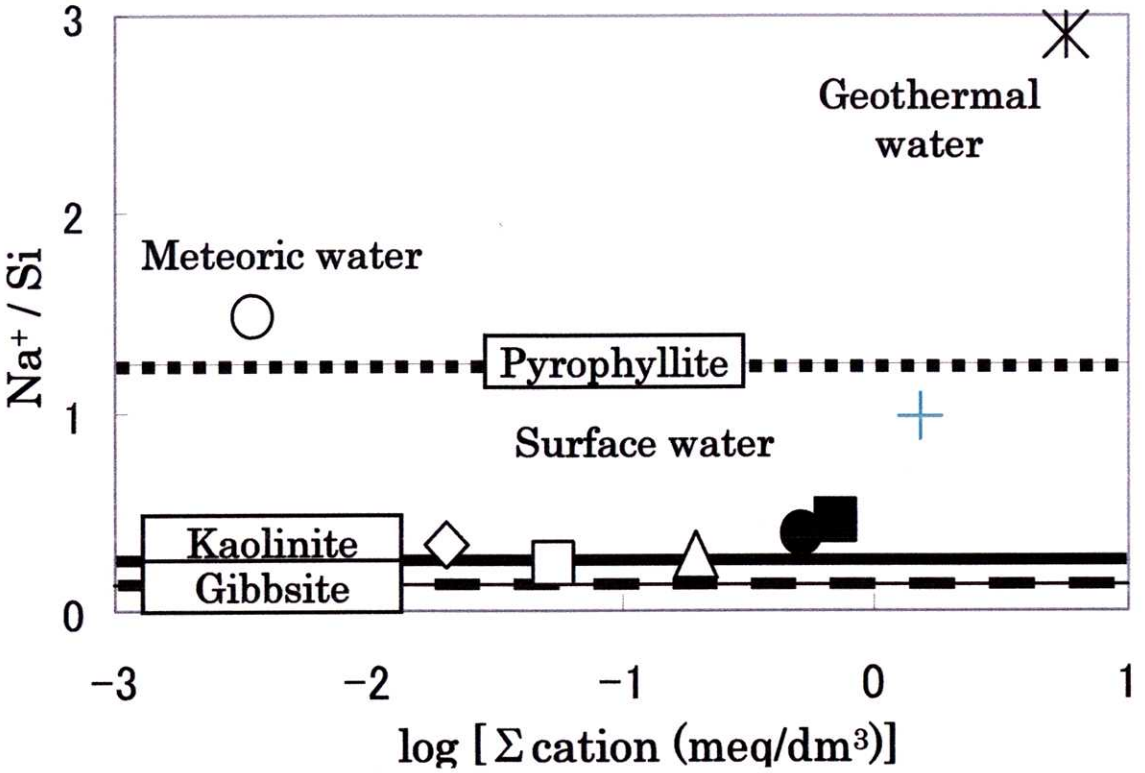

Fig. 3-2(b)

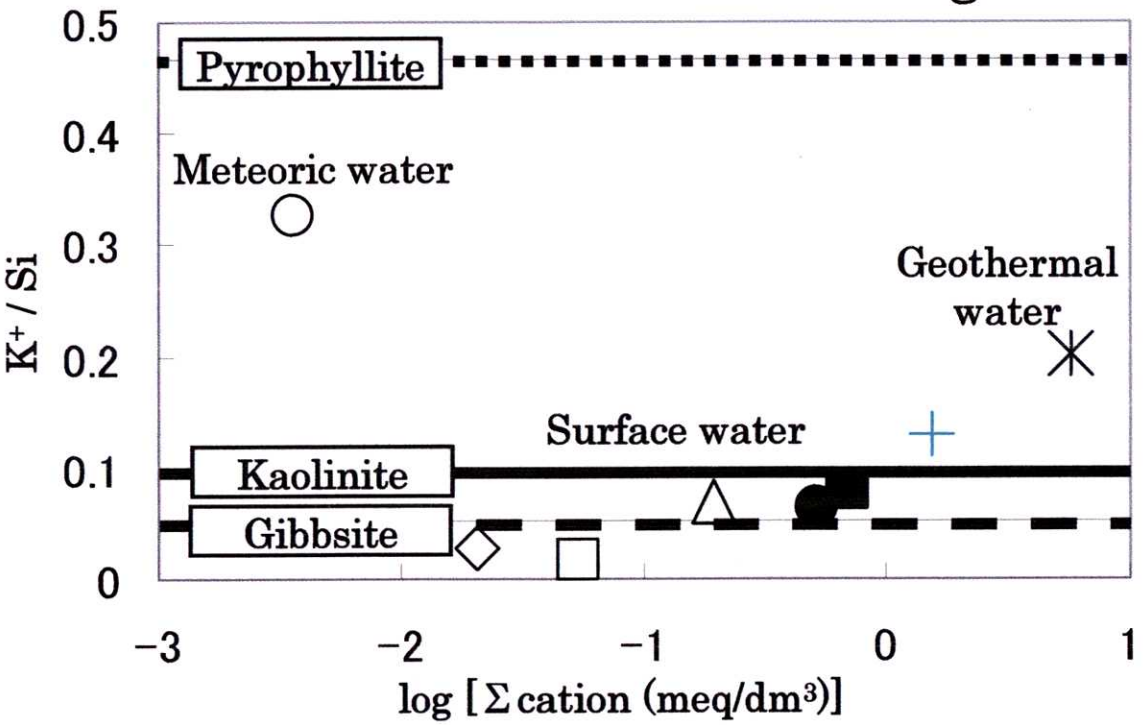

Fig. 3-2 Scatter plot of cation/silicon ratio against total cations. The dashed line is the theoretical value obtained by gibbsite coexistent solution, and solid line is obtained by kaolinite, and dotted line is obtained by pyrophyllite. (a) Na^+—Si system, (b) K^+—Si system, (c) Mg^{2+}—Si system and (d) Ca^{2+}—Si system. Symbols are the same as in Table 2-3.

Fig. 3-2(c)

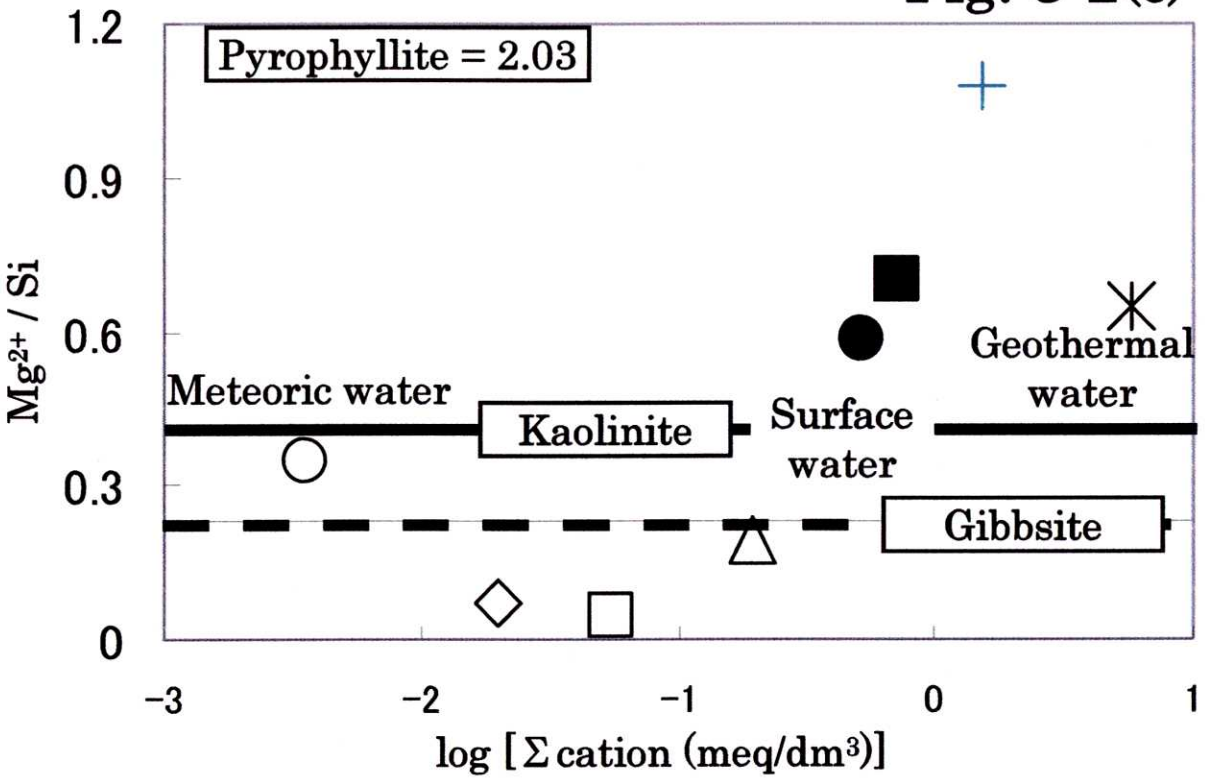

Fig. 3-2(d)

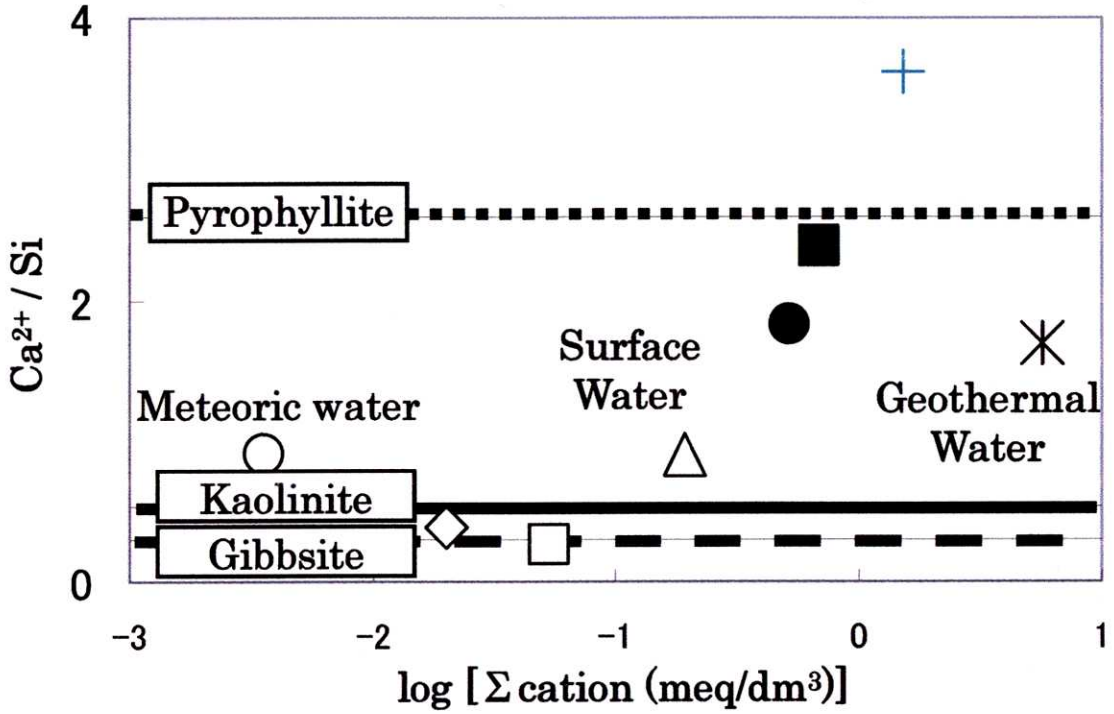

Fig. 3-3(a)

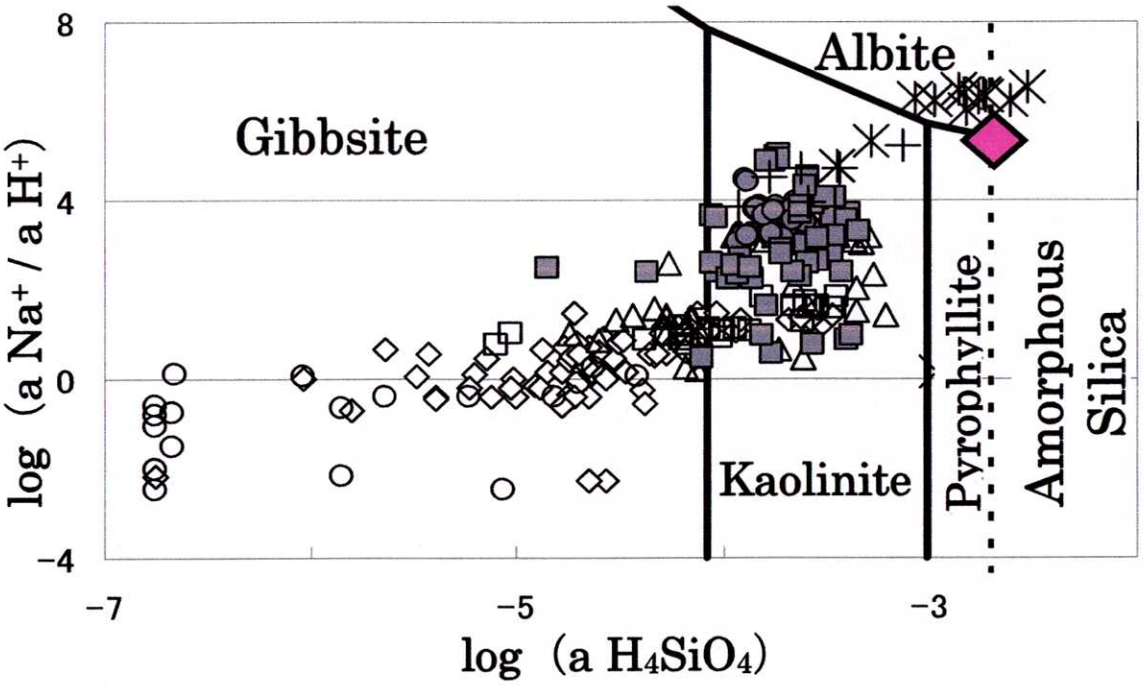

Fig. 3-3(b)

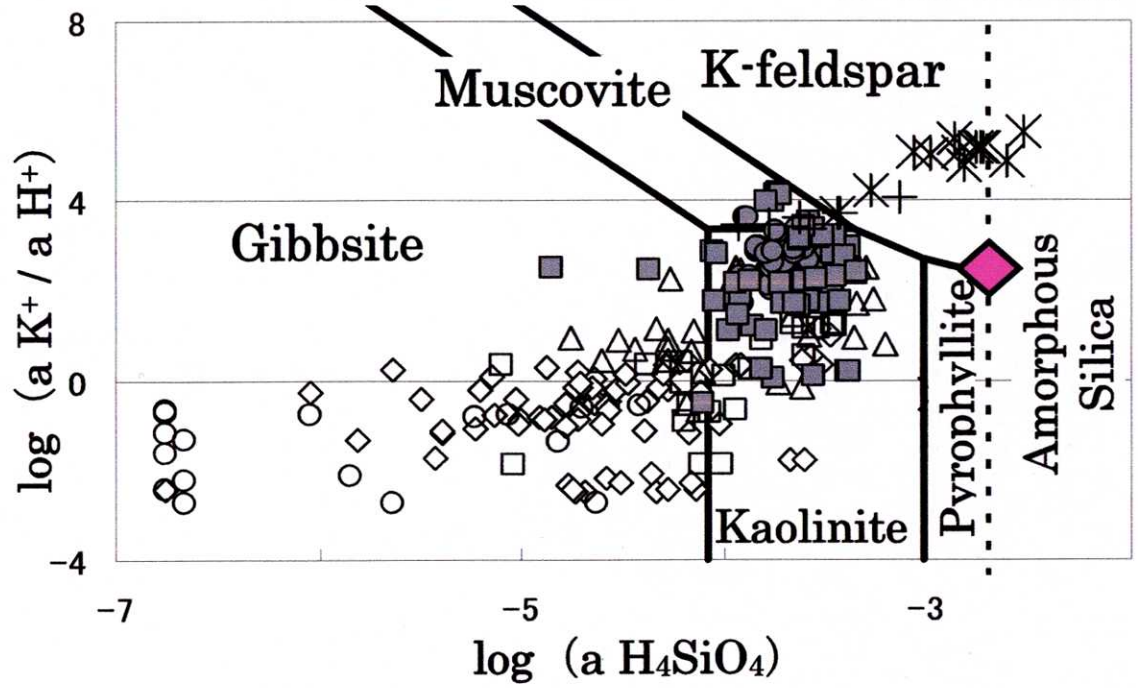

Fig. 3-3 Stability diagrams at 25 ℃. (a) Na^+—Si system, (b) K^+—Si system. Symbols are the same as in Table 2-3. ◆ is the theoretical final solution (product).

Fig. 3-3(c)

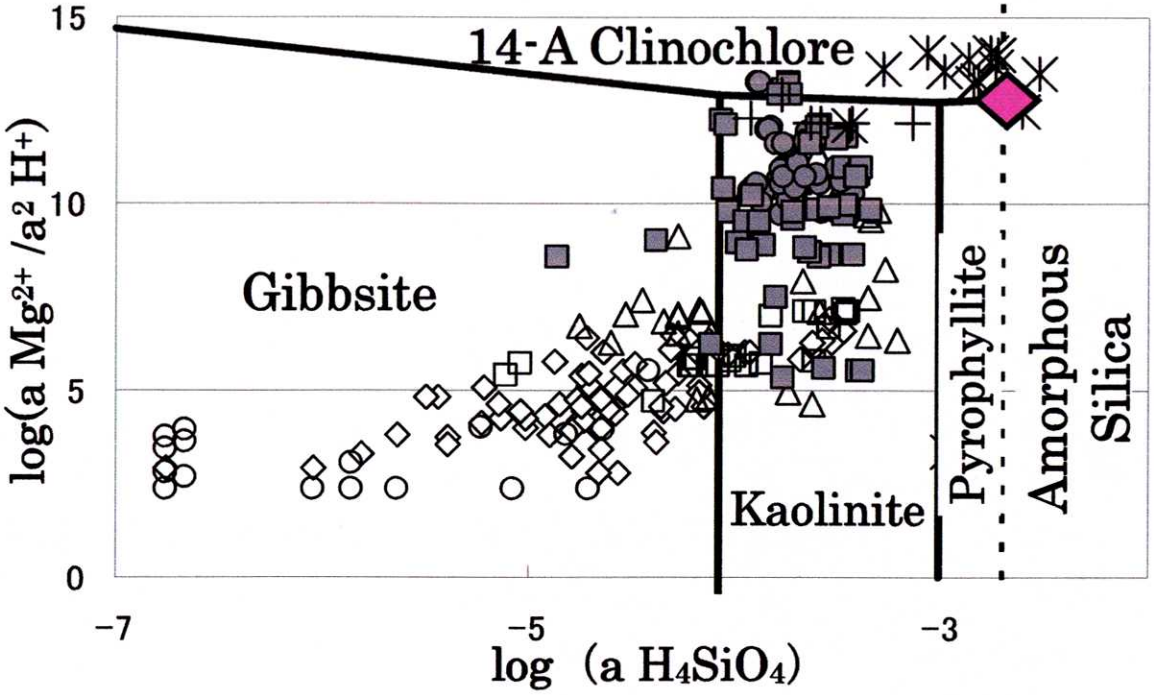

Fig. 3-3(d)

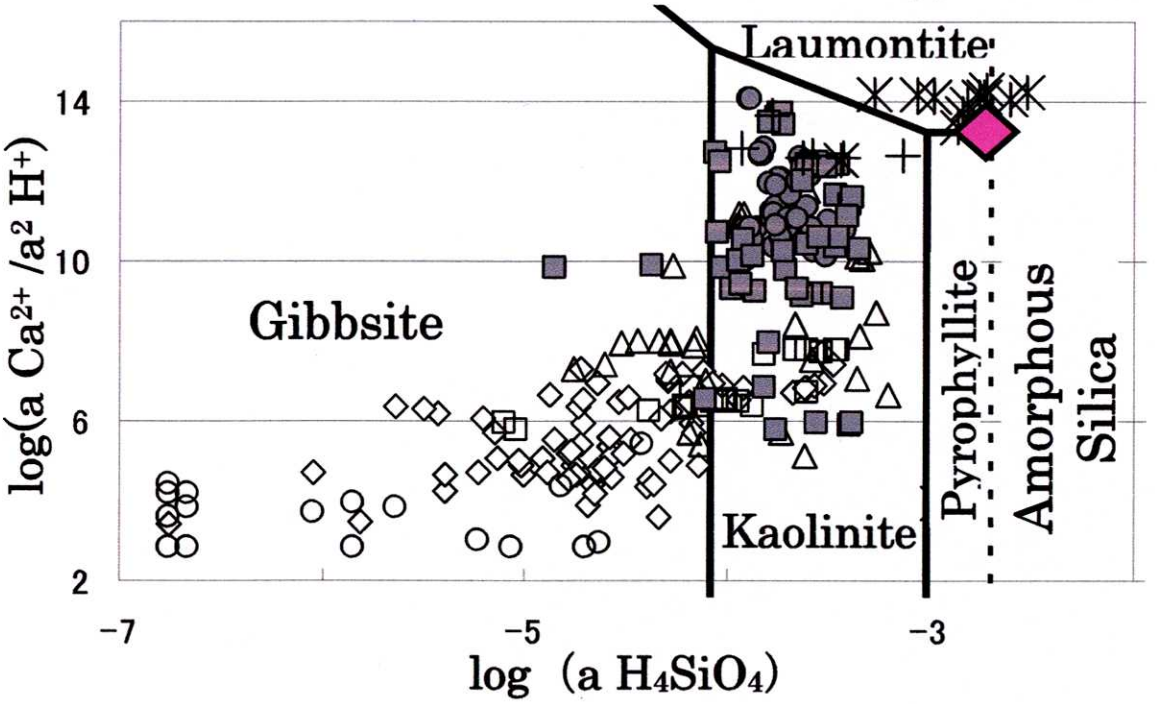

Fig. 3-3 Stability diagrams at 25℃. (c) Mg^{2+}—Si system and (d) Ca^{2+}—Si system. Symbols are the same as in Table 2-3. ◆ is the theoretical final solution (product).

Fig. 3-4

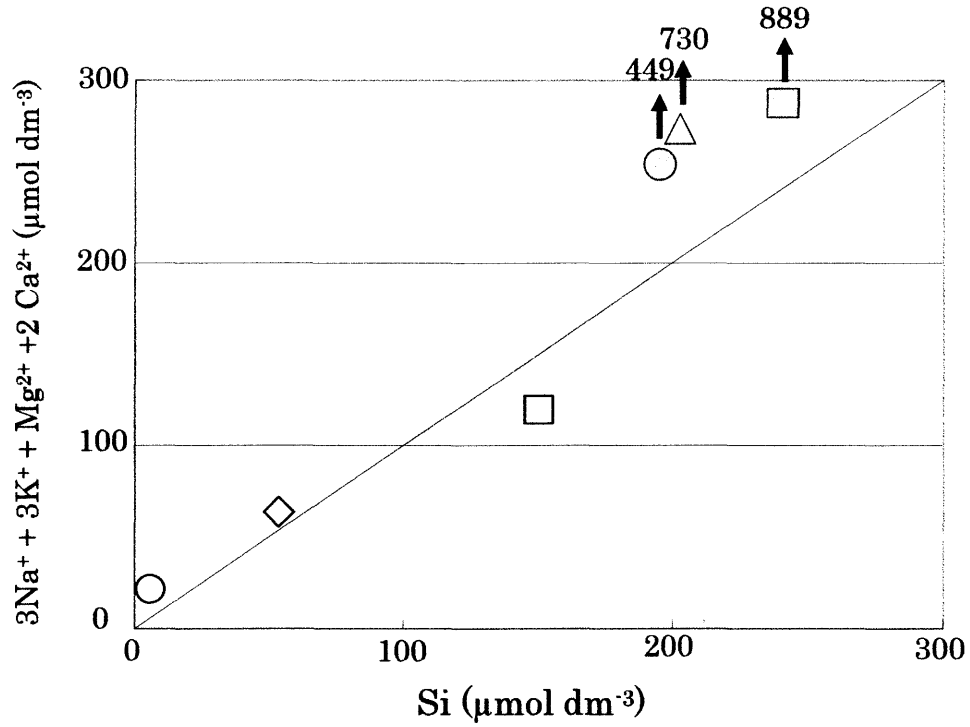

Fig. 3-4(a) Measured and estimated Si concentration (gibbsite as the secondary mineral). Estimated [Si] is given by (3 [Na^+] + 3 [K^+] + [Mg^{2+}] + 2 [Ca^{2+}]). Symbols are the same as in Table 2-3.

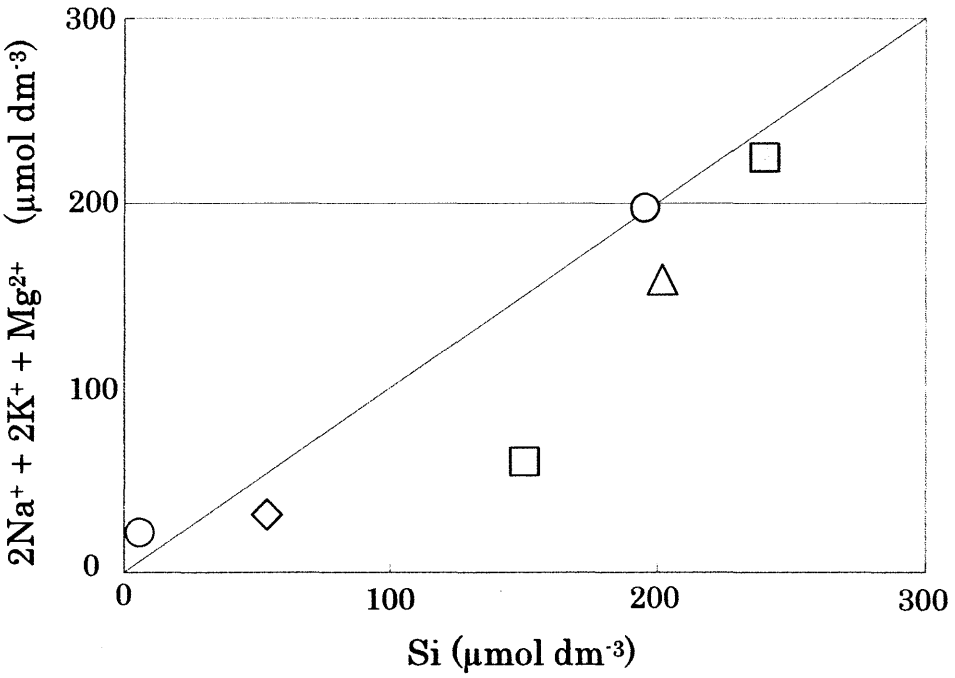

Fig. 3-4(b) Measured and estimated Si concentration (kaolinite as the secondary mineral). Estimated [Si] is given by (2 [Na^+] + 2 [K^+] + [Mg^{2+}]). Symbols are the same as in Table 2-3.

Fig. 3-5

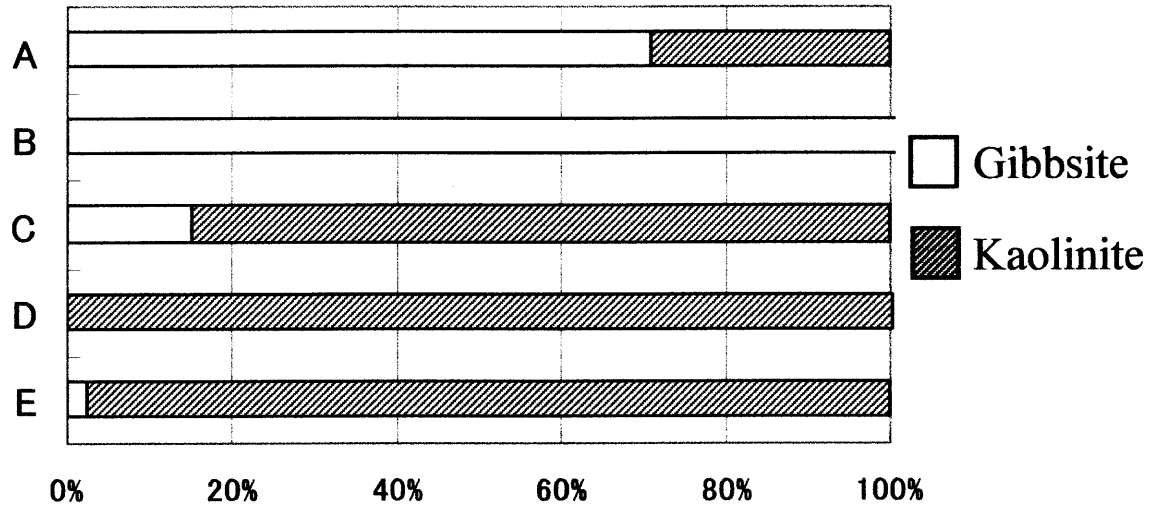

Fig. 3-5. Estimated ratio of coexistent secondary mineral on water groups. The estimation was performed using chemical weathering equation. The kaolinite contribution of Group B gave negative value; consequently, the gibbsite ratio was over 100% (151%).

Fig. 3-6(a)

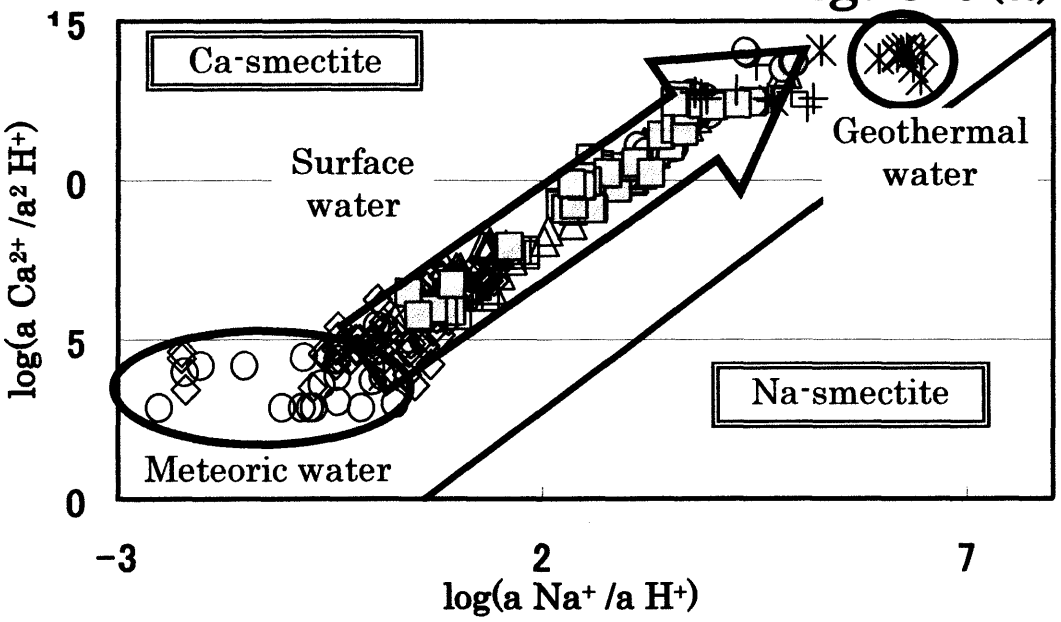

Fig. 3-6(b)

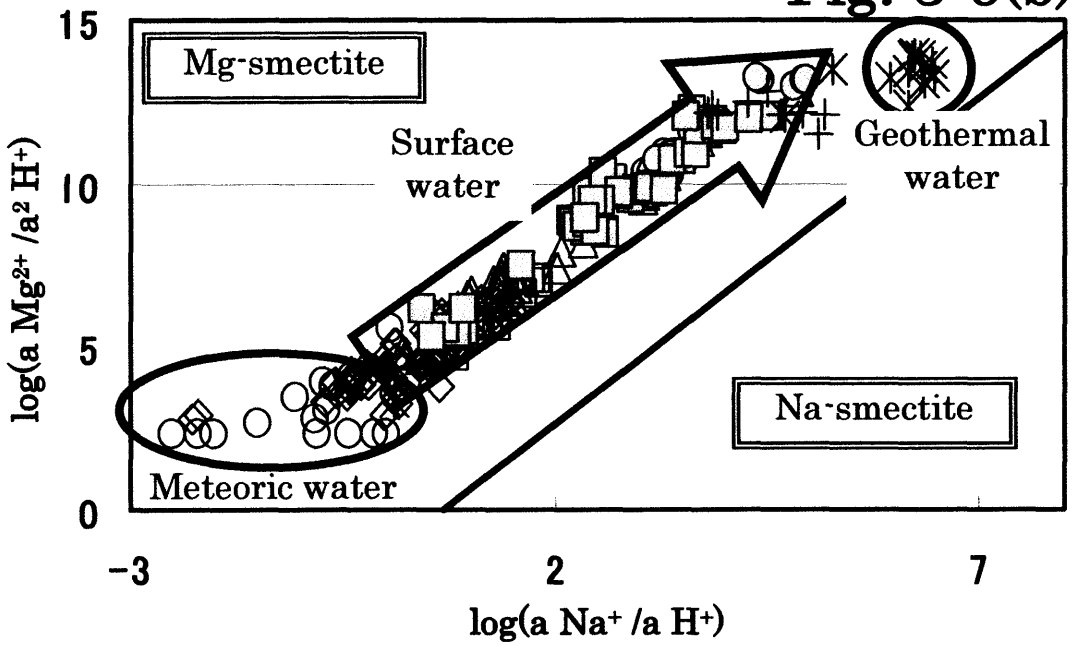

Fig. 3-6 Stability diagrams at 25℃. (a) Na^+-Ca^{2+} system, (b) Na^+-Mg^{2+} system. The line is the boundary between smectites. The arrow shows the direction of the water-rock interaction rate. The regression equation for the surface waters is

(a) $\log (a_{Ca2+}/a^2_{H+}) = 2.0 \times \log (a_{Na+}/a_{H+}) + 4.5$ (r=0.98 n=222).

(b) $\log (a_{Mg2+}/a^2_{H+}) = 2.0 \times \log (a_{Na+}/a_{H+}) + 3.8$ (r=0.92 n=222).

Symbols are the same as in Table 2-3.

Fig. 3-6(c)

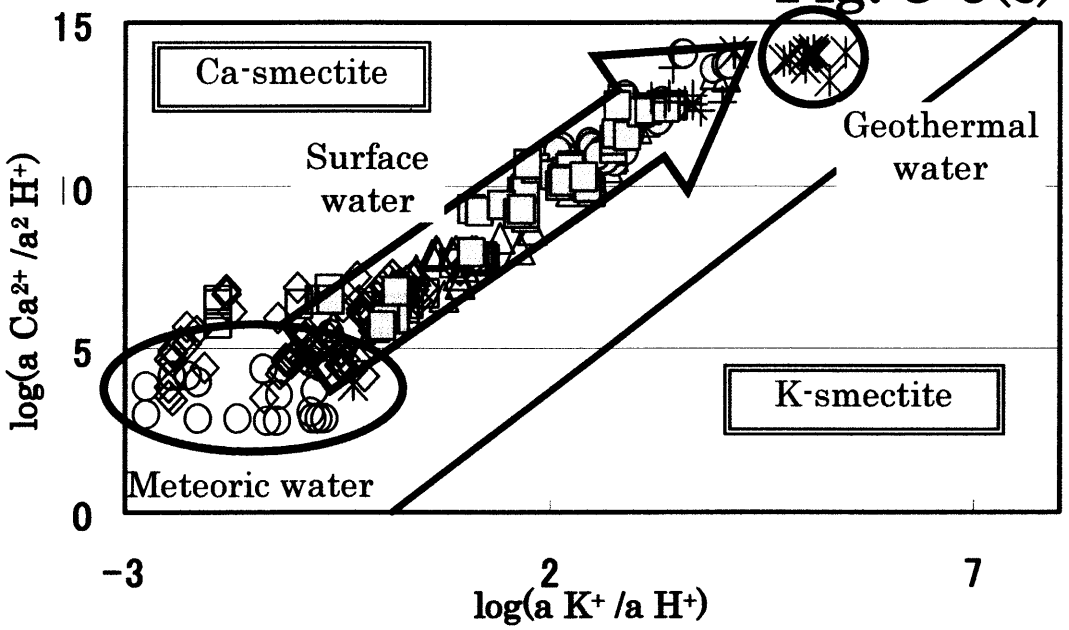

Fig. 3-6(d)

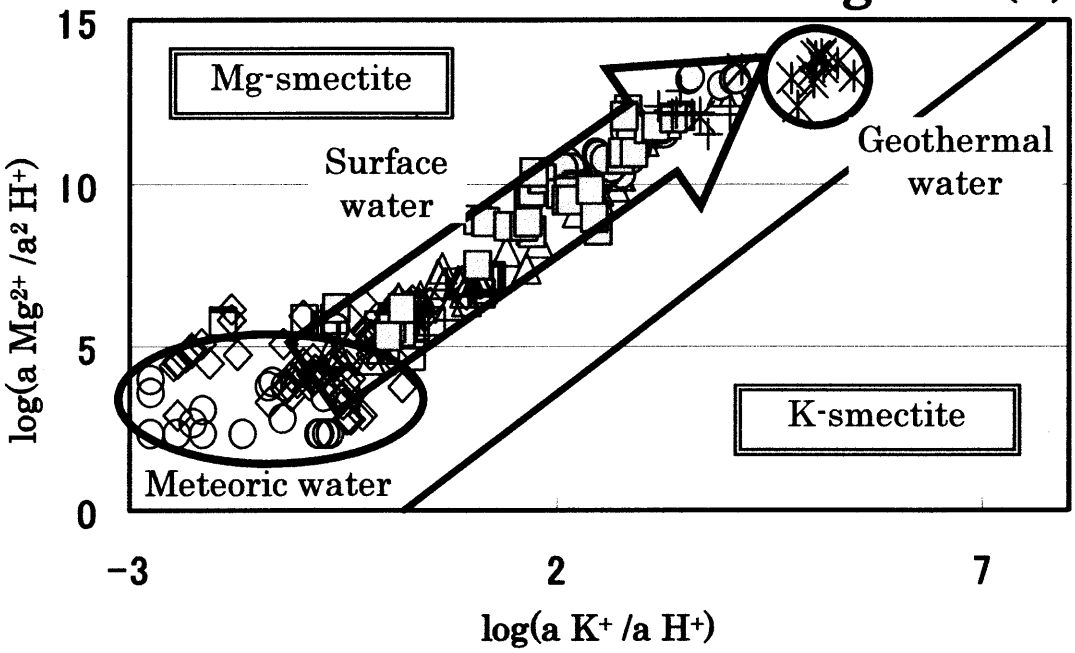

Fig. 3-6 Stability diagrams at 25 ℃. (c) K^+-Ca^{2+} system and (d) K^+-Mg^{2+} system. The line is the boundary between smectites. The arrow shows the direction of the water-rock interaction rate. The regression equation for the surface waters is

(c) $\log (a_{Ca2+}/a^2_{H+}) = 2.0 \times \log (a_{K+}/a_{H+}) + 6.0$ (r=0.92 n=222).

(d) $\log (a_{Mg2+}/a^2_{H+}) = 2.0 \times \log (a_{K+}/a_{H+}) + 5.5$ (r=0.89 n=222).

Symbols are the same as in Table 2-3.

Table 3-1. Average composition of major elements and normative minerals of the rocks in Norikura area (n=30). The analytical data set is after Nakano et al., 1987.

chemical compositions(wt.%)		norms (wt.%)	
SiO_2	56.99	Ilmenite	2.02
TiO_2	1.06	Apatite	0.66
Al_2O_3	17.37	Orthoclase	11.35
Fe_2O_3	3.22	Albite	28.31
FeO	4.30	Anorthite	26.08
MnO	0.14	Magnetite	4.41
MgO	3.56	Diopside	3.76
CaO	6.56	Quartz	10.82
Na_2O	3.35	Hypersthene	10.95
K_2O	1.92	Others	1.63
H_2O+	0.89		
H_2O-	0.36		
P_2O_5	0.28		

Table 3-2 Mole ratio (major cation / silica) of the theoretical solutions: 1) mole ratio of rock compositions. 2) theoretical solution formed by deducting the normative quartz from the rock composition(precipitation of gibbsite). 3) theoretical solution formed by deducting the normative quartz and kaolinite from the rock composition. 4) theoretical solution formed by deducting the normative quartz and pyrophyllite from the rock composition.

	1)	2)	3)	4)
	rock	rock-Q	rock-Q-KLN	rock-Q-PrL
Na/Si	0.11	0.14	0.25	1.24
K/Si	0.04	0.05	0.10	0.47
Mg/Si	0.09	0.12	0.21	1.01
Ca/Si	0.12	0.15	0.26	1.30

Table 3-3. Real and predicted silicon concentration in water samples; concentrations in μmol dm^{-3}.

		Predicted silicon concentration			
Sample	Si (real)	Gibbsite [1)]	Kaolinite [2)]	Kaolinite [3)]	Pyrophyllite [4)]
O	6.27	21.58	12.79	10.71	-0.16
A	54.12	63.39	31.71	28.20	-6.98
B	150.09	119.54	59.77	50.70	-18.14
C	202.22	448.77	158.22	127.92	-192.92
D	195.51	729.77	196.98	167.40	-394.98
E	240.21	889.05	224.31	190.97	-507.11
H	306.59	2894.78	1200.85	1118.39	-658.00
K	1502.27	24821.75	14816.22	13811.48	2801.22

1) "Albite–K-feldspar–Enstatite–Anorthite" forms Gibbsite: 3Na+3K+1Mg+2Ca
2) "Albite–K-feldspar–Enstatite–Anorthite" forms Kaolinite: 2Na+2K+Mg
3) "Albite–Muscovite–Enstatite Anorthite" forms Kaolinite: 2Na+Mg
4) "Albite–K-feldspar–Enstatite–Anorthite" forms Pyrophyllite: Na-3K+Mg-2Ca

4. Water chemistry in Shirasu ignimbrite area

4.1. Introduction

The previous chapters showed that the chemical behavior of natural surface water in Norikura volcanic area is mainly controlled by the water-rock interaction. The above results were, however, only given from a limited andesitic area, and the derived mechanism is needed to be certified in the other types of volcanic area to generalize the theory. In this chapter, the water research was performed in a granitic ignimbrite area. This observation area is covered by almost a single granitic ignimbrite layer, and there are cultivated farms or residential district and even inflows of geothermal waters are found in the area. The aim of this study is to extract and evaluate possible factors, which contribute the hydrochemistry, and to compare the water chemistry between Norikura volcanic area and the ignimbrite area. The research strategy is based on the same statistical and thermodynamic calculations as in the previous chapters.

4.2. Sampling points and methods

4.2.1. Geographical and geological characteristics of the sampling points

The observation area is in Kagoshima Prefecture, southern Kyushu Island, which is the most south-western island among the four major islands in Japan. Geographically, this area is just the point where the southwest Japanese arc meets the Ryukyu arc (Fig. 4-1). The average annual temperature is about 19 ℃, the maximum temperature in summer is 36 ℃, the minimum temperature in winter is -0.8 ℃, and the area belongs to the warm climatic zone in Japan. The average annual precipitation is 2,300 mm, of which the greatest concentration falls in the rainy season from May to July. The geological feature is that volcanic ash and debris (Ito pyroclastic flow deposits, termed "Shirasu") cover the whole area. The pyroclastic flow deposit "Shirasu" is a typical non-welded and unconsolidated ignimbrite with uniform chemical composition (age 24,500 years before present; Yokoyama, 1999), which is composed of volcanic glass and rather small amounts of feldspar, accompanied with quartz, augite, amphibole and magnetite etc.

Kotsuki River, which is the main subject of this research, flows across the Shirasu plateau. Kotsuki River begins in Mount Yae (Elevation: 677 m, Latitude:N31°44", Longitude: E130°26") , flows through Kagoshima City which is the largest city in Kagoshima Prefecture, and into Kinko Bay at N31°34", E130°34" (Fig.

4-1). The total length is 27 km with the catchment area 110 km^2. Most of the area is covered by "Shirasu" and only a limited part of the upstream area (in Mt. Yae) is covered by basaltic rocks. In the downstream area of Kotsuki River, dozens of hot springs (c.30 springs) and inflows of geothermal water from public baths are observed. The inflows of municipal wastewater are also observed in the urban district that spreads around the downstream region.

4.2.2. Sampling and analytical procedure

The field investigation was performed every 2 months between March 2001 and February 2003. Sampling points were selected from the water basin of the Kotsuki River (Kotsuki Pond in Mt. Yae) down to the estuary for every 4 km, as well as tributaries of Kotsuki River (Fig. 4-1). Altogether 106 samples were collected from 8 stationary measurement points and other additional points. The altitudes of sampling points were between 4 m and 408 m above sea level (Table 4-1). Besides those primary samples, highly polluted municipal wastewaters from the urban district were collected to evaluate anthropogenic influence to the surface water chemistry. In addition, rainwater samples were collected in Kagoshima City during the investigation period.

The water samples were filtered and placed in polyethylene bottles and transported to the laboratory, then subjected to chemical analysis. The temperature, pH and electrical conductivity (EC) were determined in the field by a digital pH meter (DKK HPH-130) and digital EC meter (Hach SensIon 5). Details of the analytical procedure and the statistical method are found in Chapter 2 (2.2. and 2.3).

4.3. Results

4.3.1. Chemical concentrations of river waters

The average chemical concentration at the stationary sampling points in the main stream of Kotsuki River and their geographic information are shown in Table 4-1. The chemical concentration at the water basin is higher than rainwater in the study area, which is about 5 times higher in EC. In comparison with Norikura samples, the water basin samples take about the same or even slightly higher chemical concentration than the mountainside samples of Norikura. The water-rock interaction seems to have fairly proceeded in those samples. This interpretation is presumably supported by the fact that the water temperature of the water basin, Kotsuki Pond in Mt. Yae, is higher in winter and lower in summer; the water has been stored in an underground reservoir for months before outflow from the pond. The outflow water should have enough time to interact

with the basement rocks under the ground. The average chemical concentrations of Kotsuki River and reference values are shown in Fig. 4-2. This figure shows that the dissolved chemical composition linearly increases downstream. In comparison with other river waters, Kotsuki River shows higher chemical concentrations than the average concentration of river waters in Japan or Kyushu Island, in spite of the shortness of the river length. A preeminent characteristic is seen in the high silicon concentration, which is a major component of Shirasu ignimbrite.

The rainwater in Kagoshima City shows extremely low chemical concentrations, which is even less than the upstream water. The chemical ratio of rainwater is far different from river waters; rainwater takes lower Si concentration and higher Na^+. The hot spring waters obtained from the vicinity of Kotsuki River show considerably higher chemical concentrations compared with the river waters.

4.3.2. Relation between the chemical concentrations and the distance from estuary

The relation between the chemical concentrations and the distance from the estuary mouth is shown in Fig. 4-3 for the major sampling points. The concentrations of most major chemical components increase downstream. Specifically, the high correlation is found between EC and the distance from the estuary mouth in the mainstream ($r^2 = 0.95$). Although the silicon concentration also increases downstream between the riverhead and the middle river area, in the downstream area, the concentration maintains a nearly constant value (Si: c. 1000 μmol dm^{-3}).

4.4. Discussion

4.4.1. Principal component analysis (PCA)

Principal component analysis was applied on the chemical concentrations in river water, municipal polluted water, hot spring water, and rainwater of Kagoshima City. The calculation results of the PCA are shown as the first three eigenvalues and eigenvectors of the correlation matrix (Table 4-2). The eigenvalue of the first principal component (P1) is 4.51, and of the second component (P2) is 2.11; both are over the critical value of 1 as often employed. The cumulative proportion of variance for the first and second principal components is 83% of cumulative proportion, i.e., P1 and P2 summarize 83% of the variability or the information in the data set. On the other hand, P3 or other components takes small variances, i.e., P3 is only 0.71 and P4 is 0.31. Therefore, the P1 and P2 were extracted as the significant components.

The PCA score of each sample is shown in Fig. 4-4. The rainwater, the

mainstream and tributary water of Kotsuki River were plotted on the straight line, which shows the direction of the hydrochemical process from rainwater to the matured river water. The hot spring water and the seawater clearly formed other groups with different direction from the river waters. This result indicates that the influences of the hot spring water or the seawater (airborne sea salt) on the river water chemistry are limited. The chemical evolution of the straight forward direction may indicate the degree of water-rock interaction or that of anthropogenic pollution.

In the next stage, to assess the major possible contributors to water chemistry, i.e., water-rock interaction and anthropogenic pollution, PCA was performed again on the representative data set. In this stage, the samples of rainwater, the mainstream of Kotsuki River and the highly polluted tributary were chosen to clarify the major contributor to the chemical evolution downstream. The first three eigenvalues and eigenvectors of the correlation matrix are shown in Table 4-3. This time, the eigenvalue of the first principal component (P_m1) is 7.34, and of the second component (P_m2) is 0.34. Only P_m1 is the significant component, which is correlated with all chemical components as a size factor. The scatter plot of PCA scores is shown in Fig. 4-5. The rain waters and the mainstream waters of Kotsuki River are plotted on a straight line, but the polluted waters in the municipal area (T6 samples) clearly separated from this line to form another group. Since the T6 samples are not only polluted waters but also the downstream samples, P_m1 would be correlated with the general chemical characteristics downstream the river, which would be mainly caused by water-rock (ignimbrite) interaction; P_m2, a minor component, would be correlated with anthropogenic pollution. Thus, the above PCA structure shows that water-rock interaction is the major contributor to the water chemistry rather than the anthropogenic pollution.

4.4.2. Factor analysis (FA)

The factor analysis (FA) was performed on the river waters to extract the underlying factors, which control the hydrochemical processes more details. As shown in PCA results, sweater or hot spring waters would be minor or tiny contributor to the water chemistry of Kotsuki River. Since entirely different data from the parent population, i.e. hot spring waters or highly influenced waters by those waters, may distort the factor solutions, the factor calculation was conducted exclusively on the mainstream of Kotsuki River samples.

Prior to factor analysis, the correlation coefficients were calculated (Table 4-4). All the components are highly correlated with each other ($r = 0.6 - 0.85$). Principal

factor extraction followed by various rotation methods gave identical factor structure. Table 4-5 shows the solution of the quartimax rotation. The first factor (F1) is highly loading on almost all chemical components with high proportionate contribution (76%); this factor is characterized as a 'size factor', which implies the integrated variances of the dissolved chemicals. The second factor (F2) is positively loading on K^+ and Si, and negatively loading on Ca^{2+} and SO_4^{2-}; the third factor (F3) is loading on Na^+ and Cl^-. The second factor (F2) may imply the negative correlation effect between the dissolution of $CaCO_3$ in the sediments (White et al., 1999), and the dissolution of Si and K in muscovite or adjacent minerals; the third factor (F3) may imply the sea salt influence. However, the contribution proportions of those factors (F2 and F3) are small as only 8.9% and 3.3 % respectively. Therefore, the influence of those factors is interpreted as of lesser importance.

4.4.3. Multiple regression analysis (MR)

Multiple regression analysis was performed to assess the dependence of river chemistry on the various sources. The chemical compositions of Kotsuki River samples (M1 – M7) were set as criterion variable and the potential sources were set as explanatory variables (predictors). Following is an expected linear equation using those predictors.

$$\text{River Water (M1 - M7)} = a_1 (Ex_1) + a_2 (Ex_2) + a_3 (Ex_3) + a_4 (Ex_4)$$

Ex : explanatory variables affecting on the river water
a_i : coefficient

Here, Ex_1 is the chemical load on the river water by sewage from the residential crowded area, Ex_2 is airborne sea salt, Ex_3 is hot spring water, and Ex_4 is rainwater in Kagoshima City. The significance of each predictor was estimated using analysis of variance (ANOVA). The significance of each explanatory variable is presented as a p-value and an F-value (Table 4-6). The coefficients of determination take only small value ($R^2 = 0.21$ to 0.29) and even the coefficients of determination adjusted for degrees of freedom are all zero ($R'^2 = 0$). The F-values of 0.01 – 0.73 (significance level is >2) and P-values of 0.46 – 0.95 (significance level is <0.05), indicate that the any of the presented explanatory variances have no significance to predict the chemical composition of Kotsuki River. This result shows that those potential sources have only a minor or no role in controlling the water chemistry of

Kotsuki River.

4.4.4. Cluster analysis (CA): Experimental water and real water

The statistical results implied that the chemistry of the river water receives only little or limited influence from the possible factors mentioned above (i.e., airborne sea salt, hot spring, sewage, rainwater contaminants). The major factor is presumably geological materials such as Shirasu ignimbrite, which represents the geology of Kotsuki River catchment. Consequently, a simulated solution was experimentally produced to compare with the real river water.

The simulated solution was made under the water-rock interaction using Shirasu ignimbrite and water with adjusted pH equivalent to the representative rainwater in Kagoshima City. The experiment was carried out using Shirasu ignimbrite marketed for the industrial use. Coarse Shirasu ignimbrite was dry ground in an agate mortar, and sieved to 100-200 mesh (corresponding to the 150-75um size fraction). The pH of the added water was adjusted by sulfuric acid to the average pH of rainwater in Kagoshima City (pH = 4.1). Twenty gram of dried Shirasu powder was put into polyethylene bottle with 5 dm^3 of pH adjusted water and keep under 20-25 ℃ for 180 days. The solution obtained was analyzed by atomic absorption spectrometry and photometric method in the same way as the river water analysis.

The chemical ratio of the mainstream waters of Kotsuki River, the experimental solution and other waters in comparison is shown in Fig. 4-6. The relative chemical compositions of the river water sample (M1 - M7) are similar to each other, and close to the composition of the experimental water, which is confirmed by cluster analysis (Fig. 4-7). An overall inspection of the dendrogram shows that the river waters (M1 – M7) and the experimental solution are classified into the same group, but other waters or possible factors (i.e., rainwater, seawater, hot spring water and municipal polluted water) are excluded from this group. This result shows that among those possible waters, only the experimental solution, which is obtained by water-rock interaction, has chemical ratio similar to the river waters. Thus the major factor to control the chemical composition in the river waters is reasonably assumed to be geological material, i.e., Shirasu ignimbrite in this case.

4.4.5. Coexistence relation between stable minerals and water solution

To assess the thermodynamic stability of waters and coexistent minerals, cation-Si stability diagrams plot were examined (Figs. 4-8 (a)-(d)). The chemical process shows a similar trend to that in shallow ground waters saturated with carbon

dioxide under atmospheric pressure (Garrels and Mackenzie, 1967); carbon dioxide dissolves plagioclase to form kaolinite (Garrels, 1967). The headwater of Kotsuki River, which is discharged from basaltic rock, contains only low concentration of silicon and cations and plots on the far left below on the diagrams. The concentration of silicon and cations increase downstream the river, and the trends on the diagram rise towards the upper right. The samples of the downstream region (M5-M7) are almost saturated with kaolinite and the sample plots change the direction up on the boundary between kaolinite and pyrophyllite. Fig. 4-3 already showed that in spite of the cation concentration still rising in the downstream region, the silicon concentration becomes nearly constant. The reason is understood as the thermodynamic barrier that keeps the silicon concentration still under the water-rock interaction when the coexisting secondary mineral changes from kaolinite to pyrophyllite.

4.4.6. Estimation of silicon concentration by cation concentrations

A stoichiometric calculation was performed under consideration of rock weathering reaction. In chemical weathering, masses of rock do not dissolve uniformly, but the mineral that is less resistant to weathering dissolves more rapidly than more resistant minerals (Goldich, 1938). Moreover, some elements such as aluminum form secondary minerals (clay minerals), and are removed from the aqueous phase. Therefore, the chemical composition of bedrock in the catchment area is not exactly reflected in the aqueous chemical composition. The stability diagram shows that the river water in this area is thermodynamically coexistent with kaolinite, and the secondary minerals produced by rock weathering are most likely kaolinite or its adjacent minerals. Among the major minerals found in Shirasu ignimbrite, the possible source mineral for sodium is albite, for potassium is muscovite, for magnesium is enstatite, and for calcium is anorthite. The weathering equations of these minerals are shown as follows.

Na^+—Si : Albite → Kaolinite

$$NaAlSi_3O_8 + 9/2H_2O + H^+ \rightarrow \underline{Na^+} + \underline{2}H_4\underline{Si}O_4 + 1/2\ Al_2Si_2O_5(OH)_4\downarrow \quad (4\text{-}1)$$

K^+—Si : Muscovite → Kaolinite

$$KAl_2(AlSi_3)O_{10}(OH)_2 + 3/2\ H_2O + H^+ \rightarrow \underline{K^+} + 3/2\ Al_2Si_2O_5(OH)_4\downarrow \quad (4\text{-}2)$$

Mg^{2+}—Si : Enstatite → Kaolinite

$$MgSiO_3 + H_2O + 2H^+ \rightarrow \underline{Mg^{2+}} + H_4\underline{Si}O_4 \quad (4\text{-}3)$$

Ca^{2+}—Si : Anorthite → Kaolinite

$$CaAl_2Si_2O_8 + H_2O + 2H^+ \rightarrow \underline{Ca^{2+}} + Al_2Si_2O_5(OH)_4\downarrow \quad (4\text{-}4)$$

If the rock weathering as expressed by the above chemical equations controls the river water chemistry, 2 moles of silicon dissolve with 1 mol of sodium dissolution; 1 mol of silicon dissolve with 1 mol of magnesium. On the other hand, in the dissolution of potassium and calcium, no silicon dissolves, since all silicon is consumed to form kaolinite. Thus, if just the above chemical reactions (4-1) - (4-4) control the river water chemistry, the following simple equation would be applicable.

$$[Si] = 2\,[Na^+] + [Mg^{2+}] \quad (4\text{-}5)$$

The scatter plot of predicted [Si] (= 2 $[Na^+]$ + $[Mg^{2+}]$) and measured [Si] is shown in Fig. 4-9(a). In this figure, most of the river water of the upstream area is plotted on the predicted line. However, predicted [Si] in the downstream area is significantly higher than the measured value. In this case, silicon is highly concentrated and is almost saturated in kaolinite; the water is even coexistent with pyrophyllite (Figs. 4-8 (a)-(d)). The formation of pyrophyllite, other than kaolinite, is a possible reason for the deviation from the predictive value.

The weathering reactions of the major minerals to form pyrophyllite are given by the following chemical equations.

Na^+—Si : Albite → Pyrophyllite

$$NaAlSi_3O_8 + 2\,H_2O + H^+ \rightarrow \underline{Na^+} + H_4\underline{Si}O_4 + 1/2\,Al_2Si_4O_{10}(OH)_2\downarrow \quad (4\text{-}6)$$

K^+—Si : Muscovite →Pyrophyllite

$$KAl_2(AlSi_3)O_{10}(OH)_2 + H^+ + \underline{3}\,H_4\underline{Si}O_4 \rightarrow \underline{K^+} + 6\,H_2O + 3/2\,Al_2Si_4O_{10}(OH)_2\downarrow \quad (4\text{-}7)$$

Mg^{2+}—Si : Enstatite →Pyrophyllite (same as kaolinite case)

$$MgSiO_3 + H_2O + 2H^+ \rightarrow \underline{Mg^{2+}} + H_4\underline{Si}O_4 \quad (4\text{-}8)$$

Ca^{2+}—Si : Anorthite → Pyrophyllite

$$CaAl_2Si_2O_8 + 2H^+ + \underline{2}H_4\underline{Si}O_4 \rightarrow \underline{Ca^{2+}} + 4H_2O + Al_2Si_4O_{10}(OH)_2\downarrow \quad (4\text{-}9)$$

As shown in the above equations (4-6)-(4-9), the chemical weathering to form

pyrophyllite yields that 1 mol of sodium and magnesium dissolution is followed by 1 mol of silicon dissolution; 3 mol of potassium dissolution causes 1 mol of silicon absorption to pyrophyllite. Likewise, 1 mol of calcium dissolution causes 2 mol of silicon absorption to pyrophyllite. Thus, the [Si] and cation relations controlled by rock dissolution to form pyrophyllite are summarized in the following equation (4-10).

$$[Si] = [Na^+] - 3\,[K^+] + [Mg^{2+}] - 2\,[Ca^{2+}] \qquad (4\text{-}10)$$

The [Si] predicted value was recalculated, under supposing that 90 % of the downstream samples (M6) plotted on the boundary between kaolinite and pyrophyllite in the stability diagram forms kaolinite and 10 % forms pyrophyllite, and 80 % of M7 forms kaolinite and 20 % forms pyrophyllite. Fig. 4-9(b) is the scatter plot of the recalculated results. The regression analysis showed that [Si] is predicted with high accuracy, 0.93 for the adjusted correlation coefficient. In this way, the major chemical behavior is quantitatively explained by the dissolution of Shirasu ignimbrite and the formation of clay minerals.

4.5. Summary

Multivariate analysis and stoichiometric calculation were performed on the major chemical composition in the river water of Shirasu ignimbrite area. The statistical calculation showed that the major hydrochemical factor is the dissolution of Shirasu ignimbrite, despite the existence of many hot spring discharges and a municipal region in the catchment area. The combination of stability diagrams and stoichiometric calculation led to a predictive equation of silicon concentration under consideration of chemical weathering followed by the formation of clay minerals. The equation is expressed as $[Si] = 2\,[Na^+] + [Mg^{2+}]$ (kaolinite precipitation region) in most of the Kotsuki River samples. In the limited downstream area, above predictive equation is complemented by $[Si] = [Na^+] - 3\,[K^+] + [Mg^{2+}] - 2\,[Ca^{2+}]$ (pyrophyllite precipitation region).

Fig. 4-1

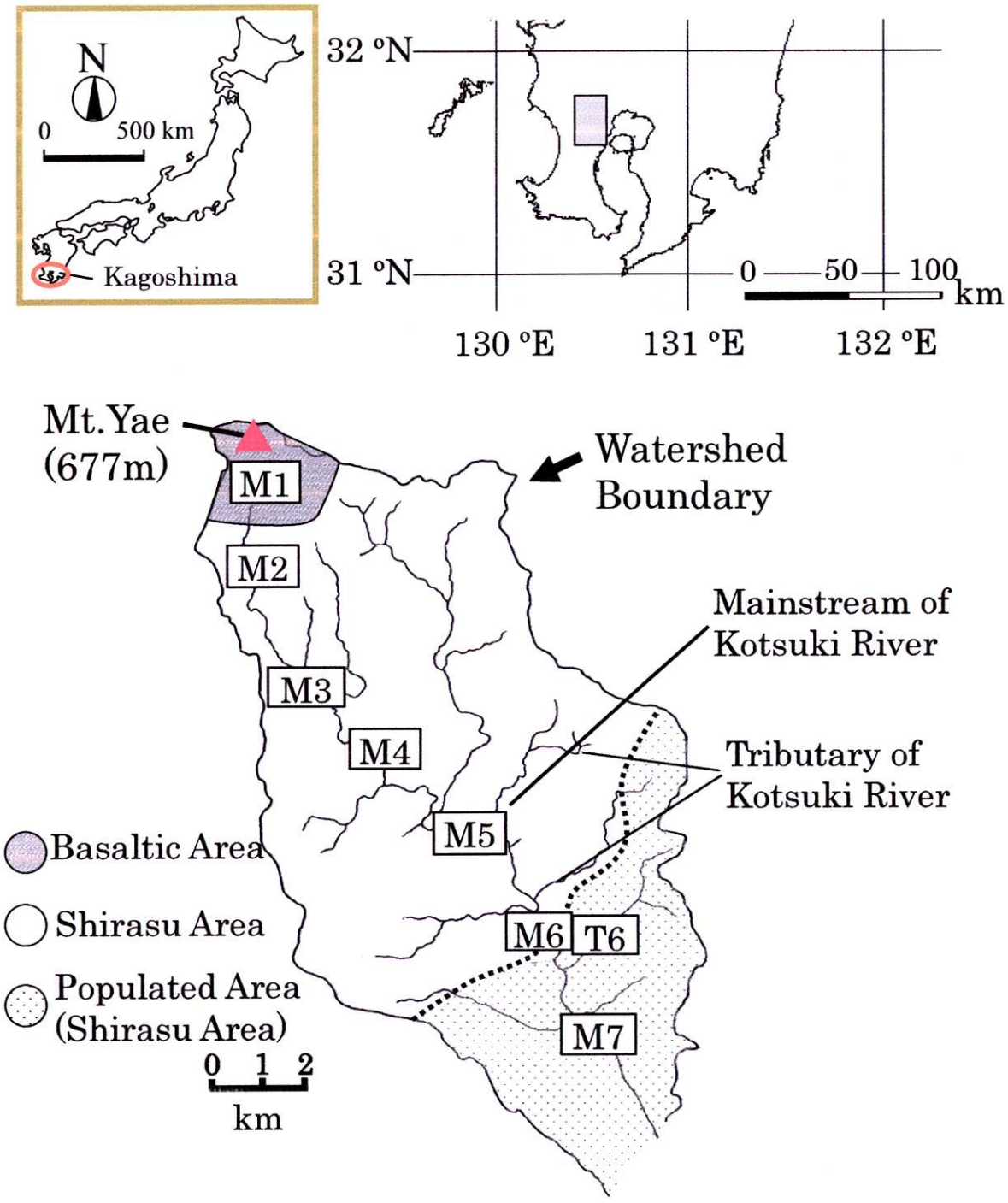

Fig. 4-1. Location map of the observation area, Kotsuki River, in southern Kyushu Island, southwest Japan. The major stationary points of M1 – M7 are on the mainstream of Kotsuki River, and T6 is on a highly polluted tributary in a populated area.

Fig. 4-2

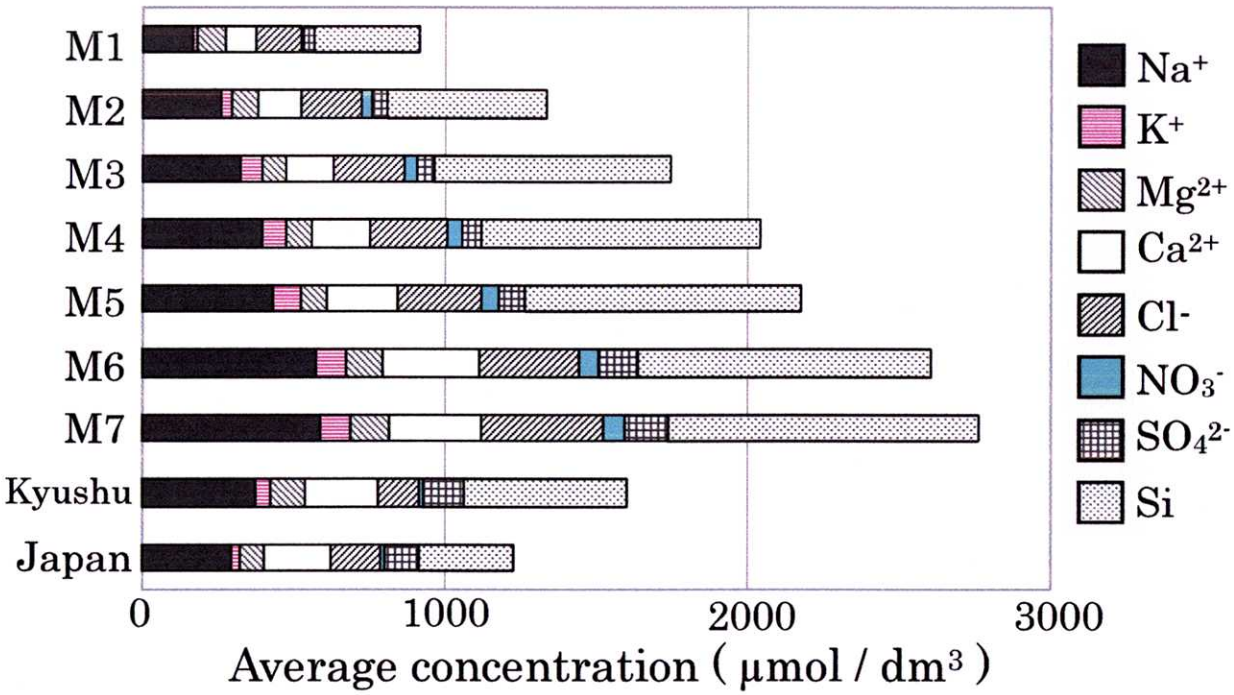

Fig. 4-2. Average concentrations of major cations and silicon in the river waters. Sampling points are shown in Fig. 1 and the sample description is in Table 1. Average chemical concentration of Kyushu or Japanese river water is after Kobayashi (1961).

Fig. 4-3

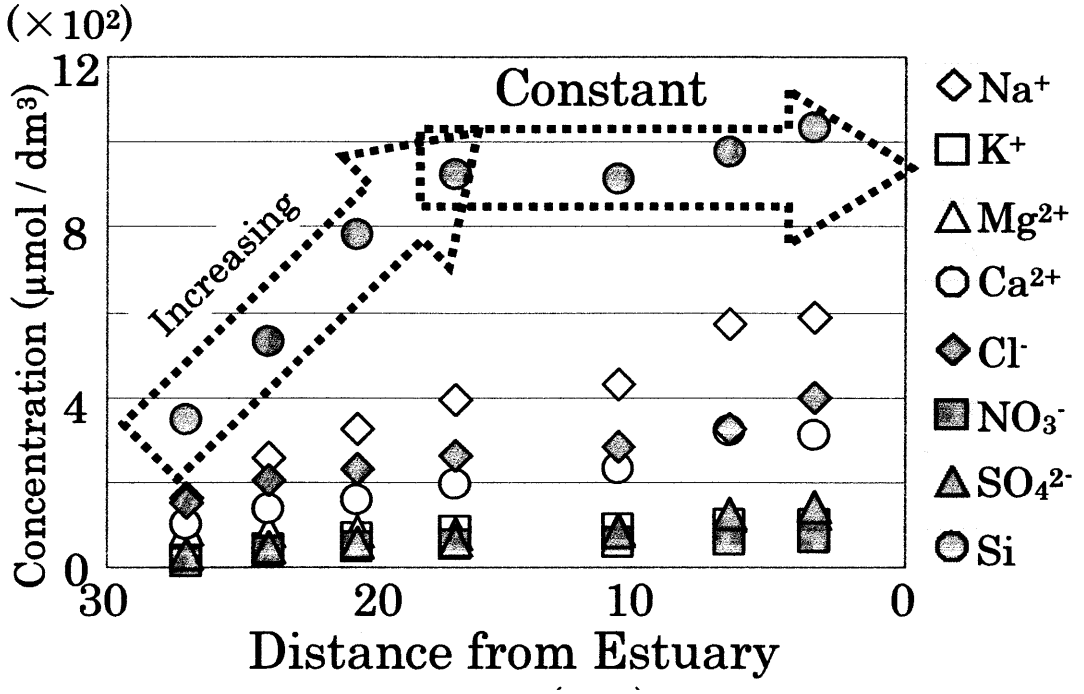

Fig. 4-3. Relation between the chemical concentrations and the distance from the estuary mouth.

Fig. 4-4

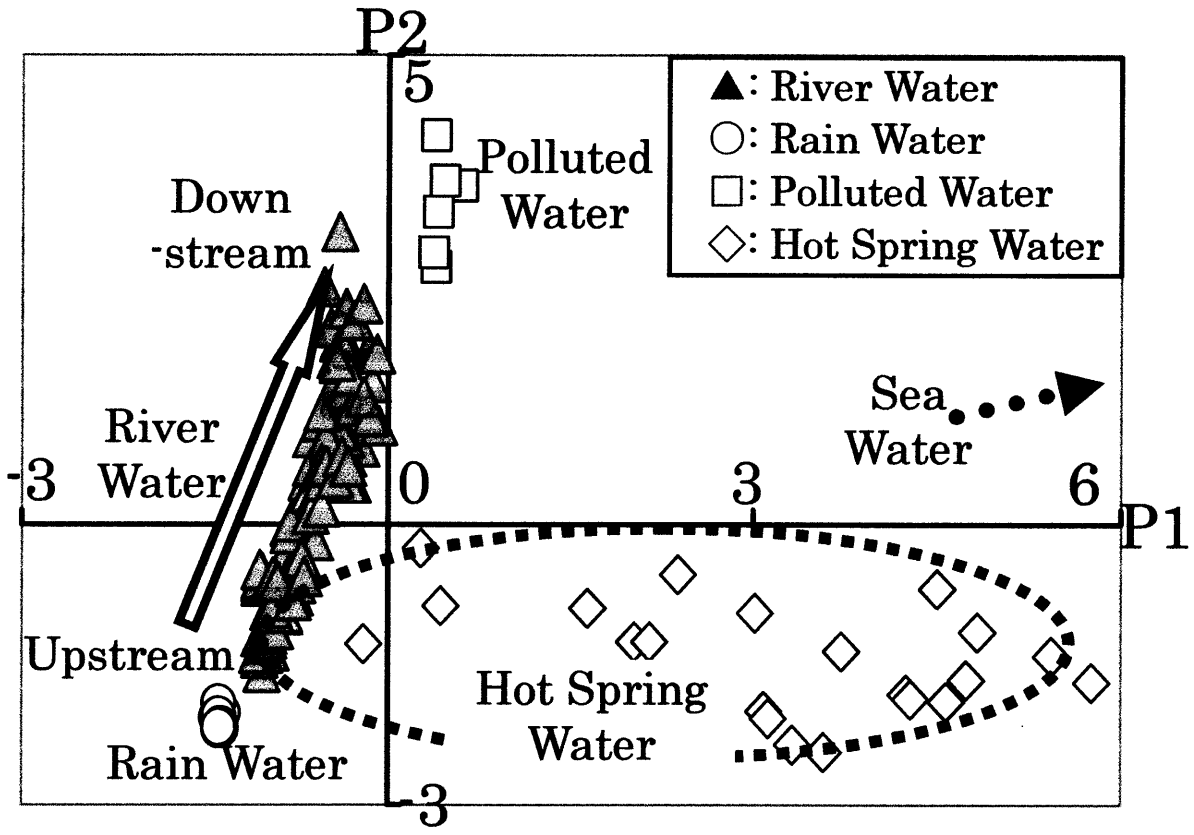

Fig. 4-4. Scatter plot of PCA scores (P1 and P2) of water samples. The arrow indicates the direction of the hydrochemical process downstream.

Fig. 4-5

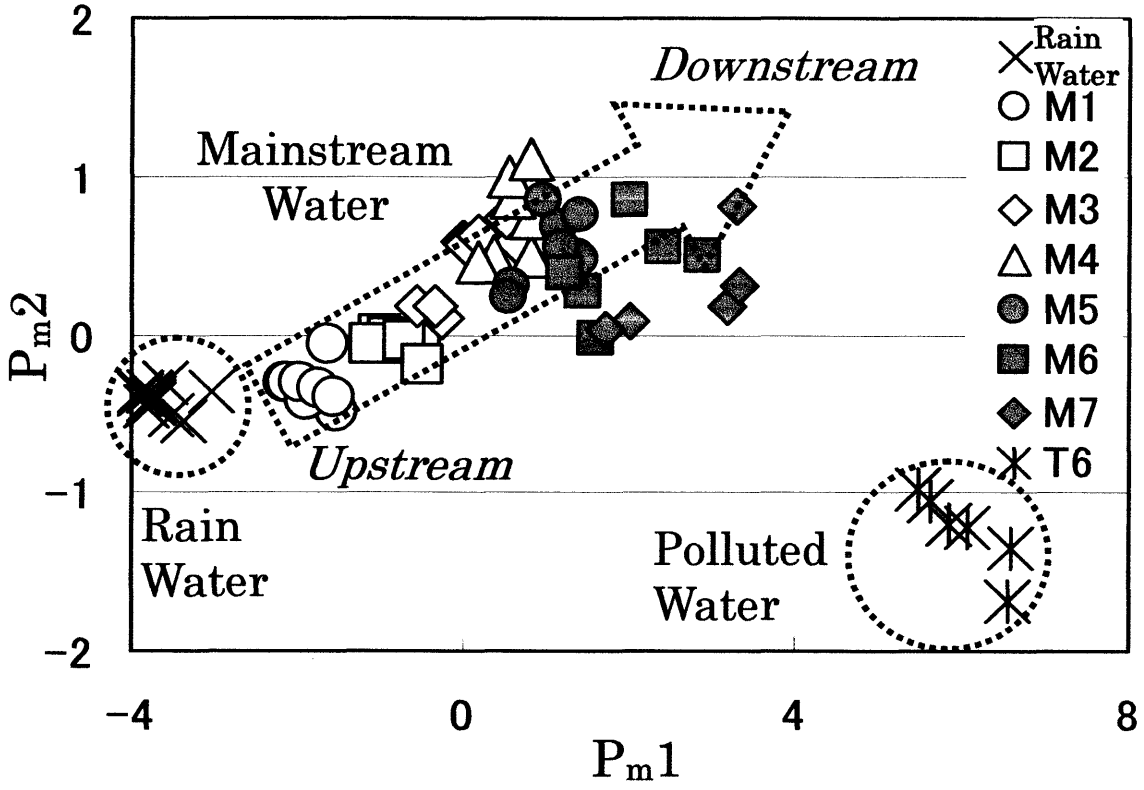

Fig. 4-5. Scatter plot of PCA scores (P_m1 and P_m2) of rainwater and the representative river water samples. The arrow indicates the direction of the hydrochemical process downstream.

Fig. 4-6

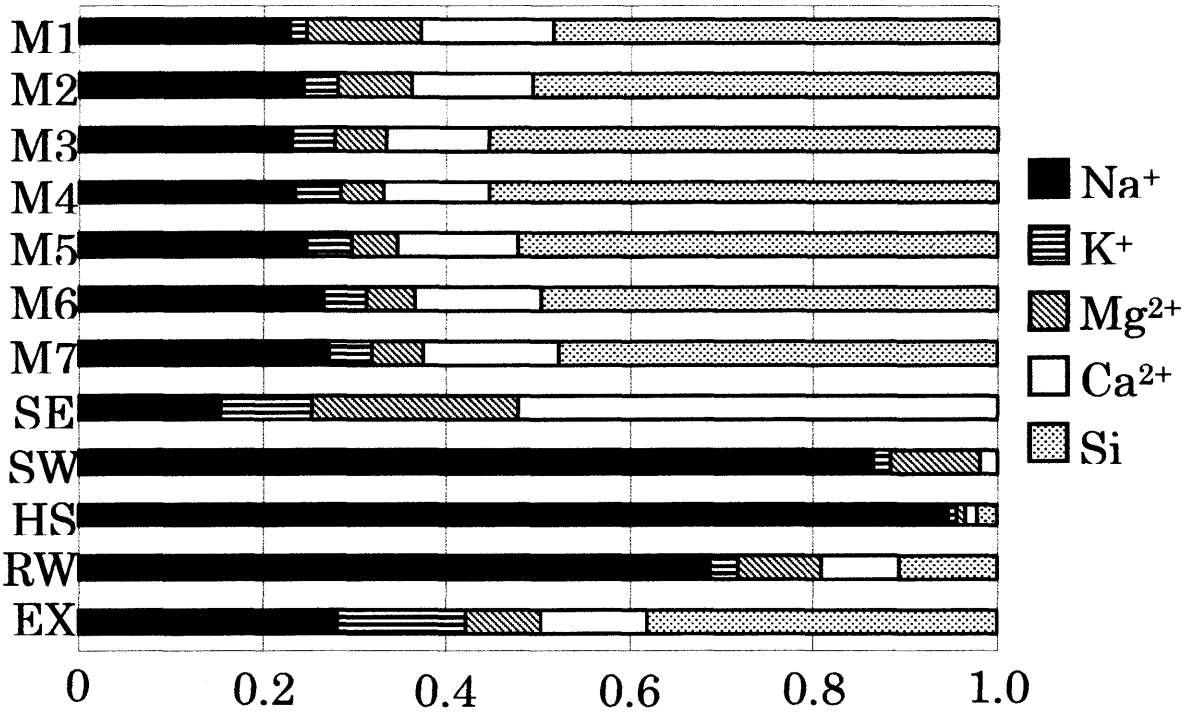

Fig. 4-6. Chemical ratio of various waters. M1 – M7: the mainstream samples of Kotsuki River found in Fig. 4-1, SE: chemical load by sewage from urban district, SW: seawater, HS: hot spring water, RW: rainwater, EX: experimental solution.

Fig. 4-7

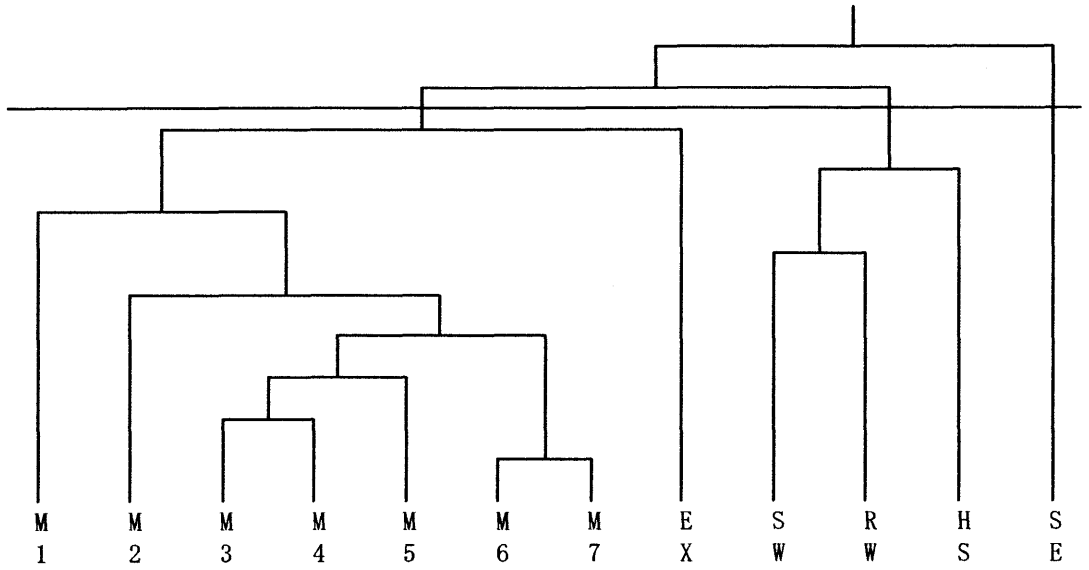

Fig. 4-7. Dendrogram for cluster analysis based on the chemical ratio of water samples. Dissimilarity is defined by Euclidean distance and combination of clusters is based on Ward method. The symbols are the same as in Fig. 4-6.

Fig. 4-8 (a)

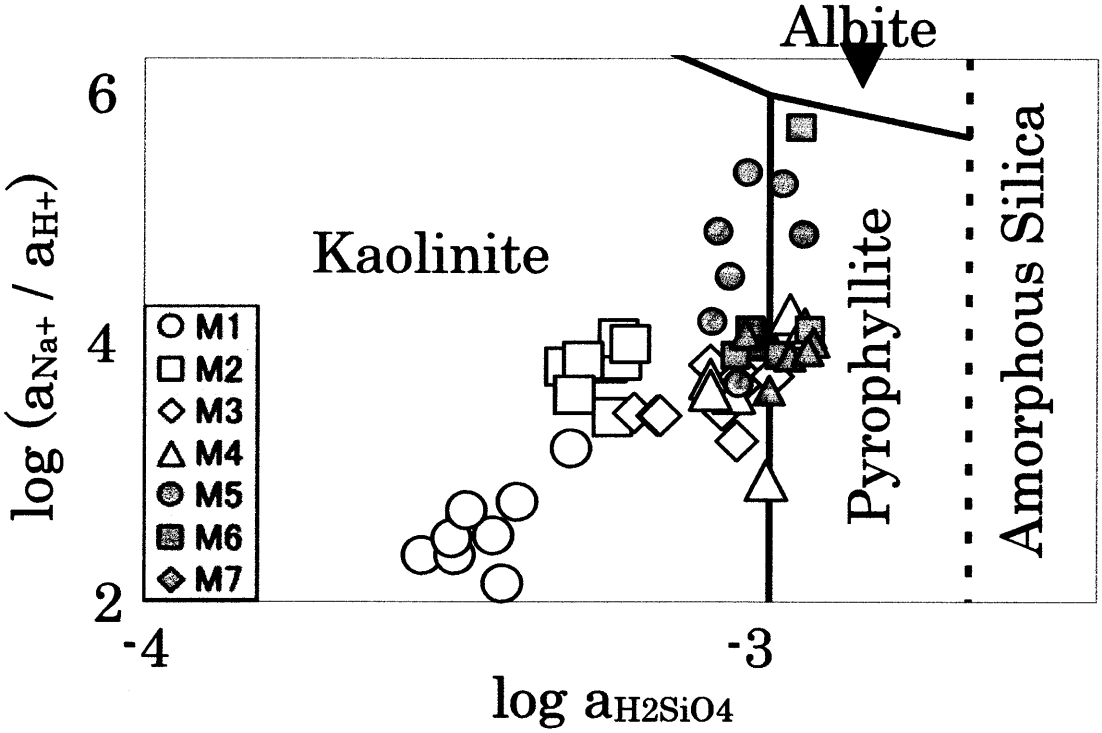

Fig. 4-8 (b)

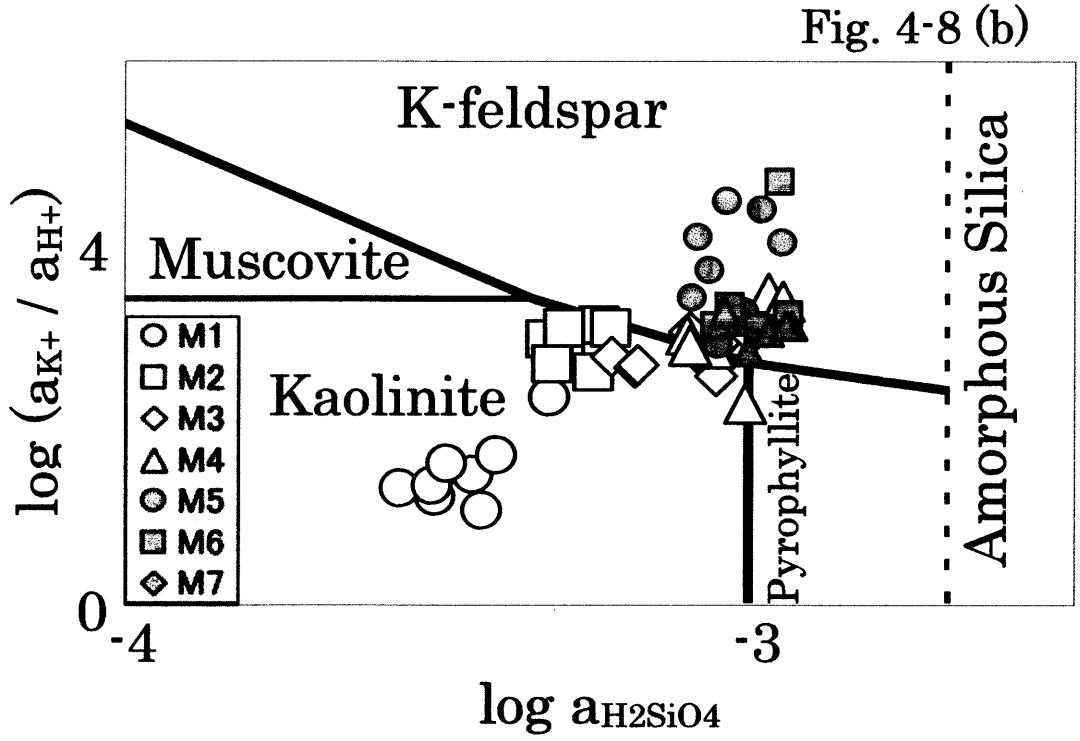

Fig. 4-8 Stability diagrams at 25 ℃. (a) Na^+—Si system, (b) K^+—Si system.

Fig. 4-8 (c)

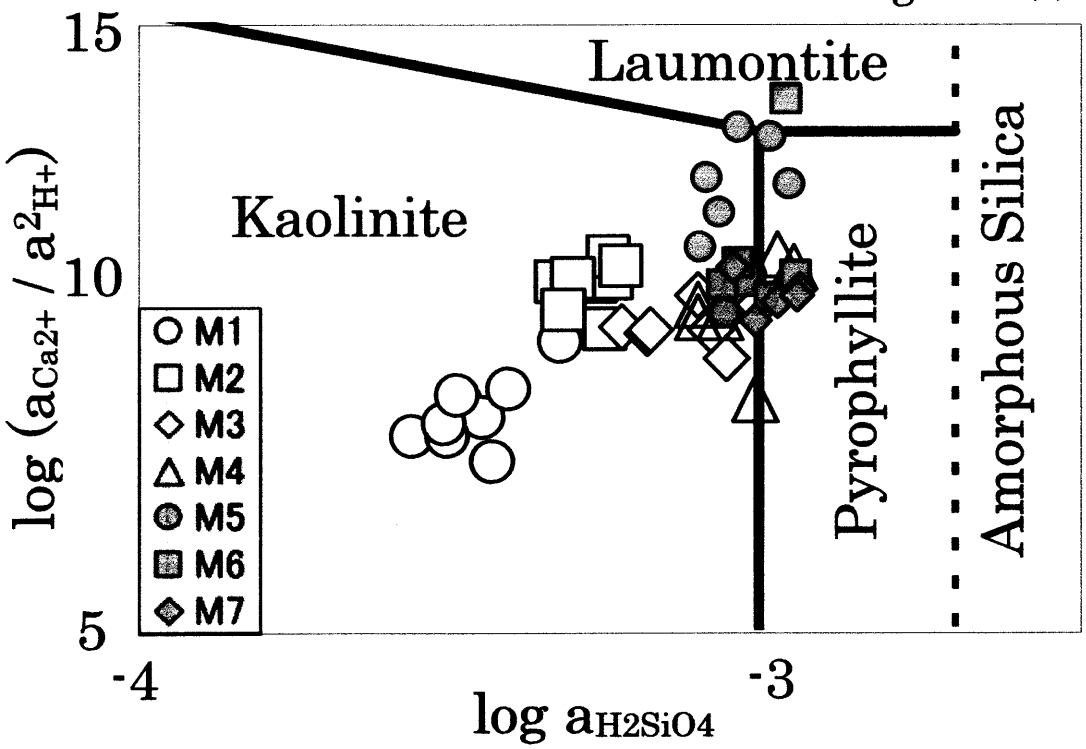

Fig. 4-8 (d)

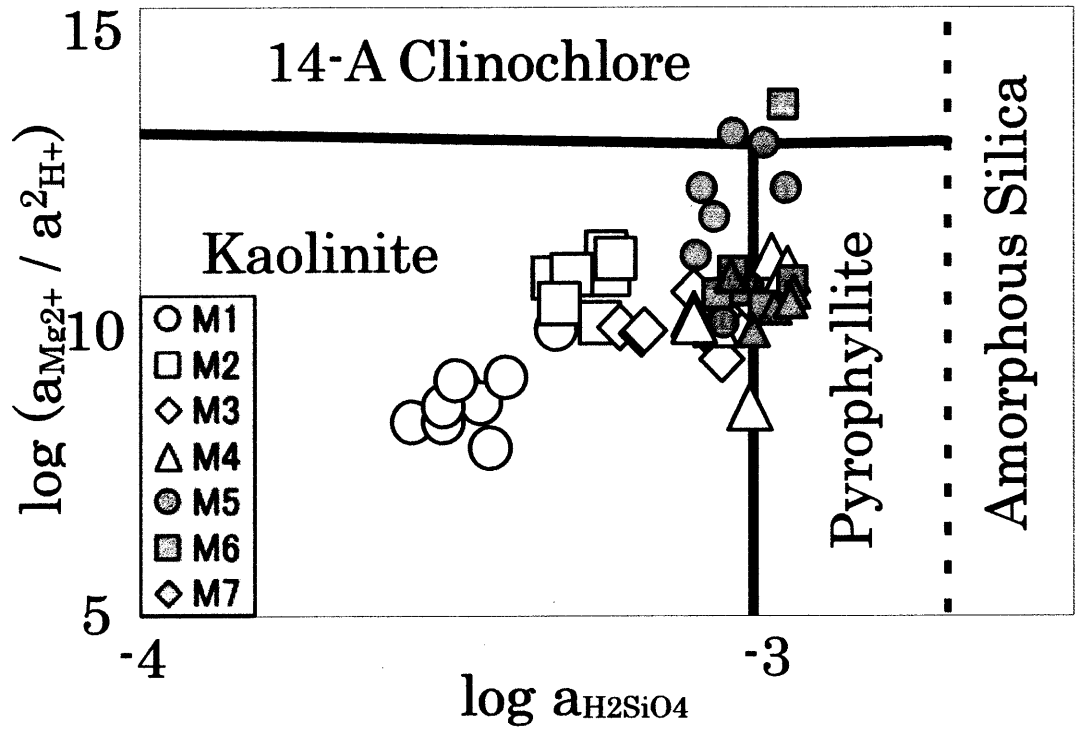

Fig. 4-8 Stability diagrams at 25 ℃. (c) Mg^{2+}—Si system and (d) Ca^{2+}—Si system.

Fig. 4-9 (a)

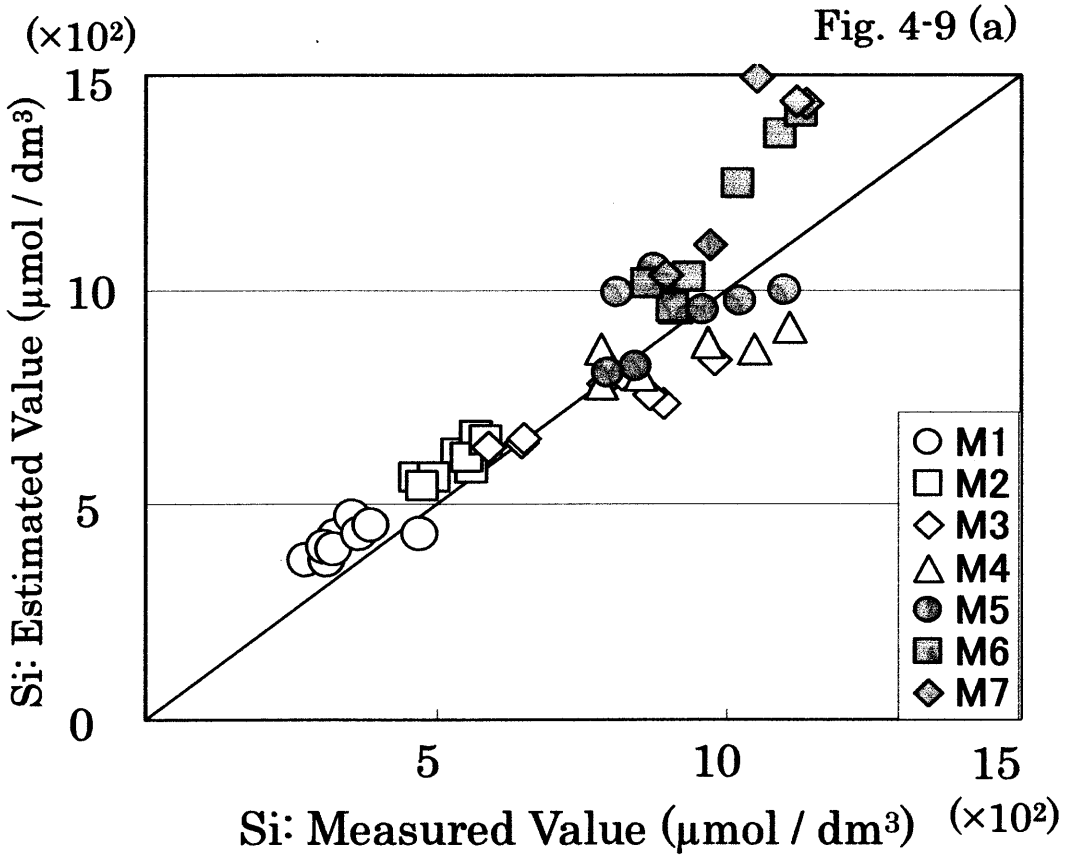

Fig. 4-9(a). Measured and simulated Si concentration. $[Si]_{Estimated}$ is given by (2 $[Na^+]$ + $[Mg^{2+}]$). Regression Equation : $[Si]_{Estimated} = 0.794\ [Si]_{Measured} - 0.000107$ (mol/dm^3). Coefficient of determination $R^2 = 0.82$, Multiple correlation coefficient $R = 0.90$, Adjusted coefficient of determination $R^{2\prime} = 0.81$, Adjusted multiple correlation coefficient $R' = 0.90$, Durbin-Watson statistic (ratio) DW = 0.98.

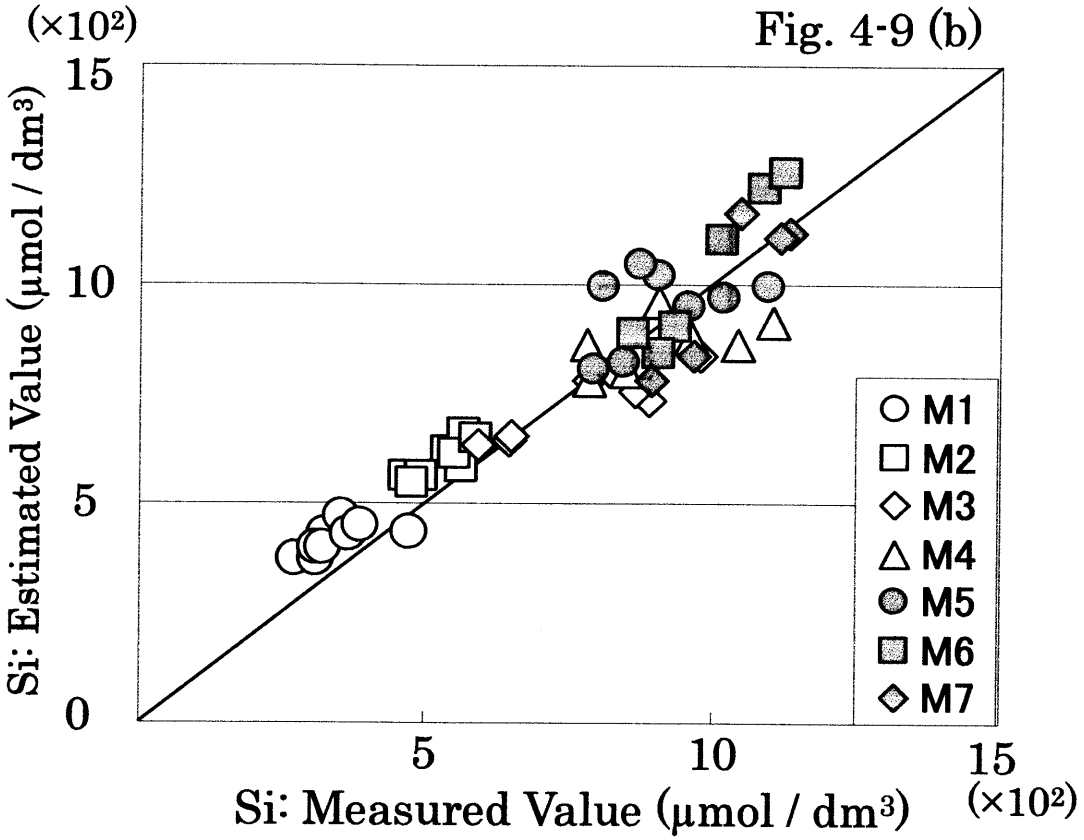

Fig. 4-9(b). Measured and simulated Si concentration. $[Si]_{Estimated}$ is given by $0.9\times(2\ [Na^+] + [Mg^{2+}]) + 0.1\times(\ [Na^+] - 3[K^+] + [Mg^{2+}] - 2[Ca^{2+}])$ on H6 samples; $0.8\times(2\ [Na^+] + [Mg^{2+}]) + 0.2\times(\ [Na^+] - 3[K^+] + [Mg^{2+}] - 2[Ca^{2+}])$ on H7 samples. [Si]Estimated of other samples are given by the same as Fig. 8(a). Regression Equation : $[Si]_{Estimated} = 1.030\ [Si]_{Measured} - 0.000036$ (mol/dm^3). Coefficient of determination $R^2 = 0.87$, Multiple correlation coefficient $R = 0.94$, Adjusted coefficient of determination $R^{2\prime} = 0.87$, Adjusted multiple correlation coefficient $R' = 0.93$, Durbin-Watson statistic (ratio) DW = 1.56.

Table 4-1 Chemical concentration of water samples (μmol dm^{-3}). M1 – M7: samples of main stream of Kotsuki River. Kyushu: average value in the river waters in Kyushu. Japan: average value in the river waters in Japan. HS: average value of hot spring waters in the observation area. RW: average value of rain water in Kagoshima City. T6: highly polluted by municipal wastewater.

Sample	n	Drainage area (km^2)	Distance from the mouth (km)	EC (mS m^{-1})	pH	Na^+ (μmol dm^{-3})	K^+ μmol dm^{-3})	Mg^{2+} (μmol dm^{-3})	Ca^{2+} (μmol dm^{-3})	Cl^- (μmol dm^{-3})	NO_3^- μmol dm^{-3})	SO_4^{2-} μmol dm^{-3})	Si (μmol dm^{-3})
M1	8	0.265	27.03	6.27	6.37	163	15	90	101	149	12	33	348
M2	9	3.914	23.862	8.24	7.31	256	40	85	137	204	36	47	531
M3	8	8.111	20.508	9.65	6.99	324	67	82	158	233	46	58	779
M4	8	10.993	16.832	11.19	7.05	392	82	80	193	260	50	63	921
M5	8	60.895	10.705	12.70	7.95	432	88	87	233	284	57	83	914
M6	6	86.636	6.49	17.46	7.82	573	101	122	321	326	63	127	975
M7	5	101.502	3.31	16.13	7.07	587	98	127	312	399	70	141	1034
Kyushu [a]						374	47	111	250	130	14	136	536
Japan [a]	225					291	30	78	220	164	19	110	316
HS [b]	24				7.91	29664	312	296	349	26182	-	2397	726
RW	14			1.23	4.13	24	1	3	3	33	6	16	4
T6	6	2.484	6.49	23.44	7.97	689	151	225	552	487	143	233	535

[a] Kobayashi, 1961, [b] Fujita and Sakamoto, 2002.

Table 4-2 Principal components (as eigenvectors) and eigenvalues on the correlation matrix of the chemical concentration in river water, rainwater, and hot spring water (n = 135).

	P1	P2	P3
Na^+	0.43	- 0.20	- 0.33
K^+	0.46	0.08	0.05
Mg^{2+}	0.37	0.13	0.68
Ca^{2+}	0.36	0.34	0.15
Cl^-	0.42	- 0.11	0.03
NO_3^-	- 0.06	0.64	- 0.06
SO_4^{2-}	0.38	- 0.20	- 0.46
Si	0.07	0.60	- 0.43
Eigenvalue	4.53	2.05	0.68
Proportion (%)	57	26	8
Cumulative Proportion (%)	57	82	91

Table 4-3 First three Principal Components (as eigenvectors) and eigenvalues on the correlation matrix of the chemical concentration in mainstream of Kotsuki River (M1-M7), rainwater(RW), and polluted tributary samples on point T6 (n = 71).

	P_m1	P_m2	P_m3
Na^+	0.36	0.30	0.06
K^+	0.36	0.24	-0.32
Mg^{2+}	0.34	-0.36	0.63
Ca^{2+}	0.36	-0.23	0.04
Cl^-	0.36	0.17	0.37
NO_3^-	0.35	-0.33	-0.58
SO_4^{2-}	0.35	-0.40	-0.15
Si	0.34	0.61	-0.04
Eigenvalue	7.34	0.34	0.15
Proportion (%)	92	4	2
Cumulative Proportion (%)	92	96	98

Table 4-4 Correlation matrix of major elements in the river water. All values show 1% significant correlations (n = 106).

	Na^+	K^+	Mg^{2+}	Ca^{2+}	Cl^-	NO_3^-	SO_4^{2-}	Si
Na^+	1.00	0.84	0.62	0.88	0.90	0.79	0.85	0.82
K^+	0.84	1.00	0.46	0.79	0.70	0.83	0.70	0.96
Mg^{2+}	0.62	0.46	1.00	0.70	0.63	0.48	0.72	0.45
Ca^{2+}	0.88	0.79	0.70	1.00	0.80	0.70	0.93	0.71
Cl^-	0.90	0.70	0.63	0.80	1.00	0.69	0.79	0.65
NO_3^-	0.79	0.83	0.48	0.70	0.69	1.00	0.67	0.85
SO_4^{2-}	0.85	0.70	0.72	0.93	0.79	0.67	1.00	0.66
Si	0.82	0.96	0.45	0.71	0.65	0.85	0.66	1.00

Table 4-5 Factor loadings of the chemical concentration in the main stream waters of Kotsuki River (principal factor method with quartimax rotation). n = 106

	F1	F2	F3
Na^+	**0.96**	0.03	**0.14**
K^+	**0.88**	**0.41**	-0.08
Mg^{2+}	**0.68**	-0.30	-0.02
Ca^{2+}	**0.94**	-0.19	-0.13
Cl^-	**0.88**	-0.13	**0.44**
NO_3^-	**0.82**	0.28	0.01
SO_4^{2-}	**0.92**	-0.29	-0.14
Si	**0.86**	**0.49**	-0.09
Proportion (%)	75.84	8.86	3.27
Cumulative proportion (%)	75.84	84.69	87.96

Table 4-6 F and p values of ANOVA on the river water and possible sources. R^2 is the coefficient of determination adjusted for degrees of freedom.

River waters	Test	Possible sources				
		Sewage	Sea Water	Hot Spring Water	Rain Water	R^2
M1	F	0.39	0.01	0.02	0.15	0.21
	p	0.58	0.93	0.91	0.72	
M2	F	0.53	0.00	0.08	0.13	0.26
	p	0.52	0.95	0.79	0.74	
M3	F	0.73	0.02	0.11	0.11	0.28
	p	0.46	0.90	0.77	0.76	
M4	F	0.70	0.03	0.14	0.12	0.29
	p	0.46	0.87	0.73	0.75	
M5	F	0.56	0.05	0.19	0.12	0.28
	p	0.51	0.84	0.69	0.75	
M6	F	0.47	0.08	0.27	0.12	0.29
	p	0.54	0.80	0.64	0.76	
M7	F	0.42	0.06	0.25	0.10	0.28
	p	0.56	0.82	0.65	0.77	

significance level of F: $F > 2$ p: $p < 0.05$

5. Conclusions

Hydrochemical research was conducted in typical volcanic areas, Norikura volcanic zone in central Honshu Island and Shirasu ignimbrite area in southern Kyushu Island. In order to clarify the chemical mechanism of natural surface waters, this research adopted mainly two methodologies, i.e., multivariate statistical analysis, and calculation of thermodynamics and stoichiometry. Multivariate analysis was applied on the major chemical components to classify the water samples and to extract potential factors, which control the water chemistry. Thermodynamic and stoichiometric calculation was performed to interpret the statistical results and to establish a theoretical model, which explains chemical behavior in the surface waters.

5.1. General water chemistry of Norikura volcano

The water samples at the summit area took extraordinary low concentrations of the chemicals (EC: 0.2-1 mS/m) and the water type belonged to the alkaline carbonate type. The waters of the mountainside were categorized as the alkaline earth carbonate type, which is typical Japanese shallow groundwater or river water. The chemical concentration was gradually increasing downstream, and the water chemistry of mountainside area was approaching to that of the typical Japanese river water.

5.2. Multivariate analysis on the hydrochemistry of Norikura volcano

The principal component analysis (PCA) on the whole chemical data clearly divided the water samples as meteoric waters, non-geothermal waters and geothermal waters. The PCA scores also showed the chemical process direction of the non-geothermal waters; the first principal component scores took high negative correlation with the altitudes of sampling points. The correlation coefficients between silicon and the major cations in the non-geothermal waters were positively high, which suggested that the volcanic rock dissolution play an important role to the water chemistry in this area.

5.2.1. Factor analysis of the summit area

The factor analysis on the summit area showed that leaching of cations in the rocks by acid rainwater was the major contributor to water chemistry (proportional contribution was 45% of all co-variances). Airborne sea salt contributed 20%, while

the biological activity contributed 10%.

5.2.2. Factor analysis of the mountainside area

The water chemistry in the mountainside area of Norikura was exclusively contributed by water-rock interaction; Na^+ and K^+ dissolution from rocks by acid water (proportional contribution was c. 45% of all co-variances), and cation exchange in the rocks or precipitation of Ca^{2+} and Mg^{2+} (c. 20%). The influence of geothermal water was small even though the sampling points were close to geothermal area.

5.2.3. Factor analysis of non-geothermal waters from the whole area

The whole chemical data of non-geothermal waters gave two major factors. The first factor showed high correlation for all cations and silica. This factor represented the characteristics of the simple rock dissolution trend with 65% of the proportionate contribution. The second largest factor took positive loadings for Na^+, K^+ and Si, and negative loadings for Mg^{2+} and Ca^{2+}. The second factor indicated the ion-exchange between (Na^+, K^+) and (Ca^{2+}, Mg^{2+}) trend with 16% of the proportionate contribution.

5.3. Interpretation of the factor structure

5.3.1. Cation and silicon behavior

The stability diagrams of $(a_{Cation+} / a_{H+}) - (a_{Si})$ and the comparison between the theoretical and the real solution showed that the above first factor was interpreted as rock dissolution (chemical weathering) followed by precipitation of secondary minerals:

$$\text{Silicate minerals} + H^+ \rightarrow M^+ + H_4SiO_4 + \text{Clay (gibbsite/kaolinite etc)}$$

In Norikura area, two major types of chemical weathering were supposed; one was gibbsite (or its adjacent minerals) yielding reaction as secondary mineral, and the other was kaolinite (or its adjacent minerals) yielding reaction. Thermodynamic calculation showed that the waters in the summit area were plotted in the gibbsite coexistent area in the stability diagram, whereas the waters in the mountainside area were plotted in the kaolinite area. Stoichiometric calculation based on the cations/silicon ratio gave the same results as the thermodynamic calculation. This

theoretical model derived the following predictive equation for silicon concentration.

Summit area; gibbsite dominant as a secondary mineral

$$[Si] = 3\,[Na^+] + 3\,[K^+] + [Mg^{2+}] + 2\,[Ca^{2+}]$$

Mountainside area; kaolinite dominant as a secondary mineral

$$[Si] = 2\,[Na^+] + 2\,[K^+] + [Mg^{2+}]$$

The chemical concentrations in the real solutions were well fitted to the above predictive equation. Those facts successfully certified the validity of this theoretical model.

5.3.2. Relation between (Ca^{2+}, Mg^{2+}) - (Na^+, K^+)

The stability diagram of (a_{Ca2+}/a^2_{H+}) - (a_{Na+}/a_{H+}) showed that the non-geothermal surface waters were plotted on a straight line, which was expressed by the following equation.

$$\log (a_{Ca2+}/a^2_{H+}) = 2 \times \log (a_{Na+}/a_{H+}) + 4.5$$

This equation is converted into the following equation.

$$\log (a_{Ca2+}/a^2_{Na+}) = \log K \quad (\log K = 4.5)$$

This correlation was interpreted that Ca^{2+} and Na^+ in the surface waters were possibly in the transitional equilibrium on an unknown ion-exchangeable phase (clay mineral).

$$2(Na^+, K^+) + (Ca^{2+}, Mg^{2+})\text{-}Clay_2 = (Ca^{2+}, Mg^{2+}) + 2(Na^+, K^+)\text{-}Clay$$

On the other hand, the logarithmic value of the equilibrium constant on the Na-Ca smectite phases, which is the most typical ion-exchangeable clay mineral, is -1.25 ($\log K = -1.25$). The equilibrium constant of smectites is far smaller than the above constant value. Therefore, the high correlation between (a_{Ca2+}/a^2_{H+}) and (a_{Na+}/a_{H+}) seems to be controlled by an ion-exchangeable solid phase, other than smectites. Further study is needed to interpret this chemical relation.

5.4. Water chemistry in Shirasu ignimbrite area

The same methods as above (i.e., multivariate analysis, thermodynamic and stoichiometric calculation) were performed on the river waters in the other volcanic area, Shirasu ignimbrite area. The multivariate analysis showed that the major hydrochemical factor is the dissolution of Shirasu ignimbrite, despite the existence of many hot spring discharges and a municipal region in the catchment area. The combination of stability diagrams and stoichiometric calculation led to a predictive equation for silicon concentration under consideration of chemical weathering followed by the formation of clay minerals. The silicon predictive equation is expressed as $[Si] = 2\ [Na^+] + [Mg^{2+}]$ (kaolinite precipitation region) in most of the Kotsuki River samples. Only in the limited downstream area, above predictive equation is complemented by $[Si] = [Na^+] - 3\ [K^+] + [Mg^{2+}] - 2\ [Ca^{2+}]$ (pyrophyllite precipitation region).

5.5. Epilogue

Above bunch of calculation showed that water chemistry in volcanic area, which characterizes Japanese hydrochemistry, is mainly controlled by the chemical interaction between silicate rocks and water. Consequently, the chemical behavior of silicon, a good indicator of silicate dissolution, would be an essential key to understand the chemical property of surface water in Japan. Caution may be needed when we apply the continental techniques, such as Piper plot or Stiff diagram, to investigate chemistry of Japanese waters. Those continental techniques have been developed to discuss the influence of airborne sea salt, dissolution of limestone and evaporite, but do not concern the chemical weathering of silicate rocks.

Acknowledgment

I wish to express my hearty thanks to Prof. Hiroo OHMORI, The University of Tokyo for many helpful suggestions and financial support throughout the entire course of the work. It has been a great pleasure to work under his supervision for over six years. I also express my sincere thanks to Prof. Shinichiro OHGAKI, Prof. Masahiko OHSAWA, Associate Prof. Jun MATSUMOTO, Associate Prof. Toshihiko SUGAI, The University of Tokyo for their critical discussions and helpful comments.

I thank Mr. Tsuyoshi Ohta, Dr. Hisao J. Iguchi, Mr. Taichi Furuhashi, Mr. Munehiro Yoshida, members of Alliance for Global Sustainability project of University of Tokyo; Mr. Hisanori ARAYA, Ms. Yoko ISHIDA, Mr. Takuji KIYOHARA, Department of Earth and Environmental Sciences, Kagoshima University, for their cooperation during the sample collections.

My sincere thanks are due to all the members of the Environmental Analysis laboratory, Department of Earth and Environmental Sciences, Kagoshima University for their help; Ms. Yurie KAWABATA, Mr. Masaomi GOTO, Mr. Yoshitsugu ARAMAKI, Mr. Hiroaki ISHIKAWA, Mr. Junpei KAMATA, Ms. Seiko YANO.

The author gratefully acknowledges the help of Ms. Jeneper Lo, Dr. Hayao SAKAMOTO, and Dr. Takashi TOMIYASU, Graduate School of Science and Engineering, Kagoshima University, for helpful comments.

I would like to thank the staff and graduate students in the Institute of Environmental Studies, Graduate school of Frontier Sciences, The University of Tokyo.

I can not help expressing my hearty thankfulness to my wife and family who consistently support me financially and spiritually.

References

Ahrens, L.H., 1954. The lognormal distribution of the elements. Geochim. Cosmochim. Acta 5, 49-73.

Alaton, I. 1999. New York Times, New York Times Co., February 28, 1999

Anazawa, K. and Ohmori, H., 2001. Chemistry of surface water at a volcanic summit area, Norikura, Central Japan: Multivariate statistical approach. Chemosphere 45, 807-816.

Anazawa, K. and Ohmori, H., 2005. The hydrochemistry of surface waters in andesitic volcanic area, Norikura volcano, Central Japan, Chemosphere, 59, 605-615.

Anazawa, K. and Yoshida, M., 1994. Volatile contents in Japanese volcanic rocks: Application of multivariate analysis. Geochem. J., 28, 307-315.

Anazawa, K. and Yoshida, M., 1997. Multivariate analysis of Japanese volcanic rocks: Volatile and major elements. Geochem. J. 30, 355-372.

Anazawa, K., Kaida, Y., Shinomura, Y., Tomiyasu, T. and Sakamoto, H., 2004. Heavy Metal Distribution in River Waters and Sediments around a "Firefly Village", Shikoku, Japan: Application of Multivariate Analysis. Anal. Sci., 20, 79-84.

Anazawa, K., Ohmori, H., Tomiyasu, T. and Sakamoto, H., 2003. Hydrochemistry at a volcanic summit area, Norikura, central Japan. Geochim. Cosmochim. Acta, 67(18S), 17.

Andrews, J. E., Brimblecombe, P., Jickells, T. D. and Liss, P. S., 1995. An Introduction to Environmental Chemistry. Blackwell Science, Cambridge, Massachusetts, USA, 90.

Baca, R.M. and Threlkeld, S.T., 2000. Inland dissolved salt chemistry: statistical evaluation of bivariate and ternary diagram models for surface and subsurface waters. J. Limnol. 59, 156-166.

Ball J. W. and Nordstrom D. K., 1991. User's manual for WATEQ4F, with revised thermodynamic data base and test cases for calculating speciation of major, trace, and redox elements in natural waters. USGS Open File Report, 91–183.

Berner, E.K., Berner, R.A., 1996. Global Environment. Prentice Hall, New York.

Berner, R.A., 1971. Principles of Chemical Sedimentology, McGraw- Hill, New York, 240.

Brewer, P.G., 1975. Minor elements in sea water. In: Chemical Oceanography (eds. J.P.

Riley and G. Skirrow), Academic Press, vol.1, pp.415-496.

Brown, C.E., 1998. Applied Multivariate Statistics in Geohydrology and Related Sciences, Springer, New York.

Chemical Society of Japan (Ed.), 1984. Kagaku Binran (Kisohen 2), 3th Ed., Maruzen, pp.2-308.

Chen, Y., Brantley, S.L., 2000. Dissolution of forsteritic olivine at 65C and 2 < pH < 5. Chemical Geology, 165, 267-281.

Chou, L. and Wollast, R., 1989. Is the exchange reaction of alkali feldspars reversible? : (Comments on "Thermodynamic and kinetic constraints on reaction rates among minerals and aqueous solutions. III. Activated complexes and pH-dependence of the rates of feldspar, pyroxene, wollastonite, and olivine hydrolysis" by W. M. Murphy and H. C. Helgeson), Geochim. Cosmochim. Acta 53, 557-558.

Clarke, F.W., 1924. U.S. Geol. Survey. Bull. Washington, D.C., U.S.A. 770, P.841.

Cross, W., Iddings, JP., Pirsson, LV. and Washington, HS., 1902. A quantitative chemico-mineralogical classification and nomenclature of igneous rocks. J. Geol., 10, 555-690.

Davis, J.C., 1986. Statistics and Data Analysis in Geology, 2nd ed. John Wiley & Sons, New York, 468-574.

Dove, P.M., Crerar, D.A., 1990. Kinetics of quartz dissolution in electrolyte solutions using a hydrothermal mixed flow reactor. Geochim. Cosmochim. Acta 54, 955-969.

Drever, J.I. (1988) The Geochemistry of Natural Waters, 2nd. ed.: Prentice Hall, New Jersey.

Felmy, A.R., Girvin, D.C. and Jenne, E.A., 1984. MINTEQ—A Computer Program for Calculating Aqueous Geochemical Equilibria (N.T.I.S. No. EPA-600/3-84-032), US Department of Commerce, Springfield, VA.

Fujita, S., Sakamoto H., 2001. Geochemical Interpretation on Hydrothermal System in Kagoshima City and its Northern Area, J. Balneological Soc. Japan (Onsenkagaku) 51, 11-20 (in Japanese).

Garrels, R.M, and Mackenzie, F.T., 1967, Origin of the chemical composition of springs and lakes, in Equilibrium concepts in natural water systems: Am. Chem. Soc., Advances in Chem. Series no. 67(ed. R.F. Gould), pp. 222-24

Garrels, R.M. and Christ, C.L., 1965. Solutions, minerals, and equiliburia. Harper & Row and John Weatherhill, Inc., pp.450.

Garrels, RM, 1967. Genesis of some groundwaters from igneous rocks. In: Abelson P.H.

(ed.), Researches in Geochemistry, 2, John Wiley & Sons, 405-420.

Geological Survey of Japan (GSJ), 1982. Geological Atlas of Japan, 119 pp

Gibbs R.J., 1970. Mechanisms controlling world water chemistry. Science 170, 1088-1090.

Gibbs,R.J., 1972. Water chemistry of the Amazon River. Geochim.Cosmochim.Acta, 36, 1061-1066.

Gieske, A., Miranzadeh, M. and Mamanpoush, A., 2000. Groundwater Chemistry of the Lenjanat District, Esfahan Province, Iran. Iranian Agricultural Engineering Research Institute

Esfahan Agricultural Research Center, International Water Management Institute, Research Report No. 4."

Goldich, S.S., 1938. A study in rock weathering. J. Geol. 46, 17-58.

Hanya, T., 1951. Int. Assoc. Hydrology, Brussels Assembly, 1.

Hara, H., 1999. Acid rain - Interpretation of ion composition. Chemical Education 47, 124-127 (in Japanese).

Helgeson, H.C., Delany, J.M.,Nesbitt,H.W. and Bird,D.K., 1978. Summary and critique of the thermodynamic properties of rock-forming minerals. Am.J.Sci,278-A,1-220.

Howard, A.G., 1998. "Aquatic Environmental Chemistry", Oxford University Press, UK.

Ishikawa, K., Yoshida, T. and Aoki, K., 1992. Ejecta geochemistry of Norikura volcano, Central Japan. Res.Rep.Lab.Nuc.Sci.Tohoku Univ. 25, 227-240 (in Japanese).

Iwatsuki, T. and Yoshida, H., 1999. Groundwater chemistry and fracture mineralogy in the basement granitic rock in Tono uranium mine area, Gifu Prefecture, Japan ?Groundwater composition, Eh evolution analysis by fracture filling minerals-. Geochem. J. 33, 19-32.

Iwatsuki,T., Sato,K., Seo,T. and Hama,K., 1995. Hydrogeochemical investigation of groundwater in the Tono area, Japan, Proc. Mat. Res. Soc. Symp., 23-27 Oct 1994, Kyoto, Japan 353, 1251-1257.

Japan Nuclear Cycle Development Institute (JNC), 2000. H12: Project to establish the scientific and technical basis for HLW disposal in Japan, Supplementary Report: Background of Geological Disposal. JNC TN1410 2000-005, 2000.

Japan Nuclear Cycle Development Institute (JNC), 2000. H12: Project to establish the scientific and technical basis for HLW disposal in Japan, Supporting

Report 3: Safty Assessment of Geological Disposal System. JNC TN1410 2000-004, 2000.

Japan Nuclear Cycle Development Institute (JNC), 2000. H12: Project to establish the scientific and technical basis for HLW disposal in Japan. Project Overview Report. JNC TN1410 2000-001.

Japan Nuclear Cycle Development Institute (JNC), 2000. H12: Project to establish the scientific and technical basis for HLW disposal in Japan. Supporting Report 1: Geological Environment in Japan.JNC Tech. Rep., JNC TN1410, 2000-02.

Japan Nuclear Cycle Development Institute (JNC), 2000. H12: Project to establish the scientific and technical basis for HLW disposal in Japan. Supporting Report 2: Repository Design and Engineering Technology.JNC Tech. Rep., JNC TN1410, 2000-03.

Johnson, J.W., Oelkers E.H., and Helgeson, H.C., 1992. SUPCRT92: A software package for calculating the standard molal thermodynamic properties of minerals, gases, aqueous species, and reactions from 1 to 5000 bars and 0 to 1000 °C, Computers Geosci. 18. pp. 899-947.

Johnson, R.A. and Wichern, D.W., 2002. Applied multivariate statistical analysis, 5th ed. Prentice Hall, 607p.

Kamei, G., Yusa, Y. and Arai, T., 1999. A natural analogue of nuclear waste glass in compacted bentonite. Applied Geochemistry 15, 153-167.

Kawakami, T., 1996. "Research on the processes which determine the acid-base status of the extremely diluted lakes in the Norikura alpine area.", Doctoral Dissertation, University of Tokyo (in Japanese).

Kehew, AE., 2001. "Applied Chemical Hydrogeology", Prentice-Hall, Upper Saddle River, New Jersey, 368pp.

Kelsey, C.H., 1965. Calculation of the CIPW norm, Mineralogical Magazine 34, 276-282.

Kobayashi, J., 1961. A chemical study on the average quality and characteristics of river waters of Japan. Nogaku Kenkyu 48, 63-106(in Japanese).

Kobayashi, S., Sakamoto, T. and Kakitani, S., 1993. Artificial alteration of granite under earth surface conditions. -Studies on the influence of acid rain on rocks and minerals (part 2)-. J. Clay Sci. Soc. Jpn. 33, 81-91.

Laaksoharju, M., Gurban, I., and Skarman, C., 1998. Summary of hydrochemical conditions at Aberg, Beberg and Ceberg, SKB Technical Report 98-03, SKB Stockholm.

Laaksoharju, M., Skarman, C. and Skarman, E., 1999. Multivariate mixing and mass balance (M3) calculations, a new tool for decoding hydrogeochemical information, Applied Geochem., 14, 1999, 861-871.

Langmuir, D., 1997. "Aqueous Environmental Geochemistry", Prentice-Hall, Upper Saddle River, 600 pp.

Lauria, D.C. and Godoy, J.M., 2002. Abnormal high natural radium concentration in surface waters. J. Environ. Radioactiv., 61, 159-168.

Livingstone, D.A., 1963. Chemical composition of rivers and lakes. In: Inorganic Geochemistry (ed. Henderson, P.), Pergamon Press, pp.263.

Martin, J.M. and Meybeck, M., 1979. Elemental mass-balance of material carried by major world previous termrivers. Marine Chem, pp. 173–206.

Meybeck, M., 1979. Rev. Geol. Dyn. Geogr. Phys., 21, 215.

Minami, Y. and Ishizuka, Y., 1996. Evaluation of chemical composition in fog water near the summit of a high mountain in Japan. Atmospheric Environment 30, 3363-3376.

Ministry of the Environment of Japan, 1999. Technical Report for a Five-Year Study (Phase 3 Survey) of Acid Deposition, Ministry of the Environment, Japan.

Ministry of the Environment of Japan, 2002. Environmental White Paper, Ohkurasyo, Tokyo, Japan, pp. 87–118.

Ministry of the Environment of Japan, 2002. Technical Report for a Three-Year Study (Phase 4 Survey) of Acid Deposition, Ministry of the Environment, Japan.

Ministry of the Environment of Japan, 2004. Environmental White Paper, Ohkurasyo, Tokyo, Japan.

Moriya, I., 1983. Eruptive prediction from the Holocene tephra layers of Norikura, Kusatsu-Shirane and Hakusan volcanoes. In: Kobayashi, T. Ed. , Reports of education through a Grant-in-Aid for Scientific Research, No. 57020017, 53-68 (in Japanese).

Nakano, S., Fukuoka, T., Aramaki, S., 1987. Trace element abundances in the Quaternary volcanic rocks of the Norikura volcanic chain, central Honshu, Japan. Geochem. J. 21, 169-172.

Nakano, S., Otsuka, T., Adachi, M., Harayama, S., Yoshioka, T., 1995. Geology of the Norikuradake district, quadrangle series. Kanazawa 10, Geol. Surv. Japan (in Japanese with English abstract).

Nambu, K., Kuniomatsu, T. amd Kyuma, K., 1994. Rates of soil acidification under different patterns of nitrogen mineralization. Soil Sci. Plant Nutr. 40, 95-106.

Négrel, P. and Lachassagne, P., 2000. Geochemistry of the Maroni River (French Guiana) during the low water stage: implications for water–rock interaction and groundwater characteristics. J. Hydrol., 237, 212-233.

Nesbitt, H.W., Wilson, R.E., 1992. Recent chemical weathering of basalts. Am. J. Sci. 292, 740-777.

Ogura, N, Ichikuni, M., 2001. Environmental Chemistry, pp.152, Shokabo, Tokyo

Ohmori, H., Saito, K., Haruyama, S., Ouchi, S., Kubo, S. and Sugai, T., 2001. Fluvial and Tectonic Landforms in Central Japan: Kanto and Chubu District. Department of Natural Environmental Studies. University of Tokyo, pp.119.

Parkhurst, D.L. and Appelo, C.A.J., 1999. User's guide to PHREEQC (Version 2)—a computer program for speciation, reaction-path, 1D-transport, and inverse geochemical calculations. US Geological Survey Water Resource Investigation Report 99-4259, 312pp.

Piper, A.M., 1944. A graphic procedure in the geochemical interpretation of water analyses, Transactions American Geophysical Union 25, 914–923.

Reimann, C., Filzmoser, P. and Garrett, R.G., 2002. Factor analysis applied to regional geochemical data: problems and possibilities. Applied Geochem., 17, 185-206.

Sakurai, T., Kazuo, K. and Yamada, T., 1998. Characteristics of River Water Quality in Relation to Geological Environments at the Eastern Foot of the Hida Mountains, Jpn. J. Limnol. 59, 87-100.

Santos, JS., Oliveira, E., Bruns, RE., and Gennari, RF., 2004. Evaluation of the salt accumulation process during inundation in water resource of Contas river basin (Bahia-Brazil) applying principal component analysis. Wat. Res., 38, 1579-1585.

Sasamoto, H., Yui, M. and Arthur, R.C., 2004. Hydrochemical characteristics and groundwater evolution modeling in sedimentary rocks of the Tono mine, Japan. Phys. Chem. Earth, 29, 43-54.

Seo, T. and Shimizu, K., 1992. Literature survey and analysis of groundwater geochemistry in Japan. PNC Technical Report, PNC-TN 7410, 92-017 (in Japanese).

Shikazono, N., 1999. Interpretation of Groundwater Chemistry and Weathering due to Mineral-Rainwater-Groundwater Interaction. J. Clay Sci. Soc. Jpn. 38, 145-152.

Shock, E.L., 1998. SLOP98 database. ftp://128.252.144.34/pub/slop98.dat.

Shock, E.L and Helgeson, H.C., 1988. Calculation of the thermodynamic an transport properties of aqueous species at high pressures and temperatures: correlation algorithms for ionic species and equation of state predictions to 5 kb and 1000°C. Geochim. Cosmochim. Acta 53, pp. 2009–2036.

Shock, E.L, Helgeson, H.C. and Sverjensky, D.A., 1989. Calculations of the thermodynamic and transport properties of aqueous species at high pressures and temperatures: standard partial molal properties of inorganic neutral species. Geochim. Cosmochim. Acta 53, pp. 2157–2183.

Simeonov, V., Sarbu, C., Massart, D.L., and Tsakovski, S., 2001. Danube river water data modeling by multivariate data analysis. Mikrochim. Acta 137, 243-248.

Singh, KP., Malik, A., Mohan, D., and Sinha, S., 2004. Multivariate statistical techniques for the evaluation of spatial and temporal variations in water quality of Gomti River (India) a case study. Wat. Res., 38, 3980-3992.

Stiff, H.A., 1951. The interpretation of chemical analysis by means of patterns. J Petrol Technol 3, 15–17.

Stillings, L.L., Brantley, S.L., 1995. Feldspar dissolution at 258C and pH 3: reaction stoichiometry and the effect of cations. Geochim. Cosmochim. Acta 59, 1483-1496.

Sugawara,K., 1964. Migration of elements through phases of the hydrosphere and atmosphere. In: Vinogradov,A.P.(ed.) Khimiya Zemnoi Kory, Vol. II., Transl. 1967 by Israel Program for Scientific Translation.

Takagi, M., Tanaka, T., Asahara, Y. Aoki, K. and Amano, K., 2001. Chemical weathering of rocks in the view of Sr isotopic ratio: Study of groundwater at Kamaishi mine. Chikyukagaku, 35, 61-72(in Japanese).

Takemura, M., 1985. Classification of river waters in different parent rocks from their chemical compositions. Jpn. J. Limnol. 46, 128-134 (in Japanese).

Tamari, Y., Tsuji, H. and Kusaka, Y., 1988. Relation between land-water quality and its surrounding geology: Analysis from leaching experiments of rocks. Chikyukagaku 22, 139-147 (in Japanese).

Turekian, K.K., 1969."Handbook of Geochemistry", Vol.1, Chapt. 10, Springer Verlag, Berlin, P.297.

van Helvoort, PJ., 2003. Complex confining layers: A physical and geochemical characterization of heterogeneous unconsolidated fluvial deposits using a facies-based approach. Utrecht: KNAG/FRW, UU. pp.49-75.

Vega, M., Pardo, R., Barrado, E. and Deban, L., 1998. Assessment of seasonal and

polluting effects on the quality of river water by exploratory data analysis. Wat. Res. 32, 3581-3592.

White, A.F., Bullen, T.D., Davison, V.V., Schulz, M.S., Clow, D.W., 1999. The role of disseminated calcite in the chemical weathering rate of grainitoid rocks. Geochim. Cosmochim. Acta 63, 1939-1953.

Wogelius, R.A., Walther, J.V., 1991. Olivine dissolution at 258C:Effects of pH, CO , and organic acids. Geochim. Cosmochim. 2 Acta 55, 943-954.

Wogelius, R.A., Walther, J.V., 1992. Olivine dissolution kinetics at near-surface conditions. Chemical Geology 97, 101-112.

World Water Assessment Program, 2003. Water for People Water for Life:next term The United Nations World Water Development Report. UNESCO Publishing, Paris.

Wu, G., Toda, H., Haibara, K. and Aiba, Y., 1998. The effects of nitrogen mineralization on water-soluble ions of forest soils. J. Jpn. For. Soc. 80, 21-26 (in Japanese).

Yokoyama, S., 1999. Rapid formation of river terraces in nonwelded ignimbrite along the Hishida Riber, Kyushu, Japan. Geomorphology 30, 291- 304.

Appendix A. Thermochemical data

Table A.Thermochemical data at 25℃ and 1 bar total pressure.

Mineral	Chemical Formula	Abbreviation	ΔG(cal/mol)	ΔH(cal/mol)	S(cal/K mol)	Reference
ALBITE,LOW	$Na(AlSi_3)O_8$	Lo-Ab	-886,308	-939,680	49.51	1)
ANORTHITE	$Ca(Al_2Si_2)O_8$	An	-954,078	-1,007,552	49.1	1)
CLINOCHLORE,7A	$Mg_5Al(AlSi_3)O_{10}(OH)_8$	7A-Cnc	-1,957,101	-2,113,197	106.5	1)
CLINOCHLORE,14A	$Mg_5Al(AlSi_3)O_{10}(OH)_8$	14A-Cnc	-1,961,703	-2,116,964	111.2	1)
GIBBSITE	$Al(OH)_3$	Gbs	-276,168	-309,065	16.75	1)
K-FELDSPAR	$K(AlSi_3)O_8$	K-Fs	-895,374	-949,188	51.13	1)
KAOLINITE	$Al_2Si_2O_5(OH)_4$	Kln	-905,614	-982,221	48.53	1)
LAUMONTITE	$Ca(Al_2Si_4)O_{12}*4H_2O$	Lmt	-1,596,823	-1,728,664	116.1	1)
MUSCOVITE	$KAl_2(AlSi_3)O_{10}(OH)_2$	Ms	-1,336,301	-1,427,408	68.8	1)
PYROPHYLLITE	$Al_2Si_4O_{10}(OH)_2$	Prl	-1,255,997	-1,345,313	57.2	1)
Amorphous Silica	SiO_2	Amor-Si	-202892	-214568	14.34	1)
Na^+	Na(+)	Na^+	-62,591	-57,433	13.96	2)
Ca^{+2}	Ca(+2)	Ca^{2+}	-132,120	-129,800	-13.5	2)
Mg^{+2}	Mg(+2)	Mg^{2+}	-108,505	-111,367	-33	2)
K^+	K(+)	K^+	-67,510	-60,270	24.15	2)
H_2O	H_2O	H_2O	-56.6874			3)
H_4SiO_4	H_4SiO_4	H_4SiO_4	-312.8			4)

[1] Helgeson et al. (1978), [2] Shock and Helgeson (1988), [3] Chemical Society of Japan (1984), [4] Berner (1971).

Appendix B. Source data

Table B-1. Chemical composition of Norikura water samples.

No.	Site	Date	pH	EC	Na	K	Mg	Ca	Si	Cl	NO_3	SO_4	Altitude
				mS/m	mg/dm^3	mg/dm^3	mg/dm^3	mg/dm^3	mg/dm^3	mg/dm^3	mg/dm^3	mg/dm^3	m
1	O	99/05/29	4.86	-	0.05	0.11	0.00	0.20	0.01	0.08	0.08	0.01	2730
2	O	99/05/29	4.86	-	0.42	0.00	0.02	0.05	0.01	0.06	0.19	0.13	2730
3	O	99/05/30	4.86	-	0.34	0.09	0.00	0.04	0.03	0.17	0.02	0.06	2700
4	O	99/07/16	4.86	-	0.24	0.13	0.00	0.01	0.56	0.12	0.02	0.01	2710
5	O	99/07/17	4.86	-	0.00	0.09	0.00	0.01	0.24	0.11	0.07	0.01	2840
6	O	99/07/17	4.86	0.2	0.12	0.00	0.00	0.05	0.07	0.20	0.18	0.06	2840
7	O	99/07/18	4.86	-	0.03	0.11	0.01	0.01	0.01	0.06	0.18	0.12	2770
8	O	99/09/29	4.86	0.6	0.59	0.00	0.04	0.01	0.65	0.23	0.17	0.11	2750
9	O	00/06/12	4.86	0.1	0.08	0.04	0.03	0.03	0.01	0.10	0.05	0.15	2780
10	O	00/06/12	4.86	-	0.00	0.00	0.00	0.07	0.04	0.02	0.02	0.02	2733
11	O	00/06/12	5.5	0.3	0.08	0.03	0.08	0.11	1.07	0.13	0.02	0.10	2733
12	O	00/06/13	4.86	0.2	0.07	0.00	0.01	0.01	0.04	0.24	0.19	0.28	2694
13	O	00/06/13	4.86	0.5	0.00	0.00	0.00	0.11	0.01	0.03	0.57	0.47	2770
14	O	00/06/13	4.86	0.3	0.06	0.03	0.04	0.01	0.01	0.20	0.20	0.29	2770
15	O	00/06/14	4.86	0.2	0.01	0.00	0.00	0.11	0.01	0.03	0.12	0.27	2770
16	O	00/06/14	4.86	0.3	0.05	0.03	0.00	0.01	0.01	0.10	0.39	0.73	2770
17	O	00/09/10	4.96	-	0.10	0.07	0.03	0.01	0.17	0.16	0.02	0.02	2733
18	O	00/09/10	4.96	-	0.10	0.02	0.02	0.11	0.43	0.27	1.05	0.06	2725
19	O	00/09/11	4.86	0.1	0.00	0.01	0.00	0.01	0.01	0.25	0.03	0.14	2770
20	A	99/07/16	5.1	0.3	0.00	0.11	0.00	0.10	0.76	0.08	0.32	0.35	2845
21	A	99/07/17	5.1	0.4	0.07	0.11	0.01	0.07	0.62	0.10	0.28	0.42	2845
22	A	99/07/17	5.1	0.4	0.00	0.12	0.00	0.07	0.62	0.10	0.27	0.39	2845
23	A	99/07/17	5.1	0.4	0.23	0.12	0.02	0.12	0.64	0.10	0.27	0.36	2845
24	A	99/07/17	5.1	0.3	0.26	0.10	0.00	0.14	0.64	0.14	0.18	0.40	2845
25	A	99/09/03	5.1	0.3	0.46	0.00	0.04	0.02	0.58	0.24	0.02	0.51	2845
26	A	99/09/03	5.1	0.3	0.52	0.00	0.04	0.13	0.52	0.22	0.17	0.50	2845
27	A	99/09/30	5.1	0.4	0.58	0.00	0.04	0.01	1.29	0.31	0.17	0.54	2845
28	A	00/06/12	5.1	0.5	0.24	0.08	0.06	0.58	0.73	0.26	0.98	1.87	2845
29	A	00/06/12	5.86	0.5	0.15	0.06	0.05	0.66	0.65	0.14	0.02	0.72	2733
30	A	00/06/13	5.46	0.4	0.10	0.09	0.04	0.58	0.18	0.18	0.02	0.95	2694
31	A	00/06/13	5.86	0.5	0.22	0.10	0.07	0.78	1.45	0.20	0.59	1.08	2730
32	A	00/06/13	5.15	0.2	0.07	0.04	0.01	0.09	0.28	0.12	0.02	0.17	2760
33	A	00/06/13	5.2	0.2	0.06	0.04	0.02	0.18	0.21	0.11	0.08	0.35	2740
34	A	00/06/13	5.1	0.5	0.13	0.05	0.03	0.28	0.34	0.16	0.46	0.80	2717
35	A	00/06/14	5.1	0.5	0.08	0.04	0.02	0.19	0.50	0.11	0.02	0.42	2770
36	A	00/06/14	5.1	0.3	0.07	0.04	0.02	0.62	0.53	0.06	0.02	0.49	2770
37	A	00/06/17	5.11	-	0.18	0.07	0.04	0.30	0.75	0.22	0.70	1.30	2845
38	A	00/09/09	5.87	0.5	0.14	0.11	0.03	0.33	0.38	0.19	0.22	1.45	2694
39	A	00/09/10	5.86	0.3	0.09	0.03	0.02	0.22	0.82	0.14	0.02	0.36	2733
40	A	00/09/10	5.43	0.3	0.12	0.02	0.01	0.18	0.40	0.15	0.02	0.60	2717

Table B-1. Chemical composition of Norikura water samples. (cont-)

No.	Site	Date	pH	EC	Na	K	Mg	Ca	Si	Cl	NO_3	SO_4	Altitude
				mS/m	mg/dm^3	mg/dm^3	mg/dm^3	mg/dm^3	mg/dm^3	mg/dm^3	mg/dm^3	mg/dm^3	m
41	A	00/09/10	5.25	0.4	0.13	0.02	0.01	0.10	0.27	0.21	0.12	0.95	2717
42	A	00/09/10	6.05	0.6	0.32	0.09	0.04	0.49	1.70	0.20	0.02	0.72	2717
43	A	00/09/10	5.16	0.4	0.06	0.02	0.01	0.03	0.11	0.18	0.17	0.40	2717
44	A	00/09/10	5.32	0.3	0.07	0.02	0.01	0.05	0.17	0.13	0.05	0.44	2717
45	A	00/09/10	5.2	0.3	0.03	0.01	0.00	0.01	0.04	0.15	0.02	0.22	2725
46	A	00/09/10	5.15	0.4	0.09	0.02	0.01	0.05	1.13	0.13	0.02	0.72	2760
47	A	00/09/10	5.15	0.5	0.11	0.04	0.01	0.10	0.36	0.25	0.02	0.48	2760
48	A	00/09/10	5.11	0.5	0.07	0.02	0.01	0.11	0.11	0.16	0.02	0.59	2845
49	A	99/05/29	5.3	-	0.32	0.25	0.02	0.51	0.20	0.31	0.16	0.42	2770
50	A	99/07/16	5.43	0.3	0.11	0.13	0.04	0.19	0.93	0.15	0.07	0.58	2717
51	A	99/07/16	5.25	0.3	0.08	0.08	0.02	0.12	0.26	0.07	0.02	0.41	2717
52	A	99/07/16	6.05	0.5	0.29	0.07	0.05	0.39	1.43	0.12	0.18	0.57	2717
53	A	99/07/16	5.16	0.3	0.16	0.15	0.00	0.10	0.03	0.14	0.24	0.30	2717
54	A	99/07/16	5.32	0.3	0.16	0.06	0.00	0.15	0.46	0.12	0.13	0.43	2717
55	A	99/07/16	5.16	0.3	0.00	0.00	0.00	0.01	0.01	0.11	0.16	0.22	2717
56	A	99/07/16	5.15	0.3	0.05	0.09	0.00	0.07	1.17	0.04	0.02	0.59	2760
57	A	99/09/04	5.43	1.7	0.68	0.00	0.04	0.22	0.74	0.32	0.21	0.66	2717
58	A	99/09/04	5.25	1.4	0.66	0.00	0.04	0.23	0.48	0.22	0.16	0.56	2717
59	A	99/09/04	6.05	1.4	0.62	0.05	0.05	0.64	0.54	0.24	0.22	0.40	2717
60	A	99/09/04	5.16	1.5	0.47	0.00	0.04	0.14	2.04	0.23	0.02	0.54	2717
61	A	99/09/04	5.32	1.5	0.72	0.00	0.04	0.13	0.85	0.27	0.02	0.64	2717
62	A	99/09/05	5.15	1.0	0.69	0.03	0.04	0.14	0.70	0.16	0.19	0.42	2760
63	A	99/09/05	5.15	0.9	0.61	0.00	0.04	0.20	1.47	0.16	0.23	0.42	2760
64	A	99/09/28	5.43	1.4	0.67	0.01	0.04	0.51	1.90	0.19	0.02	0.63	2717
65	A	99/09/28	5.25	0.3	0.64	0.15	0.04	0.02	0.63	0.17	0.17	0.41	2717
66	A	99/09/28	6.05	0.6	0.61	0.02	0.04	0.53	2.14	0.19	0.39	0.66	2717
67	A	99/09/28	5.16	0.3	0.43	0.00	0.04	0.08	0.51	0.24	0.16	0.32	2717
68	A	99/09/28	5.32	0.5	0.64	0.00	0.05	0.44	1.93	0.28	0.16	0.64	2717
69	A	99/09/28	5.15	0.3	0.59	0.00	0.04	0.05	1.23	0.22	0.19	0.50	2760
70	A	99/07/17	5.86	0.3	0.12	0.00	0.00	0.12	0.10	0.17	0.32	0.23	2740
71	A	99/07/17	5.86	0.4	0.13	0.16	0.05	0.23	1.84	0.12	0.15	0.22	2733
72	A	99/09/03	5.86	0.5	0.35	0.11	0.05	0.27	3.22	0.16	0.17	0.41	2733
73	A	99/09/03	5.86	1.0	0.53	0.11	0.09	0.71	8.51	0.50	0.21	0.53	2760
74	A	99/09/28	5.86	0.8	0.88	0.01	0.04	0.57	2.65	0.20	0.21	0.48	2760
75	A	99/09/28	5.86	0.7	0.65	0.11	0.05	0.52	3.39	0.21	0.16	0.37	2733
76	A	99/09/04	5.8	1.2	0.77	0.00	0.04	0.53	5.94	0.23	0.02	1.48	2650
77	A	99/09/04	5.8	1.2	0.83	0.00	0.09	0.70	7.01	0.24	0.26	1.60	2650
78	A	99/05/30	5.6	-	0.26	0.16	0.00	0.55	0.07	0.13	0.30	0.60	2694
79	A	99/09/29	5.6	0.6	0.61	0.06	0.04	0.43	1.50	0.25	0.21	0.01	2570
80	A	99/09/29	5.46	0.3	0.50	0.09	0.04	0.41	0.55	0.15	0.02	0.01	2694

Table B-1. Chemical composition of Norikura water samples. (cont-)

No.	Site	Date	pH	EC	Na	K	Mg	Ca	Si	Cl	NO_3	SO_4	Altitude
				mS/m	mg/dm^3	mg/dm^3	mg/dm^3	mg/dm^3	mg/dm^3	mg/dm^3	mg/dm^3	mg/dm^3	m
81	A	99/09/28	5.8	0.8	0.77	0.22	0.14	0.74	7.54	0.37	0.16	0.37	2740
82	A	99/09/28	5.8	0.9	0.84	0.17	0.11	0.69	6.80	0.18	0.58	1.76	2730
83	A	00/06/13	5.5	0.5	0.24	0.08	0.06	0.86	0.51	0.30	1.48	1.12	2620
84	A	00/06/13	5.5	0.5	0.08	0.05	0.02	0.78	0.09	0.13	0.02	0.29	2620
85	A	00/06/13	5	0.4	0.06	0.04	0.02	0.14	0.46	0.12	0.02	0.50	2740
86	A	00/09/10	5.58	0.5	0.23	0.07	0.03	0.30	1.33	0.17	0.28	0.62	2620
87	A	00/09/10	5.86	0.6	0.23	0.07	0.02	0.29	0.92	0.27	1.01	0.58	2620
88	A	00/09/10	5.9	0.3	0.11	0.04	0.01	0.22	0.55	0.16	0.44	0.44	2600
89	A	00/09/10	5.9	0.5	0.33	0.09	0.04	0.53	2.40	0.09	0.06	0.41	2600
90	A	00/09/10	6.02	1.1	0.60	0.35	0.09	0.95	9.54	0.20	0.02	2.77	2600
91	A	00/09/10	6.2	1.1	0.55	0.33	0.08	0.87	8.24	0.39	0.40	2.34	2600
92	A	00/09/10	6.14	0.5	0.17	0.04	0.02	0.31	1.40	0.13	0.31	0.75	2400
93	B	99/07/17	5.7	0.4	0.26	0.17	0.02	0.15	0.22	0.22	0.25	0.58	2610
94	B	99/07/17	5.7	0.5	0.35	0.18	0.04	0.35	1.76	0.16	0.33	0.55	2620
95	B	99/07/17	5.7	0.5	0.31	0.17	0.00	0.27	1.15	0.24	0.55	0.66	2620
96	B	99/09/03	5.7	0.8	0.26	0.02	0.07	1.11	1.88	0.27	0.21	1.07	2600
97	B	99/09/03	5.7	0.7	1.00	0.00	0.04	0.34	2.16	0.19	0.18	0.53	2610
98	B	99/09/03	5.7	0.6	0.37	0.00	0.06	0.49	2.73	0.21	0.02	0.36	2610
99	B	99/09/03	5.7	0.6	0.42	0.01	0.06	0.39	1.80	0.23	0.18	0.86	2600
100	B	99/09/03	5.7	0.8	0.56	0.13	0.05	0.38	3.81	0.20	0.35	0.77	2600
101	B	99/09/28	5.7	0.6	0.61	0.02	0.04	0.51	2.38	0.16	0.21	0.54	2640
102	B	99/09/28	5.7	0.9	0.65	0.07	0.04	0.32	1.72	0.18	1.11	0.56	2610
103	B	99/09/29	5.7	0.5	0.56	0.10	0.07	0.56	2.84	0.29	0.02	0.33	2600
104	B	99/09/29	5.7	0.6	0.58	0.02	0.04	0.51	3.25	0.21	0.30	0.47	2600
105	B	99/09/29	5.7	0.9	0.82	0.28	0.05	0.79	6.96	0.38	0.22	1.10	2640
106	B	99/09/29	5.7	0.3	0.49	0.00	0.05	0.09	0.26	0.17	0.18	0.33	2750
107	B	99/07/17	6.2	1.2	0.55	0.45	0.14	0.92	9.67	0.16	0.45	2.67	2600
108	B	99/07/17	6.2	1.2	0.58	0.43	0.12	1.00	6.24	0.23	0.83	2.01	2550
109	B	99/09/03	6.2	1.2	0.56	0.39	0.11	0.94	9.91	0.15	0.22	3.37	2600
110	B	99/09/03	6.2	1.1	0.64	0.34	0.04	0.77	8.25	0.23	0.31	2.02	2600
111	B	99/09/03	6.2	1.1	0.77	0.33	0.12	1.00	7.07	0.21	0.65	2.01	2600
112	B	99/09/29	6.2	1.2	0.94	0.42	0.12	0.99	10.12	0.19	0.35	2.42	2600
113	B	99/09/29	6.2	0.9	0.96	0.20	0.09	0.72	4.34	0.16	0.94	1.52	2700
114	C	00/06/14	6	0.4	0.17	0.11	0.04	1.01	0.70	0.12	0.19	0.88	2640
115	C	00/06/14	6	1.1	0.23	0.11	0.09	0.74	1.50	0.18	0.45	0.99	2550
116	C	00/06/14	6.1	1.0	0.20	0.27	0.08	0.48	0.50	0.35	0.90	0.98	2300
117	C	00/06/14	6.25	0.9	0.26	0.17	0.08	1.17	0.84	0.26	0.28	1.13	2200
118	C	00/06/14	6.1	0.6	1.98	1.48	0.46	3.21	12.70	0.29	0.02	6.22	1900
119	C	00/06/15	7.2	4.0	1.64	0.55	0.78	4.88	5.68	0.36	0.02	2.58	1450
120	C	00/06/15	7.49	5.6	1.21	0.60	1.01	6.83	5.85	0.31	0.04	11.31	1460

Table B-1. Chemical composition of Norikura water samples. (cont-)

No.	Site	Date	pH	EC	Na	K	Mg	Ca	Si	Cl	NO_3	SO_4	Altitude
				mS/m	mg/dm^3	mg/dm^3	mg/dm^3	mg/dm^3	mg/dm^3	mg/dm^3	mg/dm^3	mg/dm^3	m
121	C	00/06/15	7.4	6.4	1.58	0.45	0.85	9.28	3.41	0.33	0.02	5.83	1460
122	C	00/06/15	7.4	5.7	1.31	0.61	1.00	7.32	5.70	0.34	0.12	10.95	1460
123	C	00/06/15	7.4	3.5	1.40	0.33	0.55	4.83	3.12	0.31	0.08	2.78	1500
124	C	00/06/15	7.42	4.1	1.87	0.85	0.67	4.86	8.92	0.38	0.02	2.13	1550
125	C	00/06/15	7.29	3.9	1.74	0.99	0.58	4.45	9.99	0.33	0.02	5.88	1500
126	C	00/06/18	6.45	1.7	0.99	0.37	0.26	1.39	6.16	1.57	0.33	0.91	1800
127	C	00/06/18	4.7	3.1	1.25	0.53	0.42	2.07	6.87	0.19	0.20	10.68	1800
128	C	00/06/18	6.5	0.6	0.18	0.06	0.06	0.40	1.01	0.19	0.02	0.99	1750
129	C	00/09/10	5.67	3.0	1.66	0.77	0.30	2.07	12.48	0.22	0.24	9.53	2250
130	C	00/09/11	6	3.0	0.88	0.55	0.16	4.17	1.29	0.28	1.74	2.17	2550
131	C	00/09/11	6.25	1.0	0.32	0.18	0.08	1.26	1.49	0.25	0.05	1.03	2470
132	C	00/09/11	6.2	1.0	0.33	0.13	0.09	1.43	1.49	0.33	0.02	1.07	2200
133	C	00/09/11	6.15	1.6	0.40	0.35	0.14	2.26	1.99	0.43	0.45	1.30	2150
134	C	00/09/11	7	5.0	2.65	1.29	0.87	4.56	13.15	0.67	0.51	8.07	1950
135	C	00/09/11	7	2.4	0.85	0.68	0.33	3.22	1.51	0.35	0.02	0.79	1600
136	C	00/09/11	7.39	4.5	1.73	0.88	0.83	5.37	6.84	0.48	0.02	2.27	1550
137	C	00/09/11	7.4	6.7	1.58	0.48	0.84	10.07	3.22	0.45	0.90	5.74	1500
138	C	00/09/11	7.49	4.0	0.91	0.52	0.71	4.67	4.47	0.42	0.19	8.61	1500
139	C	00/09/11	7.4	4.1	1.47	0.45	0.68	5.28	3.22	0.46	1.07	2.98	1450
140	C	00/09/11	7.42	5.3	1.30	0.59	0.97	6.68	4.97	0.42	0.20	7.80	1440
141	C	00/09/13	7	7.6	3.48	1.28	1.69	7.52	14.20	1.70	0.05	11.11	1400
142	C	00/09/13	5.1	1.2	0.84	0.27	0.14	1.34	5.24	0.22	0.02	1.70	2080
143	C	00/09/13	5.3	5.4	3.14	1.19	1.39	4.42	17.52	0.59	0.03	4.28	2060
144	C	00/09/13	6	0.5	1.02	0.41	0.30	1.45	7.38	0.28	0.02	1.74	2060
145	C	00/09/13	6.4	5.7	2.06	0.99	0.68	3.14	15.25	0.29	0.13	19.97	1970
146	C	00/09/13	6	0.9	0.23	0.06	0.08	0.38	2.19	0.25	0.05	1.11	1960
147	C	00/09/13	6.4	0.6	0.22	0.07	0.06	0.46	1.92	0.23	0.05	0.69	1860
148	C	00/09/13	5.18	0.7	0.24	0.06	0.07	0.43	2.12	0.27	0.04	0.74	1860
149	C	00/09/13	5.18	0.8	0.28	0.08	0.06	0.87	1.86	0.42	0.17	1.47	1620
150	C	00/06/18	7	5.7	2.73	0.99	1.15	5.41	12.36	0.39	0.44	9.66	1450
151	C	00/06/18	7.75	6.8	2.21	0.80	1.64	7.83	7.14	1.14	0.56	11.13	1000
152	C	00/09/09	8.5	10.3	5.83	1.62	1.97	10.88	5.32	5.51	1.69	11.66	560
153	C	00/09/09	8.5	10.7	5.17	1.15	2.03	12.13	4.62	4.37	0.75	13.46	700
154	C	00/09/09	7.75	11.8	2.76	1.00	3.17	13.54	6.69	1.11	0.72	19.17	1000
155	D	00/06/16	7.49	2.6	1.17	0.17	0.75	2.90	3.55	0.54	0.18	0.83	1428
156	D	00/06/16	7.49	5.3	1.55	0.19	1.19	7.38	4.70	0.61	0.02	0.94	1400
157	D	00/06/16	7.6	4.4	1.51	0.31	1.44	5.52	4.94	0.95	1.07	1.16	1050
158	D	00/06/16	8.73	9.2	1.21	0.29	1.44	15.58	3.63	0.64	0.10	5.46	1000
159	D	00/06/16	6.86	6.1	0.79	0.27	1.17	8.31	3.46	1.37	0.02	5.22	900
160	D	00/06/16	7.2	3.0	2.13	0.69	0.57	2.99	7.66	0.59	0.22	0.90	1300

Table B-1. Chemical composition of Norikura water samples. (cont-)

No.	Site	Date	pH	EC	Na	K	Mg	Ca	Si	Cl	NO_3	SO_4	Altitude
				mS/m	mg/dm^3	mg/dm^3	mg/dm^3	mg/dm^3	mg/dm^3	mg/dm^3	mg/dm^3	mg/dm^3	m
161	D	00/06/16	7.2	3.3	2.11	0.24	0.50	3.86	4.82	0.63	0.02	1.85	1350
162	D	00/06/16	7.4	3.3	2.11	0.66	0.81	3.38	9.61	0.41	0.02	0.65	1350
163	D	00/06/16	7.4	2.5	1.06	0.32	0.80	2.76	3.38	0.32	0.02	2.62	1300
164	D	00/06/16	7.4	3.7	2.18	0.99	0.71	3.79	10.83	0.32	0.02	1.41	1320
165	D	00/06/16	7.4	5.8	2.41	0.84	1.59	5.67	9.36	0.31	0.02	8.84	1325
166	D	00/06/16	7.4	3.6	1.62	0.30	0.73	4.21	3.97	0.31	0.02	2.90	1350
167	D	00/06/16	7.4	7.7	1.92	0.92	3.61	6.44	8.90	0.41	0.02	5.90	1400
168	D	00/06/16	7.4	4.6	1.59	0.59	1.64	4.51	5.72	0.35	0.02	3.72	1400
169	D	00/06/16	7.4	2.1	1.45	0.32	0.40	2.07	3.84	0.38	0.02	1.48	1640
170	D	00/06/16	7.4	2.6	1.62	0.45	0.45	2.65	5.24	0.39	0.55	1.92	1417
171	D	00/09/14	7.5	2.6	1.14	0.20	0.76	2.79	3.67	0.98	0.73	1.13	1428
172	D	00/09/14	7.4	5.4	1.59	0.20	1.29	7.58	4.76	0.72	1.24	1.06	1420
173	D	00/09/14	7.6	4.0	1.37	0.32	1.23	4.17	4.82	1.49	3.44	1.05	1050
174	D	00/09/14	7.4	5.5	1.25	0.65	0.93	7.96	5.64	0.66	0.30	1.41	1200
175	D	00/09/14	7.16	3.1	1.68	0.71	0.63	2.71	8.81	0.39	0.02	4.58	1300
176	D	00/09/14	7.4	4.5	2.20	0.75	1.20	4.17	7.43	0.58	0.07	4.89	1325
177	D	00/09/14	7.46	4.2	1.34	0.52	1.59	4.01	4.91	0.78	0.22	3.49	1400
178	D	00/06/16	8.02	11.9	1.28	0.27	2.04	19.40	4.11	0.90	0.02	2.76	1000
179	D	00/06/16	8	11.4	1.47	0.31	2.18	17.70	4.07	1.92	0.13	4.01	900
180	D	00/06/16	8	12.3	1.56	0.34	2.31	18.61	4.22	1.87	0.22	4.30	800
181	D	00/06/16	8	11.7	2.10	0.92	2.16	16.94	6.44	2.00	0.91	4.28	750
182	D	00/06/16	7.84	9.5	3.34	1.21	2.60	11.02	7.29	1.88	1.64	4.14	700
183	D	00/06/16	7.41	10.9	2.66	1.17	2.23	14.29	7.14	2.02	1.71	4.09	650
184	D	00/06/16	7.61	8.2	2.48	0.94	1.86	10.49	5.78	1.69	1.23	4.07	600
185	D	00/09/14	8.73	9.5	1.14	0.30	1.56	15.79	3.72	0.67	0.94	5.66	1000
186	D	00/09/14	8.02	13.1	1.32	0.32	2.34	23.97	4.31	1.00	0.68	3.48	1000
187	D	00/09/14	8	10.9	1.49	0.35	2.33	20.96	4.16	1.65	1.03	4.70	900
188	D	00/09/14	6.86	6.3	0.80	0.28	1.31	9.15	3.51	1.58	0.79	5.25	900
189	D	00/09/14	7.8	9.4	2.69	1.20	2.16	12.27	5.19	2.24	3.16	4.72	760
190	D	00/09/14	7.8	8.6	2.12	1.25	2.11	11.57	5.12	1.25	0.70	5.14	760
191	D	00/09/14	7.8	7.6	1.60	0.42	2.53	9.63	4.54	0.96	2.19	3.25	730
192	D	00/09/14	7.8	8.2	2.29	0.41	2.79	9.90	6.25	1.05	6.20	2.34	730
193	D	00/09/14	7.84	5.8	1.90	0.43	1.93	6.31	4.97	1.54	3.20	2.04	900
194	D	00/09/14	7.6	3.3	2.12	0.79	0.81	2.79	6.27	1.44	1.50	1.00	750
195	D	99/06/04	8.6	8.6	4.14	0.92	1.66	9.68	4.95	3.80	0.50	10.36	700
196	D	99/06/04	8.7	8.6	4.37	0.99	1.60	8.81	5.16	3.93	0.41	9.83	650
197	D	99/06/04	8.68	9.2	4.85	1.18	1.70	9.54	5.26	4.43	0.78	11.15	560
198	E	99/09/28	7	2.9	1.83	0.19	0.92	2.53	5.50	0.36	0.06	1.96	1250
199	E	99/09/27	7	3.2	0.56	0.21	1.49	2.87	2.65	0.31	0.43	10.68	1350
200	E	99/09/28	6.4	10.0	1.52	0.20	3.22	13.51	2.96	0.23	0.09	4.97	1250

Table B-1. Chemical composition of Norikura water samples. (cont-)

No.	Site	Date	pH	EC	Na	K	Mg	Ca	Si	Cl	NO_3	SO_4	Altitude
				mS/m	mg/dm^3	mg/dm^3	mg/dm^3	mg/dm^3	mg/dm^3	mg/dm^3	mg/dm^3	mg/dm^3	m
201	E	99/09/27	6.4	7.4	1.56	0.25	2.83	11.83	3.95	0.27	0.07	7.80	1400
202	E	99/09/05	7	-	1.15	0.28	3.91	14.26	3.44	0.17	0.70	3.62	1250
203	E	99/07/16	7	13.3	1.35	0.46	1.30	9.97	9.68	0.96	0.70	15.26	1300
204	E	99/09/02	7	9.4	2.24	0.64	1.65	11.13	7.09	0.32	0.25	20.56	1400
205	E	99/09/28	7	15.2	0.90	0.23	6.23	22.10	2.51	0.09	0.38	3.39	1250
206	E	99/09/27	6.4	9.1	3.79	0.81	1.56	9.40	8.18	1.24	0.62	21.51	1400
207	E	99/09/05	4.9	-	0.84	0.14	6.88	23.96	2.22	0.85	0.26	3.11	1300
208	E	99/09/02	4.9	7.6	2.71	0.77	1.27	5.52	11.83	0.55	0.31	26.47	1400
209	E	99/09/02	6.4	-	2.18	0.87	1.55	7.25	10.63	0.69	0.41	26.18	1350
210	E	99/09/30	7	12.3	3.40	0.77	2.22	17.10	9.93	0.46	0.40	15.33	1300
211	E	99/09/02	7.9	13.2	3.12	0.82	2.40	18.14	9.93	0.55	0.30	14.72	1400
212	E	99/09/03	7.9	13.0	3.21	0.81	2.41	17.95	9.89	0.49	0.33	14.82	1250
213	E	99/07/15	4.9	8.0	2.19	0.80	1.21	5.18	11.29	0.31	0.61	28.22	1400
214	E	99/09/27	7.9	12.5	3.19	0.80	2.28	17.12	9.91	0.83	0.50	15.42	1400
215	E	99/09/27	7.5	8.7	2.45	0.73	1.32	5.62	11.19	0.17	0.32	31.42	1400
216	E	99/07/18	7.5	-	1.89	0.72	1.55	10.72	11.37	1.42	0.60	24.62	1250
217	E	99/07/15	7.5	12.7	2.82	0.79	2.31	18.76	9.66	1.00	0.73	15.27	1400
218	E	99/09/02	7.5	12.8	3.61	1.11	2.41	15.95	11.66	1.09	0.26	21.84	1250
219	E	00/06/14	7.9	10.7	3.05	0.73	1.98	15.34	8.22	1.02	0.74	12.34	1400
220	E	00/06/14	4.93	7.4	1.48	0.59	1.38	5.01	7.80	0.28	0.02	24.05	1400
221	E	00/06/14	6.4	8.5	3.65	0.86	1.38	9.27	7.39	1.15	0.73	20.74	1400
222	E	00/06/14	6.5	7.0	1.66	0.36	1.33	10.46	3.31	0.30	0.02	12.79	1400
223	E	00/06/14	5	20.2	2.13	0.66	4.27	27.69	4.34	0.38	0.02	39.56	1350
224	E	00/06/14	6.5	6.4	1.42	0.56	1.17	5.74	6.66	0.29	0.47	21.74	1350
225	E	00/06/14	6.5	7.2	1.80	0.62	1.61	7.99	6.29	0.66	0.31	20.80	1280
226	E	00/06/14	7	10.8	3.06	0.73	1.95	15.43	8.14	1.00	0.76	12.57	1250
227	E	00/06/15	8	13.4	7.74	1.27	3.09	12.35	7.38	5.74	0.29	23.48	1250
228	E	00/06/15	8.06	12.2	0.86	0.25	3.42	15.90	2.46	0.39	0.02	5.60	1300
229	E	00/06/15	7	5.9	1.39	0.56	1.38	7.35	5.44	0.32	0.05	9.31	1440
230	E	00/06/15	7.89	8.5	1.55	0.64	1.94	12.27	6.73	0.63	0.02	3.89	1300
231	E	00/06/15	8	8.1	1.90	0.87	1.72	11.77	7.78	0.77	0.13	3.75	900
232	E	00/09/11	4.93	5.9	1.00	0.52	0.71	3.22	4.92	0.30	0.02	19.13	1400
233	E	00/09/11	6	4.9	0.98	0.51	0.77	3.77	4.57	0.28	0.10	18.74	1350
234	E	00/09/11	7.9	11.7	3.21	0.78	2.19	15.35	8.79	1.17	0.27	14.97	1400
235	E	00/09/11	7	3.9	0.83	0.54	0.78	4.03	3.19	0.32	0.09	12.66	1650
236	E	00/09/11	7	5.4	0.69	0.59	0.82	5.51	3.79	0.20	0.02	19.09	1650
237	E	00/09/11	7	2.0	0.70	1.24	0.09	2.66	0.39	0.16	0.09	1.71	1430
238	E	00/09/11	7	2.4	0.53	1.13	0.23	3.30	1.19	0.22	3.63	1.00	1350
239	E	00/09/13	7	7.5	4.67	1.02	1.64	7.70	12.87	2.94	0.58	2.90	1150
240	E	00/09/13	8	11.0	4.90	0.98	2.83	11.35	7.10	3.09	0.04	21.05	1300

Table B-1. Chemical composition of Norikura water samples. (cont-)

No.	Site	Date	pH	EC	Na	K	Mg	Ca	Si	Cl	NO_3	SO_4	Altitude
				mS/m	mg/dm^3	mg/dm^3	mg/dm^3	mg/dm^3	mg/dm^3	mg/dm^3	mg/dm^3	mg/dm^3	m
241	E	00/09/13	8	8.81	0.87	0.27	2.95	12.95	2.59	0.59	0.11	4.69	1300
242	H	99/09/27	8	18.7	1.76	0.67	6.51	25.56	4.73	0.13	0.18	32.03	1350
243	H	99/09/27	8	28	20.95	2.03	4.41	31.14	8.88	14.98	1.86	19.32	1350
244	H	99/09/02	8	28	4.81	0.00	10.31	36.05	5.68	4.61	2.09	51.59	1350
245	H	00/09/12	8	23.8	32.74	2.56	0.95	9.20	13.44	43.73	0.99	5.19	1000
246	H	00/06/15	8	12.83	2.05	0.95	3.73	17.60	7.39	0.57	0.43	6.55	950
247	H	00/06/15	8	17.81	12.49	2.07	3.58	16.27	10.41	9.49	0.66	23.08	910
248	H	00/06/14	8	17.6	11.26	1.67	3.88	17.05	6.66	9.27	0.07	23.68	1250
249	H	00/06/15	8	29.45	38.42	4.70	3.77	18.71	20.79	15.87	0.83	22.61	910
250	H	00/09/11	4	22.9	1.57	1.09	4.60	28.38	3.36	0.39	0.10	46.90	1350
251	H	00/09/12	8.5	11.6	2.49	0.37	1.96	19.18	4.76	2.74	0.02	9.10	980
252	K	99/07/16	8.5	103.6	186.9	14.78	4.13	22.97	40.84	145.9	0.02	33.75	1250
253	K	99/09/27	8.5	98.2	121.4	13.74	9.25	54.88	29.50	125.0	4.65	57.05	1250
254	K	99/09/02	8.5	131.2	177.2	19.06	13.46	54.88	51.15	187.3	5.73	28.25	1250
255	K	99/07/15	8.5	140	167.6	18.93	29.07	95.84	53.21	134.6	0.65	79.47	1250
256	K	95/08/02	8.5	153	247.0	45.10	7.80	75.90	83.70	224.0	0.02	78.00	1250
257	K	00/06/14	8.5		139.1	15.92	29.82	74.65	24.18	108.4	0.02	138.8	1250
258	K	00/06/14	8.5	13.37	145.2	18.40	31.92	64.40	48.31	110.0	0.02	102.8	1250
259	K	00/06/15	8.5		231.4	28.78	18.66	9.68	38.69	132.9	0.02	35.07	1250
260	K	00/06/15	8	17.54	12.93	2.07	3.36	15.30	10.14	10.30	0.42	26.05	1000

Table B-2. Chemical composition of Kotsuki river water samples.

No.	Site	Date	pH	EC	Na	K	Mg	Ca	Si	Cl	NO_3	SO_4	HCO_3
				mS/m	mg/dm^3	mg/dm^3	mg/dm^3	mg/dm^3	mg/dm^3	mg/dm^3	mg/dm^3	mg/dm^3	mg/dm^3
1	M1	01/6/18	6.39	6.33	3.77	0.57	2.43	4.39	9.18	5.64	0.35	3.06	
2	M1	01/6/29	6.17	5.31	3.38	0.51	1.89	3.40	7.74	5.02	0.05	3.34	
3	M1	01/8/5	6.25	7.08	4.11	0.60	2.72	4.88	10.03	5.62	1.07	2.96	
4	M1	02/2/15	6.89	6.57	3.97	1.03	2.08	4.25	13.26	5.03	0.86	2.98	
5	M1	02/4/26	6.17	5.35	3.41	0.43	1.81	3.32	8.75	4.83	0.42	3.50	
6	M1	02/5/1	6.27	6.24	3.61	0.46	2.06	3.58	8.69	5.31	1.13	3.19	11.7
7	M1	02/6/28	6.49	6.14	3.59	0.46	2.05	3.74	9.12	5.15	0.42	3.08	22.9
8	M1	02/9/20	5.91	6.6	3.89	0.54	2.26	4.44	10.35	5.47	0.75	3.21	26.8
9	M1	02/11/19	6.49	6.64	4.06	0.59	2.36	4.51	10.92	5.58	1.50	3.08	25.0
10	M2	01/4/6	7.33	0	6.00	1.43	2.29	5.68	15.13	7.65	1.77	4.32	
11	M2	01/6/18	7.35	7.78	5.57	1.49	1.89	5.41	13.07	7.82	1.59	4.31	
12	M2	01/8/4	7.33	9.07	6.49	1.65	2.32	6.35	15.98	7.83	2.38	4.67	
13	M2	02/2/15	7.55	8.36	5.72	1.41	2.04	5.47	15.83	6.55	2.27	4.46	
14	M2	02/4/26	7.39	7.72	5.62	1.78	1.78	4.80	13.92	6.93	2.37	4.68	
15	M2	02/6/28	7.15	7.56	5.43	1.32	1.73	4.62	13.41	6.88	2.09	4.38	25.1
16	M2	02/9/20	6.95	8.98	6.02	1.68	2.09	5.65	15.52	7.10	2.45	4.54	29.3
17	M2	02/11/19	7.46	9.01	6.31	1.60	2.37	6.01	16.48	7.05	3.10	4.85	34.1
18	M3	01/4/6	7.22	0	7.99	2.51	2.12	6.28	22.05	9.28	2.00	5.43	
19	M3	01/6/18	6.96	8.74	6.42	2.49	1.81	6.06	16.61	8.66	3.00	5.61	
20	M3	01/8/5	6.88	10.94	8.11	2.99	2.28	7.49	23.03	9.22	3.20	5.96	
21	M3	02/2/15	7.13	10.05	7.55	2.68	1.89	6.12	24.99	7.23	3.03	5.65	
22	M3	02/4/26	6.92	8.78	6.55	1.97	1.77	5.55	18.13	6.93	2.60	5.29	
23	M3	02/6/28	6.93	9.14	6.67	2.12	1.80	5.78	18.29	8.28	3.02	5.20	31.2
24	M3	02/9/20	6.67	10.68	7.76	3.02	2.00	6.74	24.36	8.13	2.64	5.81	39.0
25	M3	02/11/19	7.11	10.48	8.60	3.13	2.17	6.65	27.50	8.22	3.28	5.77	40.0
26	M4	01/6/18	7.06	11.08	9.06	3.34	1.83	8.39	21.92	11.34	3.90	6.40	
27	M4	01/8/5		0	9.97	3.20	2.19	9.26	25.53	10.24	2.55	6.41	
28	M4	02/2/15	7.53	11.16	8.99	3.25	1.89	6.90	29.40	7.72	3.58	5.95	
29	M4	02/4/26	6.99	10.74	8.32	2.86	1.90	7.31	23.91	8.55	3.59	5.91	
30	M4	02/6/28	7.02	10.82	8.11	2.77	1.84	6.85	22.02	8.52	3.07	6.11	39.3
31	M4	02/9/20	6.3	12.08	9.16	3.46	1.96	7.92	27.12	9.31	2.12	5.83	42.2
32	M4	02/11/19	7.41	11.28	9.54	3.65	2.03	7.45	31.13	8.87	3.04	5.99	42.7
33	M5	01/4/6	8.51	0	10.71	3.53	2.10	8.48	25.45	11.15	3.83	7.28	
34	M5	01/6/18	8.07	12.99	10.38	3.94	2.23	10.57	22.77	12.18	3.10	8.59	
35	M5	01/8/4	6.94	12.3	10.91	3.50	2.38	11.05	24.51	11.52	3.57	7.79	
36	M5	02/2/15	8.43	12.78	10.19	3.41	2.06	8.62	28.74	8.59	4.40	8.61	
37	M5	02/4/26	7.83	11.56	8.52	2.89	1.99	8.50	23.71	8.61	3.49	7.88	
38	M5	02/6/28	7.52	12.21	8.32	2.91	2.01	8.56	22.28	8.94	3.21	8.21	43.9
39	M5	02/9/20	7.27	13.82	9.98	3.73	2.02	9.71	26.92	9.91	2.37	7.68	52.4
40	M5	02/11/19	8.05	12.85	10.43	3.68	2.16	9.11	30.89	9.52	4.38	8.00	46.1

Table B-2. Chemical composition of Kotsuki river water samples. (cont-)

No.	Site	Date	pH	EC	Na	K	Mg	Ca	Si	Cl	NO_3	SO_4	HCO_3
				mS/m	mg/dm^3	mg/dm^3	mg/dm^3	mg/dm^3	mg/dm^3	mg/dm^3	mg/dm^3	mg/dm^3	mg/dm^3
41	M6	02/2/15	8.71	17.1	14.39	3.58	2.73	10.64	30.62	12.43	5.04	11.18	
42	M6	02/4/26	7.21	14	10.67	3.25	2.41	10.31	26.28	10.19	4.04	10.22	
43	M6	02/6/28	7.38	14.11	9.95	3.42	2.23	9.67	25.49	10.26	3.59	9.56	61.2
44	M6	02/9/20	7.06	10.56	13.16	3.85	2.47	11.65	28.59	13.69	2.59	10.66	83.4
45	M6	02/11/19	7.21	17.8	14.71	4.05	3.31	13.04	31.63	13.40	4.08	13.04	39.5
46	M6	02/6/28	7.16	21	10.43	3.31	2.62	11.43	24.21	10.50	3.21	13.08	48.0
47	M7	02/2/15	7.12	19.04	14.86	3.82	3.41	12.92	31.90	13.56	5.24	14.89	
48	M7	02/4/26	6.87	15.49	11.39	3.47	2.71	11.61	27.25	11.24	4.56	12.21	
49	M7	02/6/28	7.32	15.6	10.67	3.28	2.59	11.25	25.11	11.16	3.78	12.57	50.7
50	M7	02/9/20	7	12.06	15.65	4.29	3.24	13.07	29.53	20.11	2.91	14.02	68.8
51	M7	02/11/19	7.05	18.45	14.91	4.36	3.43	13.61	31.48	14.61	5.11	13.87	59.0
52	E1	02/4/26	6.79	6.1	3.66	0.55	1.41	3.14	8.48	5.04	0.61	3.44	
53	E1	02/4/26	6.63	5.6	3.62	0.50	1.78	3.68	9.07	4.93	0.80	3.43	
54	E1	02/6/28	6.72	6.34	3.80	0.51	2.11	4.49	10.49	5.27	0.53	3.06	11.7
55	E1	02/9/20	6.25	6.42	4.40	0.73	2.44	5.35	12.27	5.49	0.90	2.87	35.2
56	E1	02/11/19	7.01	6.72	4.32	0.68	2.30	4.72	12.18	5.34	1.02	2.78	27.3
57	T1	01/6/18	6.46	5.74	5.91	1.34	0.56	3.58	13.54	7.03	2.47	1.86	
58	T1	01/8/5	6.44	5.88	5.93	1.33	0.60	3.63	13.58	6.63	2.52	1.89	
59	T1	02/2/15	7.24	5.67	5.69	1.25	0.56	3.06	13.49	6.05	2.08	1.66	
60	T1	02/4/26	6.23	5.68	5.86	1.28	0.54	3.00	13.88	6.07	2.21	1.87	
61	T1	02/6/28	6.38	5.92	5.92	1.37	0.58	2.97	13.92	6.43	2.16	1.45	18.5
62	T1	02/9/20	6.12	6.27	5.73	1.26	0.53	3.10	13.98	6.10	2.27	1.74	18.9
63	T1	02/11/19	6.88	5.74	6.32	1.40	0.54	3.01	14.59	6.37	2.48	1.51	16.6

論文内容の要旨

論文題目　Chemistry of Natural Surface Water in Volcanic Area
火山地域における天然陸水の水質形成機構

氏　名　穴澤活郎

水の世紀と呼称される２１世紀、水環境の悪化は人類が抱える大きな地球環境問題の一つである。水環境問題の根本的な解決のためには、天然陸水の化学的特性を理解した上で、人為的な環境負荷を求め、対策を立てる必要がある。すなわち、天然陸水を本質的に決定づける溶存化学成分の挙動を把握することが不可欠である。それにもかかわらず、河川水や浅層地下水の主要な溶存成分に関する知見はいまだに乏しく、特に源泉の集中する火山地域における陸水の主要成分の挙動については、ほとんど研究されていない。

一方、研究対象となる化学成分に根ざした”水質”に関する研究は、化学分析値などの数量データに基づいたものであっても、その解釈は概念的になっているものが多い。たとえばナトリウムイオンや塩化物イオンの定量値を用いて、海水混入の大小を論じ、あるいはカルシウムイオンや炭酸水素イオンにより、石灰岩の溶出の度合いを考えるなど、量の大小関係を論じるにとどまっており、各成分が何ゆえにその値をとらなければならなかったのか、定量的な因果律まで追求した例は少ない。しかし、水質を決定づける主要成分の化学組成には、「各成分が一定の濃度であってそれ以外ではあり得ない」、という必然性が介在しているはずである。この必然性に答えるための一つの古典的な解法として利用されてきたのが、化学平衡論に代表される熱力学的な計算である。この手法は、深部熱水や海水のように、基盤岩と水との化学反応が十分に進行し、平衡状態に達している環境水については広く用いられてきたが、反応が未成熟であると想定される浅層地下水や表流水については、ほとんど適用されてこなかった。

こうした背景のもと、本研究では、わが国における水環境を理解するための基礎となる天然の陸水の姿を把握するため、河川水の水源が集中的に存在する火山地域における陸水中の溶存化学成分の挙動について調査研究を行うこととした。調査地としては、わが国の典型的な安山岩質火山であり、陸水環境への人為的な影響や風送海塩の影響が小さく、水量が豊富な中部山岳地帯の乗鞍岳を主たる調査地として選定した。また、同じケイ酸塩鉱物を主体とする岩盤で構成される地域ながら、人為的な影響や風送海塩の影響が予想される南九州のシラス台地で同様の調査を行い、乗鞍岳での調査結果と比較の上、より普遍的な水質形成機構の解明を試みた。

定量的な因果律の解明という問題に対しては、多変量解析法を用いて表流水の化学成分の挙動を支配する要因を統計的に求め、それが岩石（ケイ酸塩鉱物を主要成分とする火成岩）と水との相互作用（化学風化反応、イオン交換反応など）であることを明らかにした。次に化学成分を必然的に決定づける定量的な反応モデル構築のため、各試料水と安定的に共存しうる二次鉱物（粘土鉱物）を熱力学的に求め、表流水の化学組成を支配するケイ酸塩岩石の化学風化式ならびにイオン交換式を求めた。さらにこれらの化学反応式から化学量論的な計算を行い、表流水中の化学成分間の関係式を導出した。そして、この理論式に実試料の化学組成を代入し、当該化学反応モデルの妥当性を検証した。

本論文は５章から構成されている。第１章では、既往研究のレビューと共に、研究の背景を整理し、研究の目的と意義を述べた。

第２章では、乗鞍岳周辺域での天水、陸水（湖沼水、河川水、湧水など）、地熱水（温泉水など）の分析結果を概観し、多変量解析法を用いて、地域ごとに水化学を支配する要因を地球統計学的に特定し、その影響を数量化した。その結果、当該調査地域における水質形成機構は、わが国の水質形成機構を代表しうること、化学成分の濃度から得られた主成分得点分布と試料採取地点の標高データにより天水・陸水・地熱水が明瞭に分別されることなどを明らかにした。また、山頂付近の水質は、ケイ酸塩鉱物を主要構成物とする火山岩の溶解反応により支配され（寄与率 45%）、若干の風送海塩の影響（寄与率 20%）、ならびに生物活動の影響（寄与率 10%）も認められることを明らかにした。乗鞍岳中腹における解析では、岩石-水相互作用が大きく作用しており、特にシリケイトの溶解反応が全水溶成分の変動のうち 45%を、カルシウムやマグネシウムの沈着反応が約 20%を占めていることを明らかにした。風送海塩や生物活動が水質変化に及ぼす影響は、相対的に小さくなり、有意な水質変動要因とはなりえなかった。調査地域全体から得られた非地熱水の因子分析結果からは、中腹域と同様の傾向を示す２つの因子が抽出された。第１因子は、全陽イオンとケイ素への正の負荷を示し（寄与率 65%）、第２因子は、(Na^+, K^+)への負の負荷と(Mg^{2+}, Ca^{2+})への正の負荷を示した（寄与率 16%）。第１因子は岩石成分の溶解、第２因子はイオン交換反応であると解釈され、当該水域における主要成分の挙動は、周辺岩盤と水との相互作用によって支配されることが示唆された。

第３章では、第２章の多変量解析の結果に基づき、岩石－水相互作用の観点から水質形成機構を熱力学的・化学量論的に考察した。第１因子が正の負荷を示すケイ素・陽イオンの挙動については、鉱物の風化系列を想定して得られた理論溶液の組成や、安定関係図を用いて議論した。その結果に基づき、主要成分である陽イオンとケイ素との関係を、長石類を主体とした岩石成分の溶出と、それに伴うギブサイトやカオリナイトなどの二次鉱物の生成反応により定量的に説明した。また、上記化学風化反応に基づく化学量論式から、以下のような陽イオン濃度によるケイ素濃度の推定式を導出した。

乗鞍岳山頂付近の陽イオンとケイ素との関係式（理論式）

$$[Si] = 3[Na^+] + 3[K^+] + [Mg^{2+}] + 2[Ca^{2+}]$$

乗鞍岳中腹付近の陽イオンとケイ素との関係式（理論式）

$$[Si] = 2[Na^+] + 2[K^+] + [Mg^{2+}]$$

実試料の化学分析値はこの式によく適合し、このことからも本論で導かれた仮説が支持された。

第２因子で表現される１価/２価陽イオンの負相関については、岩石—水相互作用で一般に言われているようなCa^{2+}型の水質からNa^+型への変化は見られず、むしろNa^+型からCa^{2+}型への明瞭な変化が観察された。また、地熱水の影響が無い地表水では、$\log (a_{Ca2+} / a^2_{Na+}) = 4.5$の関係式が成り立つことが判明した。この関係式が成り立つ要因については、準安定なイオン交換性鉱物による過渡的な平衡反応を仮定することにより説明がついた。このように天水および地熱水を含めた当該地域全般の水質変動は、天水の溶液組成と、安定鉱物と水との最終平衡条件で算出した溶液組成とを両端成分とする、比較的単純な岩石—水相互作用により説明することができた。

第４章では、南九州のシラス台地を流れる河川水、および周辺地域の温泉水や雨水試料の化学成分を定量し、主要成分の挙動を上記手法により解析した。まず多変量解析により、河川水の溶存主要成分が当該調査地域に数多く見られる温泉や住宅地の排水からの影響をほとんど受けず、主として火砕流堆積物から構成される周辺地質によって支配されることを明らかにした。また、シラス台地を構成する主要鉱物の風化反応式から、陽イオン濃度からケイ素濃度の推定式を導出した（$[Si] = 2[Na^+] + [Mg^{2+}]$）。このことから、当該水域においても、溶存化学成分は岩石成分の溶出と二次鉱物の生成反応に支配されることが明らかになった。

以上本研究では、わが国の水環境に関わる化学的研究において、いままで欠落していた火山地域における天然陸水を調査対象として選定した。注目した要素としては、陸水の性質を本質的に決定づける主要な溶存化学成分を選び、その挙動を多変量解析法と熱力学的・化学量論的計算により定量的に議論した。その結果、わが国の陸水形成機構については、火山岩の主要構成物であるケイ酸塩鉱物の溶解反応が重要な役割を果たしていることが判明した。このことは、陸水の水質特性と形成機構がケイ素濃度を中心とする熱力学的・化学量論的計算によって把握できることを明示している。これは、火山国であるわが国の水質形成機構を特徴づけるものであり、大陸における石灰岩・蒸発岩の溶解や風送海塩の影響を議論するために開発されたPiper plotやStiff diagramなど、溶存イオンのみを扱う手法でわが国の陸水を把握するのは不合理であることを示唆する。こと陸水の溶存化学成分を研究する上では、わが国の水理・地質学的特徴を考慮せずに、欧米で採用されている手法を無批判に導入するようなことは厳に慎まねばなるまい。